Stability and Kinetic Studies on Recombinant Pyroglutamyl Peptidase I and Two Mutant Forms.

By

Karima Mtawae B.Sc. (Hons)

A thesis submitted for the degree of

Master of Science (MSc)

Supervised by Dr. Ciaran O' Fagain

Dublin City University November 2005

DECLARATION

I hereby certify that this material, which I now submit for assessment on the programme of study leading to the award of Master of Science (MSc), is entirely my own work and has not been taken from the work of others save and to the extent that such work has been cited and acknowledged within the text of my work.

Signed: Karima Mt Student Number.: 53134290

Karima Mtawea

Date: 9/01/2006

ACKNOWLEDGEMENTS

I would like to thanks Dr Ciaran Fagan for giving me the opportunity to carry out this research. I greatly appreciate his help, support and advice over the last two years.

I wish to thank Libyan Peoples' Bureau for funding.

Thanks to Dr. Brendan O' Connor's Laboratory, School of Biotechnology, DCU, for permission to use recombinant PAPI and mutants, Ms Zelda Kilbane for materials and advice and Ms Pam O'Brien for help in use of equipment.

A very special thanks to Barry Ryan for all his help and support, Neil and Deborah for their help and encouragement.

Thanks to Technical staff and Library staff.

Family

A very special thanks to my super husband Khaled Elmashaikh and his family for their support, help and patience over the period of my study.

Thanks to my kids Dania, Mohamed and Sarah for giving me their time.

Finally, A very special thanks to my loving Parents Khalifa & Masouda and my sisters, brothers for their support, encouragement and help from the beginning of my life, and thanks to all my friends in my country.

ABBREVIATIONS

Å	Absorbance
ACN	acetonitrile
AD	Alzeimher's Disease.
ALT	Alanine aminotransferase
AMC:	7-Amino-4-methyl-Coumarin
BCA	Bicinchoninic acid
Bov ser DPP IV	Bovine serum dipeptidyl peptidase IV
BSA	Bovine serum albumin
bp	Basepair.
C_{50}	Solvent concentration at which half-inactivation of enzyme is observed
cDNA	Complementary DNA.
CHPNA	(N-[1(R,S)-carboxy-2- phenylethyl]-N-imidazole benzyl- histidyl- β-naphthylamide).
CNS	Central Nervous System
Da:	Dalton
DMF:	Dimethylformamide
DMSO:	Dimethylsulphoxide
DMS	Dimethyl Suberimidate
DNA	Deoxyribo Nucleic Acid.
DTT:	Dithiothreitol
EDTA:	Ethylenediaminetetra Acetic Acid
EtOH	Ethanol
eu	Enzyme units

Flu	Fluorescence Intensity
GRH	Gonadotropin Releasing Hormone.
HRP	Horseradish peroxidase
HPLC	High performance liquid chromatography
His:	Histidine
IPTG:	Isopropyl-beta-D- thiogalactopyranoside
k_{cat}	Catalytic constant
K_m	Michaelis Menten Constant
kDa	kilo Daltons.
LB	Luria- Bertani medium
LHRH	luteinizing hormone-releasing hormone
MeOH	methanol
mM	millimolar
Mw:	Molecular weight
min	minute
µM	micromolar
N:	Native state of protein
NEM	N-Ethylmaleimide
PAP	Pyroglutamyl Peptidase.
PAPI , R hu PAPI	Pyroglutamyl Peptidase I (E.C.3.4.19.3).
PAPII	Pyroglutamyl Peptidase II (E.C.3.4.19.6).
Pcp	Pyrrolidone Carboxylpeptidase
pGCK	pGlu chloromethyl ketone.
pGlu	Pyroglutamic Acid.
pGlu-AMC	Pyroglutamyl-7-amino-4-methyl coumarin
Pyr-O-pcp	Pyroglutamyl pentachlorophenol

Methionine	Met	M
Phenylalanine	Phe	F
Proline	Pro	P
Serine	Ser	S
Threonine	Thr	T
Tryptophan	Trp	W
Tyrosine	Tyr	Y
Valine	Val	V

Units

°C	Degrees Celsius
g	Grams
L	Litres
lb/in^2	Pounds per Square Inch
M	Moles
mg	milligrams
ml	millilitres
µg/ml	Micrograms per millilitre
µL	Microlitres
w/v	Weight per volume
$Units.ml^{-1}$	(micromol product formed/ minute)

TABLE OF CONTENTS

Abstract

This thesis investigates the kinetic and stability characteristics of recombinant human brain pyroglutamyl peptidase PAPI, an omega exopeptidase which cleaves pyroglutamic acid from the N-terminus of peptides and proteins. Three classes of pyroglutamyl peptidase have been found in a variety of bacteria, plant, animal, and human tissues; the first class includes the bacterial and animal type 1, pyroglutamyl peptidase I. The genes encoding bacterial PAPI have been cloned and characterized previously, allowing the study of the primary structure of this enzyme and its over-expression in heterologous organisms. Researchers have also been able to clone and characterize the human form of the peptidase. Recombinant human PAPI was over expressed in *E. coli* grown in LB culture medium and purified by nickel affinity chromatography. The enzyme has a molecular weight of 23kDa, by SDS-PAGE. The estimated T_{50} was 60°C and the half-life at this temperature was 15 min, $k = 0.046 \pm 0.002$ min^{-1}. With regard to solvent tolerance, PAPI was tested in dimethyl sulphoxide, methanol, acetone, tetrahydrofuran, acetonitrile, dimethyl formamide and ethanol over a range of v/v concentrations. It was not stable in most solvents and methanol and DMSO were the least injurious for PAPI activity: 56% and 50% residual PAPI activity remained at 10% v/v methanol and DMSO, respectively. Chemical modification with dimethyl suberimidate gave only 20% recovery of initial activity and did not stabilize the enzyme. The effect of polyol additives was investigated and it was found that the enzyme's activity and stability increased with xylitol. Trehalose, glycerol and ammonium sulphate did not stabilize PAPI. Michaelis-Menten kinetics of PAPI were determined at pH 8.0 with pyroglutamyl 7-aminomethylcoumarin as substrate, $K_m = 0.132 \pm 0.024$ mM and $k_{cat} = 2.68 \times 10^{-5}$ s^{-1}. Both mutant Phe16→Tyr (F16Y) and Tyr147→Phe (Y147F) were compared with wild type PAPI. The T_{50} of F16Y was 51°C and the half-life at 70°C was 27 min, $k = 0.026 \pm 0.002$ min^{-1}. For Y147F, T_{50} was 78°C and the half-life at 70°C was 25 min, $k = 0.028 \pm 0.001$ min^{-1}. Kinetic values for F16Y were $K_m = 0.162 \pm 0.020$ mM and $k_{cat} = 5.75 \times 10^{-5}$ s^{-1}, while Y147F had $K_m = 0.115 \pm 0.019$ mM and $k_{cat} = 2.45 \times 10^{-5}$ s^{-1}.

CHAPTER ONE

INTRODUCTION

1.0 Introduction

This thesis describes experiments on recombinant human PAPI and two mutant forms. This Introduction reviews properties of bacterial and mammalian PAPI, with special reference to its structure, catalysis and possible roles in the body, and compares it with PAPII and thyroliberinase.

1.1 PROTEASES

1.1.1 Definition of proteases

A protease is defined as an enzyme that hydrolyses one or more peptide bonds in a protein or peptide. Thus, proteases can, potentially, degrade anything from a dipeptide up to a large protein containing thousands of amino acids. However, many proteases have a preference for protein substrates, while others will only cleave short peptides or even just dipeptides.

Proteases can be divided into endopeptidases, which cleave internal peptide bonds in substrates, and exopeptidases, which cleave the terminal peptide bonds. Exopeptidases can be further subdivided into aminopeptidases and carboxypeptidases.

1.1.2 Endopeptidases and exopeptidases

Exopeptidases are peptidases that hydrolyse the peptide bonds of the terminal amino acids of the peptide chain while endopeptidases are peptidases cleave peptide bonds in the middle of a peptide chain. (Hooper, 2002)

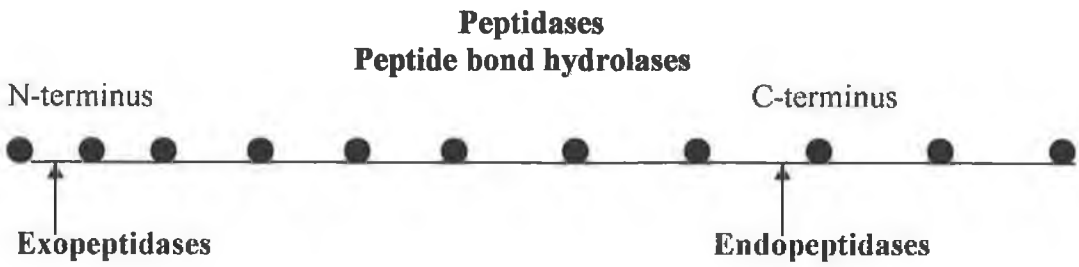

Figure 1.1. A schematic diagram to show the difference between exopeptidases and endopeptidases (Website: burnham.org/labs/salvesen/classification)

1.1.3 Families of proteases

Proteases can also be classified as aspartic proteases, cysteine proteases, metalloproteases, and serine proteases, depending on the nature of the active site. Different inhibitors can be used experimentally to distinguish between these classes of protease. Protease activity can be regulated in *vivo* by endogenous inhibitors, by the activation of zymogens and by altering the rate of their synthesis and degradation.

Table 1.1. Classification of proteases

Family	Examples	Essential residue	Active site Composition	Cleavage mechanism
Serine	Trypsin, subtillsin	Serine	Ser-His-Asp Catalytic triad	Acyl-enzyme intermediate
Cysteine	Papain, ficin	Cysteine	Cys-His Charge transfer	Acyl-enzyme Intermediate
Aspartate	Pepsin, chymosin	Aspartate	One charged One uncharged Asp	General acid-base
Metallo-	Thermolysin	*Zn^{2+}	Coordinated Zn^{2+}	Zn^{2+} acts as Lewis acid

*Zinc ion is not an amino acid, and hence is not a 'residue' but it is essential for metalloprotease function, (Creighton, 1993).

1.2 Pyroglutamyl Peptides

Pyroglutamyl peptides, which are often neuropeptides of up to 40 amino acids, possess an N-terminal pGlu (pyroglutamic acid) residue (Fig. 1.2). An N-terminal pGlu residue can define the highly specific biological properties of neuropeptides. There are many reports of the enzymatic formation of pGlu from glutamic acid and glutaminyl peptides, as reviewed by (Orlowski and Meister 1971). This cyclisation of the N-terminal glutamic acid allows them to have a longer half-life than other peptides of similar size (De Gandarias *et al*, 2000). Pyroglutamyl substrates are often neuropeptides: typically, they are short polypeptide chains released in the autocrine, paracrine and endocrine systems allowing cells to communicate and hence regulate the basic functions of life such as metabolic activity, cell differentiation and growth. (Hardie, 1992). Many biologically active peptides (thyrotropin-releasing hormone, luteinizing hormone-releasing hormone, neurotensin, etc.) and proteins have pyroglutamyl residues. Only a small number of peptidases can degrade the amino terminal pGlu; these are described in the following sections.

1.2.1 Types of Pyroglutamyl Peptidase

Three classes of Pyroglutamyl Peptidase have been found in a variety of plant, animal, and human tissues and classified as Pyroglutamyl Peptidase I (E.C 3.4.19.3), Pyroglutamyl Peptidase II (E.C 3.4.19.6), and Serum Thyroliberinase (E.C 3.4.19.6). (Cummins and O'Connor, 1998). Two pyroglutamyl peptide hydrolases have been found and recognised in the brain: the cysteine peptidase pyroglutamyl-peptidase I (EC 3.4.19.3) that hydrolyses pGlu-X bonds, where X is any amino acid except proline, and the metallopeptidase pyroglutamyl-

peptidase II (EC 3.4.19.6) that degrades thyrotropin-releasing hormone in a highly specific manner (Alba *et al*, 1995). PAPI is widely distributed in bacteria, plants, and animals (Robert-Baudouy and Thierry, 1998).

While PAPI is the principal focus of this review, the main features of PAPII and ST are summarised in sections 1.4 and 1.5 below.

1.3 PYROGLUTAMYL PEPTIDASE I (PAPI)

1.3.1 Classification and occurrence of PAPI

Classification

Pyroglutamyl-peptidase I (PAPI, EC 3.4.19.3) is an omega exopeptidase that is able to specifically remove the amino-terminal pyroglutamyl residue from oligopeptides and proteins. It can be classified as an omega exopeptidase rather than aminopeptidase because the substrate contains no free N-terminal amino group. from oligopeptides and proteins, including thyrotropin-releasing hormone, luteinizing hormone-releasing hormone, neurotensin, bombesin, gastrin, fibrinopeptides, and collagen (Alba *et al*, 1995). PAPI hydrolyses N-terminal pyroglutamyl residues. Pyroglutamyl-peptidases I (EC3.4.19.3) are enzymes of class 3, the hydrolases, and subclass 3.4, the peptide hydrolases or peptidases. PAPI has been identified as a cysteine peptidase-type protease. PAPI has been referred to under several different names including pyrrolidonyl peptidase, pyrrolidone carboxyl peptidase, 5-oxoprolyl-peptidase, PYRase and pyroglutamyl aminopeptidase.

The sequences of the bacterial and archaeal enzymes (see Section 1.3.5) place them in peptidase family C15 of the MEROPS classification (Barrett and Rawling, 2001). Estimates of the molecular mass of the subunit of type I

pyroglutamyl peptidases, as determined by SDS– PAGE under denaturing conditions, are similar for bacterial and mammalian enzymes, ranging from 22 to 25 kDa.

PAPI has been used in protein sequencing to unblock proteins and polypeptides with the amino-terminal pyroglutamyl residue prior to Edman degradation.

Occurrence

PAPI has been found in a variety of bacteria (but not all bacteria), archaea, plant, animal, and human tissues for over two decades, but as yet no form has been found in the *Saccharomyces cerevisiae* genome or in any fungus.

Pyroglutamyl peptidase I occurs as a soluble, intracellular cytosolic cysteine peptidase with broad specificity for pGlu-substrates, and was distributed in many sources such as human cerebral cortex, kidney and skeletal muscle, bovine whole brain, rat, bovine, guinea pig brain, and various rat organs including liver (Cummins and O'Connor, 1998).

In vertebrates the liver and kidney show relatively high PAPI activities compared with other tissues. PAPI was later reported in hamster (*Mesocricetus auratus*) hypothalamus (Prasad and Peterkofsky, 1976) and feline (*Felis domesticus*) brain (DeGandarias *et al*, 1992).

PAPI was localized in the renal proximal tubules; also, imunohistochemical localization study of PAPI demonstrated intracellular distribution in the pituitary. Other, different tissues were tested including heart, liver, spleen, lung, and intestine. PAPI activity has also been noted in non- mammalian sources such as avian, fish, amphibian tissues and bacterial sources (Szewczuk and Kwiatkowska, 1970). Among plants, it occurs in parsley, carrot, bean, oats,

wheat, cauliflower, and potato. Tissues tested included leaves, seeds, sprouts and roots.

PAPI was documented in a wide range of prokaryotes including *Bacillus subtilis* (Szewczuk and Mulczyk 1969), *Klebsiella cloacae* (Kwiatkowska *et al*, 1974), *Streptococcus cremoris* (Exterkate 1977), *Streptococcus faecium* (Sullivan *et al*, 1977), *Bacillus amyloliquefaciens* (Tsuru *et al*, 1978), *Streptococcus pyogenes* (Cleuziat *et al*, 1992), *Staphylococcus aureus* (Patti *et al*, 1995), *Enterococcus faecalis* (Mineyama and Saito 1998), *Pyrococcus horikoshii* (Kawarabayasi *et al*, 1998), *Pyrococcus furiosus* (Tsunasawa *et al*, 1998), *Thermococcus litoralis* (Singleton *et al*, 1999a) and *Mycobacterium bovis* (Kim *et al*, 2001) Doolittle and Armentrout (1968) found that *Pseudomonas fluorescens* could grow on media having free pGlu as the sole carbon and nitrogen source.

1.3.2 Substrates and inhibitors of PAPI

PAPI can be said to hydrolytically remove L-pGlu from $_{L}$-pGlu-$_{L}$-X, where X is any amino acid (except proline), a peptide or an arylamide such as AMC. PAPI has a broad Pyroglutamyl substrate specificity, with its activity being regulated by the amino acid directly after the pGlu residue. In mammals, it may be involved in the inactivation of biologically active peptides that contain an N-terminal pyroglutamyl residue such as TRH (thyrotropin-releasing hormone), LHRH (luteinizing hormone-releasing hormone), bombesin and anorexigenic peptide. More recent studies found that PAPI is involved in the hydrolysis of some xenobiotic compounds having an LpGlu or L-pGlu-related structure (Abe *et al*, 2003; Abe *et al*, 2004a,b) (See physiological role, Section 1.3.4).

Synthetic substrates such as pGlu-Mca, pGlu- Ala, pGlu-pNa, pGlu-βNA and pGlu-Val Cummins and O'Connor (1996); Browne and O'Cuinn, (1983); Bauer et al., (1980); Albert and Szewczuk (1972) are the enzyme's substrates. pGlu-Pro bonds are normally not hydrolysed by mammalian PAPI (Cummins and O'Connor 1996).

A recent study by (Abe *et al,* 2004b) has shown that PAPI can tolerate some single atom substitutions on the pGlu ring such as pGlu-Ala replaced with sulphur (L-OTCA-$_L$-Ala), oxygen (L-OOCA-$_L$-Ala) and nitrogen (L-OICA-L-Ala).

The inhibition of PAPI by many cations such as Hg^{2+}, Zn^{2+}, Cu^{2+}, Co^{2+}, Ca^{2+}, Mn^{2+}, Mg^{2+}, Ni^{2+}, Ba^{2+}, Sr^{2+} and Cd^{2+} has been demonstrated Szewczuk and Mulczyk, (1969); Albert and Szewczuk, (1972); Szewczuk and Kwiatkowska, (1970); Kwiatkowska *et al*, (1974); Prasad and Peterkofsky, (1976); Tsuru *et al*, (1978); Mantle *et al*, (1991); Awadé *et al*, (1992a,b); Bharadwaj *et al*, (1992); Patti *et al*, (1995); Cummins and O'Connor, (1996); Mineyama and Saito, (1998); Tsunasawa *et al*, (1998); Dando *et al*, (2003).

The catalytic importance of a cysteine thiol group in PAPI activity has been demonstrated by its absolute requirement for a thiol-reducing agent such as DTT. PAPI loses activity when treated with a standard cysteine protease inhibitor such as (NEM), as stated earlier.

Inhibition studies confirmed that PAPI belongs to the thiol enzyme family and is completely inhibited by micromolar concentrations of thiol blocking reagents (e.g. iodoacetate, iodoacetamide, p-chloromercurybenzoate (p-CMB), p-mercuriphenylsulphonate, N-ethylmaleimide and sodium tetrathionate). (Doolittle and Armentrout, 1968; Szewczuk and Mulczyk, 1969; Szewczuk and

Kwiatkowska, 1970; Mudge and Fellows, 1973; Kwiatkowska *et al*, 1974; Prasad and Peterkofsky, 1976; Tsuru *et al*, 1978; Bauer and Kleinkhauf, 1980; Tsuru *et al*, 1978; Browne and O'Cuinn, 1983; Awadé *et al*, 1992a,b; Gonzalès and Robert-Baudouy, 1994; Patti *et al*, 1995; Cummins and O'Connor, 1996; Tsunasawa *et al*, 1998; Mineyama and Saito, 1998; Singleton *et al*, 2000; Singleton and Littlechild, 2001; Dando *et al*, 2003).

Chemical modification studies also indicated the involvement of acidic residues, in addition to a His residue, in the enzymatic activity on the basis of experiments with 1-ethyl-3-(3- imethylaminopropyl) carbodiimide (EDAC) at acidic pH and diethylpyrocarbonate (LeSaux *et al*, 1996). To elucidate the catalytic mechanism and biological significance of the enzyme, several specific inhibitors have been synthesized (Fujiwara *et al*, 1981; Friedman *et al*, 1985).

Site directed PAPI inhibitors were first synthesized for bacterial cells, *B. amyloliquifaciens* in particular, the most potent being pGlu chloromethyl ketone (pGCK), Z-pGlu chloromethyl ketone (Z-pGCK), and Z-pGlu diazomethyl ketone (Z-pDMK). (Fujiwara *et al*, 1981) reported that pGlu diazomethyl ketone, did not enhance TRH levels in the brain *in vivo* or *in vitro*, but (Faivre-Bauman *et al*, 1986) observed increased levels of TRH when primary cultures of hypothalamic cells were treated with Z-Gly-ProCHN_2, also known as a PAPI inhibitor. In mammalian cultures inhibition of the enzyme can be due to absence of a thiol-reducing agent, DTT, or the presence of sulfhydryl-blocking reagents, for example 2-iodoacetamide (Bauer and Kleinkauf, 1980).

(Fujiwara *et al*, 1981) noted a decrease in enzyme activity upon addition of pGCK. However, these tests were carried out in the absence of DTT. Several workers have used 2-pyrrolidone to stabilize type I pyroglutamyl peptidases

during purification and storage (Armentrout and Doolittle, 1969; Mudge and Fellows 1973).

A synthetic aldehyde analog of pGlu, 5-oxoprolinal, was also found to be a potent inhibitor of PAPI (Friedman *et al*, 1985). Competitive inhibition by these compounds is due to their binding to the PAPI active site instead of the substrate. Several other inhibitors have been observed for mammalian PAPI. (Yamada *et al*, 1990) noted the inhibitory effects of 1,10-phenanthroline, excess DTT and EDTA. (Cummins and O'Connor, 1996) reported that bovine brain PAPI was 28% inhibited by 1mM 1,10-phenanthroline. Two compounds, benarthin and pyrizinostatin, isolated from the genus *Streptomyces*, were found to be inhibitors of PAPI (Aoyagi *et al*, 1992a; Aoyagi *et al*, 1992b). Also, the inhibitory effect of an oligosaccharide gum from *Hakea gibbosa* on PAPI activity was reported (Alur *et al*, 2001). Benzamidine was also described as an inhibitor of the bacterial enzyme (Awad *et al*, 1994). Other studies carried out by (Mantle *et al*, 1991), noted inhibitory effects of amastatin, arphamenine, chymostatin, elastinal and leupeptin.

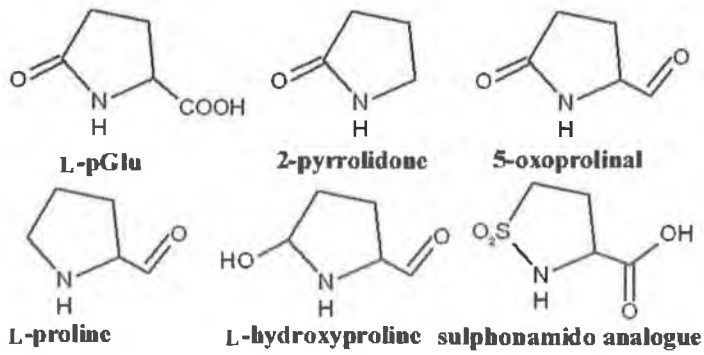

Figure 1.2: chemical structures of L-pGlu, 2-pyrrolidone, 5-oxoprolinal, L-proline, L-proline, L-hydroxyproline, sulphonamide.

1.3.3 PAPI characterisation

PAPI enzymes from a range of prokaryotic and eukaryotic organisms have been characterised biochemically. The molecular weight of PAPI was determined mainly by SDS-PAGE and gel filtration and it was mostly been reported as around 24 kDa. The optimal activity for the enzyme was in the pH range 6.0 to 9.5. The isoelectric point (pI), where reported, is around 5.0. The physiological temperature of 37°C has been widely used as the standard reaction temperature for analysis of eukaryotic PAPI. Optimum temperatures for activity of mesophilic prokaryotic PAPI have mostly been reported as ranging from 30 - 45°C, but two thermophilic enzymes *T. litoralis* PAPI and *P. furiosus* PAPI exhibit optimum activity at 70°C and 90°C, respectively. (Singleton & Littlechild, 2001; Ogasahara *et al*, 2001)

The purification of PAPI from several strains of the species *Bacillus* and the characterisation of its enzymatic properties have been well documented. *Bacillus amyloliquefaciens* PAPI has been particularly well studied, including cloning, sequencing and expression of its gene in *Escherichia coli*. The peptide comprises 215 amino acid residues, has a homodimer structure with a deduced subunit molecular mass of 23.3kDa and a pH optimum of 6.5. (Yoshimoto *et al*, 1993).

1.3.4 Physiological role(s) of PAPI

The physiological role of PAPI currently remains unclear. (Albert and Szewczuk, 1972) suggested a possible role for PAPI in the absorption of peptide and proteins from the alimentary tract by the presence PAPI in the small intestine and intestinal mucous membrane and duodenum, in addition to its broad substrate specificity (Pierro and Orsatti, 1970). From many studies it was suggested that PAPI was a cytosolic enzyme. The cytosolic location of PAPI excludes a

significant role in extracellular peptide degradation (Charli et al., 1987; Abe et al., 2004a,b). O'Cuinn et al. (1990) suggested that PAPI may represent a mechanism for returning pGlu terminating neuropeptides released from damaged or ageing vesicles back to the cellular amino acid pool. PAPI may contribute to the intracellular catabolism of peptides to free amino acids which are then re-incorporated into biosynthetic pathways. Thus, it may be involved in regulating the cellular pool of free pGlu.

PAPI might contribute to neuropeptide break down where secretion from neuropeptide-synthesising cells is suppressed to degrade neuropeptides that are produced in excess. The findings by Faivre-Bauman *et al.* (1986) showing that the addition of specific PAPI inhibitors to TRH-synthesising hypothalamic cells in culture results in a significant increase of TRH content and release from cells, under both basal and K^+ stimulated conditions.

More recently it was found that PAPI is involved in the hydrolysis of some xenobiotic compounds with an LpGlu or L-pGlu-related structure, (Abe *et al*, 2003; Abe *et al*, 2004b). PAPI may also be involved in detoxification of pGlu-peptides, since high levels of such peptides would abnormally acidify the cell cytoplasm.

The study of subcellular localisation of peptidases could form an important platform for understanding the regulatory mechanisms that control the activity of neuropeptides in the cell. The high level of Pyroglutamyl Peptidase in the human brain cortex agrees with the inactivation of TRH is higher in the human brain cortex than in other regions (Griffiths *et al*, 1985). Cortex is the area of the brain closely related to memory, cognition and learning, thus this may suggest a

possible role for the PAPI in the higher parts of the human brain. (Coyle et al, 1983).

Roles in health

A TRH regulation study carried out by Irazusta *et al.* (2002) showed that both soluble and particulate pyroglutamyl peptidase activities were higher in human brain. A correlation between PAPI activity and TRH levels in mammalian brain has been observed in many studies (De Gandarias *et al*, 1992; 1994; 1998; 2000). A decrease in PAPI activity coincides with increasing levels of TRH as brain development progresses, indicating that PAPI plays a part in the normal development of mammalian brain. Also, during earlier stages of development, high PAPI activity is linked to elevated levels of cyclo(His-Pro), a correlation which was previously indicated (Prasad *et al*, 1983). The wide distribution of TRH throughout the central nervous system, and, the findings of various biochemical, pharmacological and behavioural studies strongly implies that TRH may act as a neuromodulator or neurotransmitter in the extrahypothalamic brain. PAPI may also have an important part to play in memory and learning, in metabolism and the possible control of neural diseases such as Alzheimer's disease (Irazusta *et al*, 2002).

The effect of light intensity on the activity of PAPI in the functionally connected retina and hypothalamus of rats was studied (Ramírez *et al*, 1991; Sánchez *et al*, 1996). PAPI exhibits a highly significant periodic fluctuation, coinciding with environmental light and dark conditions. Results suggest a possible function of PAPI within the "body clock" of a human Sanchez *et al*, (1996). Substrates of PAPI (such as TRH or GRH, gonadotropin releasing hormone) may play a

functional role in the retina, apart from their well-known role in the hypothalamus.

Involvement in disease

The concentration of TRH in the hippocampus of elderly controls and Alzheimer's disease (AD) patients was recorded by radioimmunoassay (RIA). He and Barrow (1999) reported that PAPI may be involved in the propensity of amyloid precursors to form insoluble plaques, resulting in Alzheimer-type diseases.

The free pGlu is known to have pharmacological properties and these have been demonstrated in certain disease states (Szewczuk and Kwiatkowska, 1970; Lauffart *et al.*, 1989; Mantle *et al.*, 1990; 1991).

The physiological implications of this involvement were explored by Falkous *et al.* (1995) who observed significantly increased levels of PAPI in the spinal cord of patients suffering from motor neuron disease. The identification of characteristic deposits of proteins in degenerating spinal cord neurons in motor neuron disease cases suggests that an abnormality of intracellular protein catabolism may contribute to the pathogenesis of this disorder.

A recent study by Valdivia *et al.* (2004) showed that sub-fertile men had higher PAPI levels in their soluble sperm fraction than normal men.

1.3.5 Structure, Sequence and Active site of PAP I

Sequence

The purification of PAPI has been reported from several prokaryotic species and its enzymatic properties have been studied; see Table 1.2 below.

Table 1.2 Known PAPI sequences of prokaryotic organisms

Organism Type	PAPI Enzyme	GenBank Accession	Molecular Weight	Amino Acids	Reference
Pseudomonas fluorescens	*Pfl*PAPI	X75919	22.438	213	Gonzalès and Robert-Baudouy, 1994
Pyrococcus horikoshii	*Pho*PAPI	AP000002	22.640	206	Sokabe *et al.*, 2002
Pyrococcus furiosus	*Pfu*PAPI	AB015291	22.822	208	Tsunasawa *et al.*, 1998
Streptococcus pyogenes	*Spy*PAPI	X65717	23.132	215	Cleuziat *et al.*, 1992
Mycobacterium bovis	*Mbo*PAPI	U91845	23.193	222	Kim *et al.*, 2001
Staphylococcus aureus	*Sau*PAPI	U19770	23.227	212	Patti *et al.*, 1995
Bacillu. amyloliquefaciens	*Bam*PAPI	D11035	23.287	215	Yoshimoto *et al.*,1993
Bacillus subtilis	*Bsu*PAPI	X66034	23.774	215	Awadé *et al.*, 1992a,b
Thermococcus litoralis	*Tli*PAPI	Y13966	24.745	220	Singleton *et al.*, 2000

Figure 1.3. shows PAPI amino acid sequences of prokaryotic organisms. Sequence similarities are coloured in gray and black indicates the highest homology. The highest degree of sequence homology exists between *Bsu*PAPI and *Bam*PAPI (72% identity, 85% similarity). The prokaryotic sequence that human PAPI shows most homology to is *Bam*PAPI (25% identity, 45% similarity); this is a higher score than among some of the eukaryotic sequences. The largest divergence exists between *Mbo*PAPI and *Sau*PAPI (27% identity, 48% similarity).

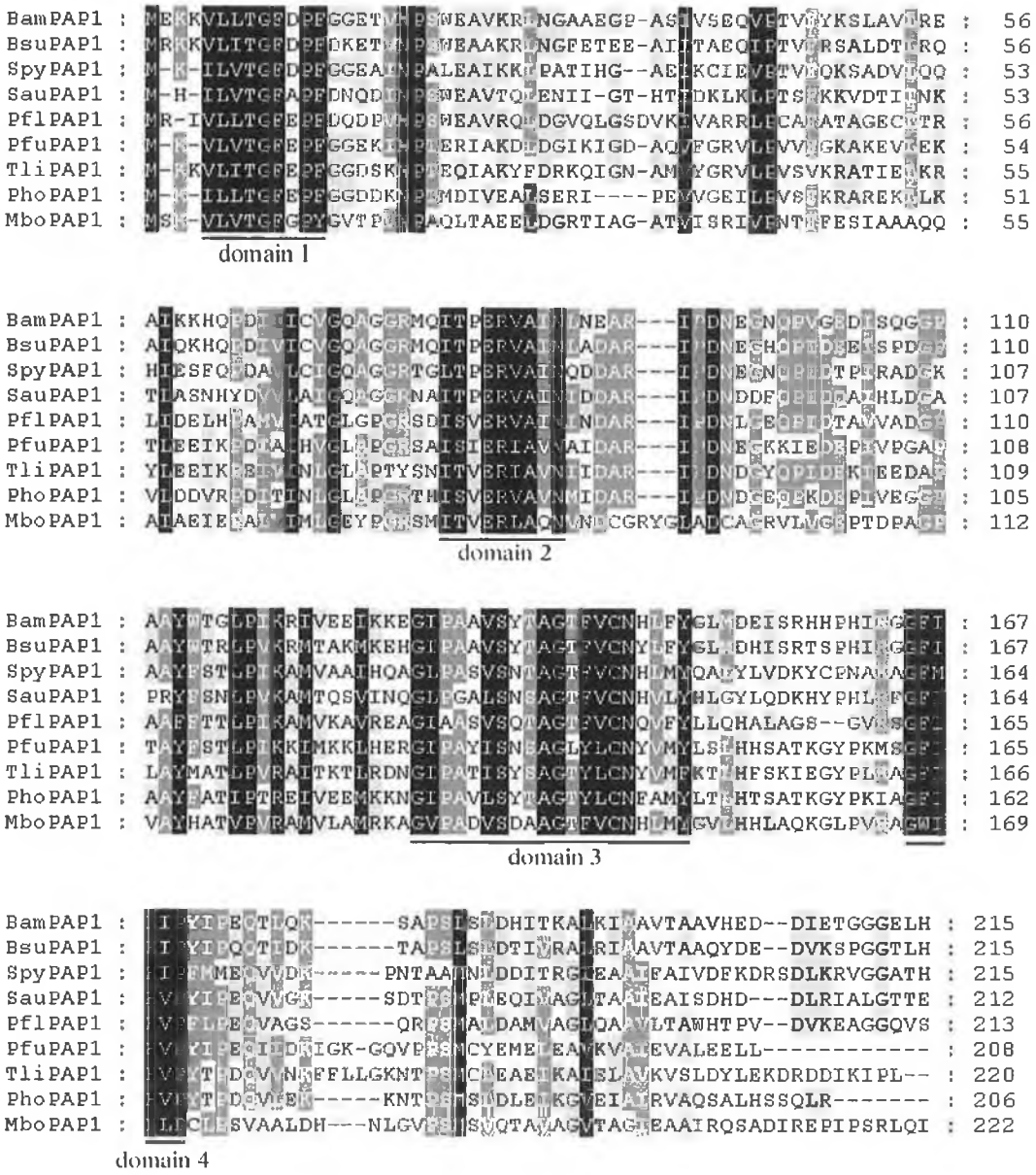

Figure 1.3 Amino acid sequence alignment of prokaryotic PAPI

Alignment was created using MultAlin with Blosum62-12-2 parameters and edited using GenDoc. **Key:** *Pseudomonas fluorescens* = *Pfl*PAPI; *Pyrococcus horikoshii* = *Pho*PAPI; *Pyrococcus furiosus* = *Pfu*PAPI; *Streptococcus pyogenes* = *Spy*PAPI; *Mycobacterium bovis* = *Mbo*PAPI; *Staphylococcus aureus* = *Sau*PAPI; *Bacillus amyloliquefaciens* = *Bam*PAPI; *Bacillus subtilis* = *Bsu*PAPI; *Thermococcus litoralis* = *Tli*PAPI. Figure reproduced from P-R Vaas (PhD thesis, DCU, 2005) by permission.

BLAST comparison of human PAPI with known PAPI sequences against the current GenBank data (2005) reveals similarities to a number of eukaryotic PAPI genes. An aminopeptidase from *M. musculus* (mouse) shows 34% compatibility, while an aminopeptidase from *C. elegans* shows 29% compatibility. [http://www.ncbi.nlm.nih.gov/UniGene].

Table 1.3 Known PAPI sequences of eukaryotic organisms

Organism Type	Common Name of organism	GenBank Accession	PAPI Enzyme	Molecular Weight	No. of Amino Acids	Reference
Apis mellifera	Honey Bee	XM_392560	Ame*PAPI*	21,941	191	[*]
Tetraodon nigroviridis	Green Pufferfish	CAAE01014609	*Tni*PAPI	22,376	205	[*]
Rattus norvegicus	Rat	AB098134	*Rno*PAPI	22,800	208	[‡]
Mus musculus	Mouse	AJ278829	*Mmu*PAPI	22,934	209	[†]
Homo sapiens	Human	AJ278828	*Hs*PAPI	23,138	209	[†]
Takifugu rubripes	Japanese Pufferfish	AJ301641	*Tru*PAPI	23,331	211	[*]
Anopheles gambiae	Mosquito	XM_308793	*Ag*PAPI	23,940	209	[*]
Arabidopsis thaliana	Cress	NM_104547	*Ath*PAPI	24,046	219	[*]
Drosophila melanogaster	Fruit Fly	NM_168616	*Dm*PAPI	24,807	224	[*]
Caenorhabditis elegans	Nematode	NM_060090	*Cel*PAPI	31,007	274	[*]

Dando et al., (2003)[†]; Abe et al., (2003) [‡]; Putative sequences; [*] Molecular weights were deduced from amino acid sequences

Figure 1.4. shows PAPI amino acid sequences of eukaryotes. Sequence similarities are coloured in gray and the highest homology is shown in black. The highest homology was between the sequences *Mmu*PAPI and *Rno*PAPI (98% identity/ similarity) and the next closest homology was to *Hsa*PAP1 (94% identity, 96% similarity). The insect sequences *Dme*PAPI, *Aga*PAPI and *Ame*PAPI (35% identity, 56% similarity) show a similar degree of homology with *Hsa*PAPI as with each other (~30% identity, ~50% similarity). The plant sequence *Ath*PAPI and nematode sequence *Cel*PAPI exhibit the greatest divergence from other eukaryotic sequences.

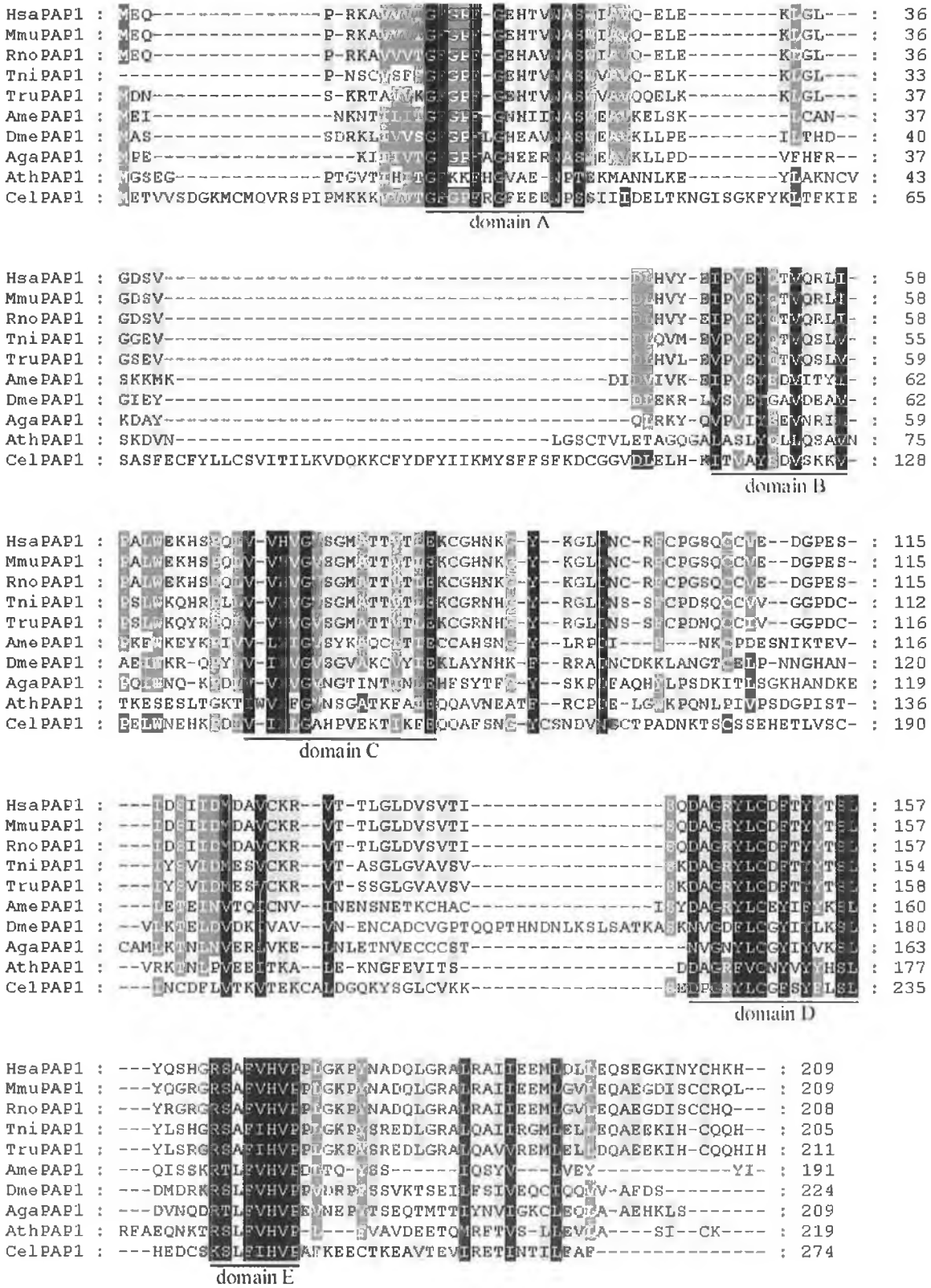

Figure 1.4 Alignment was created using MultAlin with Dayhoff-8-0 parameters and edited using GenDoc homology. **Key:** *Apis mellifera, Ame*PAPI. *Tetraodon nigroviridis, Tni*PAPI. *Rattus norvegicus, Rno*PAPI. *Mus musculus, Mmu*PAPI.

*Homo sapiens, Hs*PAPI. *Takifugu rubripes, Tru*PAPI. *Anopheles gambiae, Ag*PAPI. *Arabidopsis thaliana, Ath*PAPI. *Drosophila melanogaster, Dm*PAPI. *Caenorhabditis elegans, Cel*PAPI. Figure reproduced from P-R Vaas (PhD thesis, DCU, 2005) by permission.

Structure

The native mammalian enzyme appears to be monomeric, but Mw values of 50–91 kDa have been reported for the native bacterial enzyme. PAPI was first isolated from *Bacillus amyloliquefaciens*. The recombinant *B. amyloliquefaciens* enzyme probably functions as a dimer (Yoshimoto *et al.*, 1993), but the protein has been crystallised as a tetramer from *B. amyloliquefaciens* (Odagaki *et al.*, 1999) and *Thermococcus litoralis* (Singleton *et al.*, 1999a,b).

The X-ray analysis and three-dimensional structure of PAPI were solved.

The first documented crystallized structure of *Bacillus amyloliquefaciens* was at 1.6 Å (Odagaki *et al.*, 1999), for *Pyrococcus furiosus* PAPI at 1.73 Å (Tanaka *et al.*, 2001), for *Thermococcus litoralis* PAPI at 2.0 Å (Singleton *et al.*, 1999a; 1999b) and *Pyrococcus horikoshii* PAPI at 2.2 Å (Sokabe *et al.*, 2002).

The monoclinic crystal form of *Bam*PAPI, *Pfu*PAPI, *Tli*PAPI and *Pho*PAPI has four crystallographically independent copies of PAPI in the asymmetric unit, and it was categorised as a tetramer of four identical subunits designated A – D. Each monomer of the tetramer makes contact with two other subunit monomers.

The structure allows the catalytic site of PAPI to be identified and begins to define some key features of the catalytic mechanism. It serves as a model system to help elucidate the mechanism of similar enzymes in higher organisms, including humans and allows comparison of the overall topology and three-

dimensional structure of PAPI to that of other similar proteins as well as a comparison of the organization of the active site with that of other proteases The polypeptide folds in an α/β globular domain with a hydrophobic core consisting of a twisted β sheet surrounded by five α helices. This structure allows the function of most of the conserved residues in the PAPI family to be identified, and it has been concluded that the catalytic triad consists of Cys144, His168 and Glu 81.

The enzyme expressed in *E. coli* was crystallized and the three-dimensional structure clarified by x-ray crystallography (Odagaki *et al.*, 1999). The active site (a catalytic triad composed of Cys-144, His-168, and Glu-81) of each monomer was located inside the doughnut-shaped tetramer. A thermostable enzyme from *Thermococcus litoralis* was also studied by x-ray crystallography (Singleton *et al.*, 1999a,b). The A-D interface of *Bacillus amyloliquefaciens* PAPI involves hydrophobic interactions and several ionic salt bridges between each monomer. The A-C interface does not have any ionic salt bridges and a thin layer of water mediates hydrogen bonds between the subunits.

The *Thermococcus litoralis* PAPI tetramer has a central cavity of 6000 Å. The A-B interface has hydrophobic interactions and salt bridges involving Arg81, Asp88, Asp101 and Arg119, the A-C interface is formed by an extended loop and a disulphide bridge exists between Cys190 of each monomer. This hydrophobic core may contribute towards the thermostability of *Thermococcus litoralis* PAPI. Other residues along this interface are generally hydrophobic.

The A-B interface of the *Pyrococcus horikoshii* PAPI tetramer consists hydrophobic interactions and has inter-subunit ion bonds and the A-C interface

has hydrogen bonds that are entirely mediated by a thin layer of water and was a dimer in solution.

Further recent studies carried out by (Kabashima et al., 2001) have again focused on the thermal stability of PAPI in the *Bacillus* strain in comparison to the PAPI activity in *Thermococcus litoralis*.

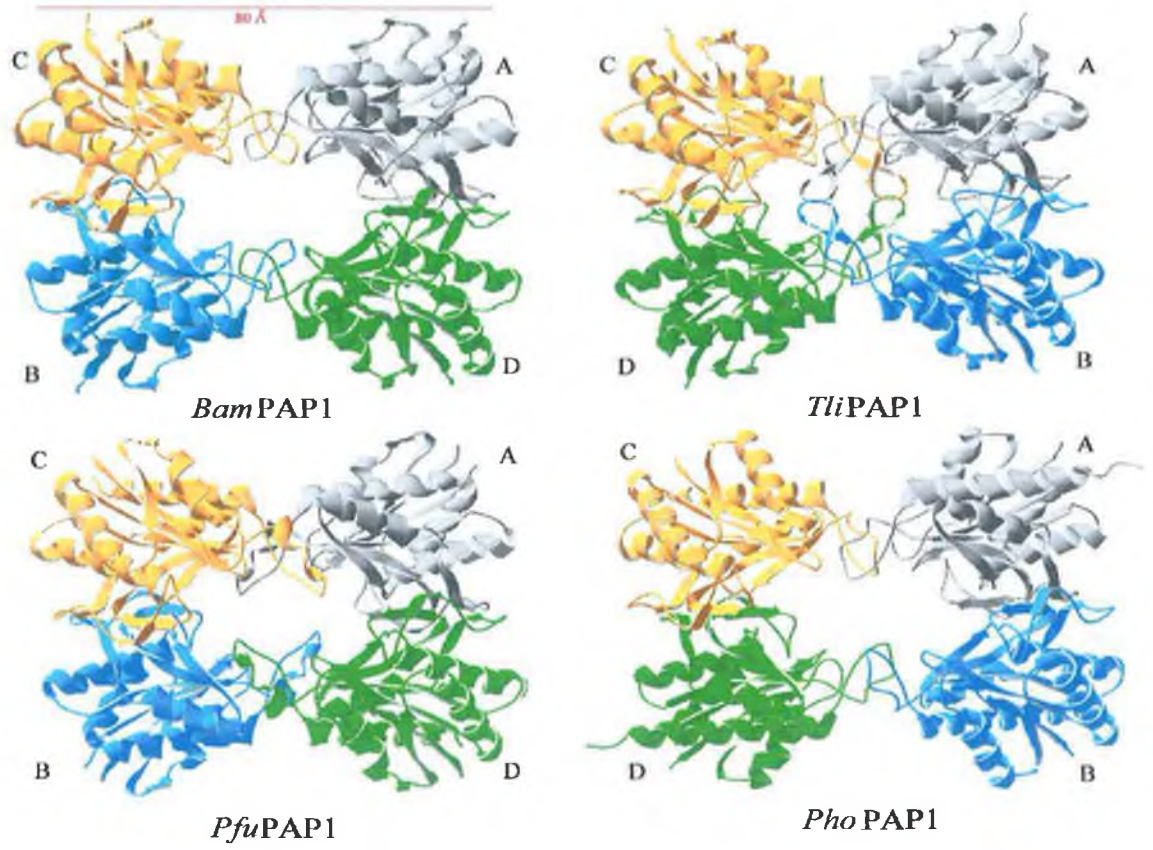

Figure 1.5 Ribbon diagrams of the tetrameric crystal structures of *Bacillus amyloliquefaciens* PAPI (1AUG), *Pyrococcus horikoshii* PAPI, *Pyrococcus furiosus* PAPI and *Thermococcus litoralis* PAPI (1A2Z). The monomeric subunits are labelled A - D. Figure reproduced from P-R Vaas (PhD thesis, DCU, 2005) by permission.

PAPI from the hyperthermophilic archaeon *T. litoralis* showed an enhanced thermal stability when compared to PAPI enzymes from mesophilic bacteria such as *B. amyloliquefaciens,* probably due to the presence of inter subunit disulphide bonds. Disulfide bonds appear to make a considerable contribution to thermal stability, an effect mainly attributed to the decreased entropy of the denatured protein. *B. amyloliquefaciens* PAPI with an engineered inter-subunit disulphide bond showed increased thermal stability, without any decrease in enzymatic performance. However, pH stability was not altered (Kabashima *et al.*, 2001).

The active sites of cysteine proteases typically have a catalytic triad, an oxyanion hole and a specificity pocket. The catalytic triad of *B. amyloquefaciens* PAPI comprises Cys144, His168 and Glu81 and this was concluded from site-directed mutagenesis of the appropriate amino acids (Odagaki *et al.*, 1999).

The two cysteine residues of BamPAPI, Cys68 and Cys144, were mutated to Ser. Mutant Cys144_ Ser has no detectable PAPI activity (Yoshimoto *et al.*, 1993), while Cys68_Ser has wild type activity, implicating Cys144 as the active site thiol. Also, by titration with 5,5'-dithio-bis-(2-nitrobenzoate), it was shown that the Cys68 is located internally. His168 is also completely conserved, and thus PAPI was thought to be a cysteine protease with a Cys-His catalytic diad or Cys-His-Asp/Glu catalytic triad.

Several residues were investigated by (Le Saux *et al.*, 1996) as possible residues contributing to the active site of *Pfl*PAPI. Substitution of the Cys-144 and His-166 residues by Ala and Ser, respectively, resulted in inactive enzymes. Proteins with changes of Glu-81 to Gln and Asp-94 to Asn were not detectable in crude extract and were probably unstable in bacteria. The results suggest that Cys-144

and His-166 constitute the nucleophilic and imidazole residues of the enzyme active site, while residue Glu-81, Asp-89, or Asp-94 might constitute the third part of the active site.

Tsunasawa *et al.* (1998) substituted Cys142 residue of *Pfu*PAPI with Ser, resulting in inactive enzyme, and by sequence analysis, showed that the catalytic triad Cys142, His166, and Glu79 corresponds to Cys144, His168 and Glu81 of BamPAPI. The location of the Cys144 at the N terminus of an α helix could have an important effect on the enzyme's reactivity. A location such as this could effect catalysis, as the helix dipole can depolarise the amide bond and enhance its reactivity. PAPI does not have a well defined oxyanion hole; however, it is possible that a tetrahedral oxyanion could be produced by the contribution of Cys144 and Arg91 and their respective side chains. A hydrophobic region close to Cys144 provides an area of high specificity. This area provides a binding site for the pGlu of the enzyme's substrate. This pocket appears to have some conformational flexibility, hence allowing for maximum interaction with the substrate. PAPI appears to only have one pocket of specificity (Odagaki *et al.*, 1999). The catalytic residues Glu81, Cys144, and His166 in the enzyme from *B. amyloliquefaciens* are all conserved in the human sequence.

1.3.6 Genetics of PAPI; Cloning strategy and sequence for pRV5

Forms of pyroglutamyl-peptidase I from bacteria and archaea have been cloned and sequenced, and the proteins have been crystallised and their three-dimensional molecular structures determined (Yoshimoto *et al.*, 1993; Singleton *et al.*, 1999a,b). Many data are available of homology and biochemical characterisation of PAPI. Genes have been cloned for the enzymes of *Bacillus*

subtilis (Awade *et al.*, 1992), *Pseudomonas fluorescens* (Gonzales and Robert-Baudouy, 1994), *Staphylococcus aureus* (Patti *et al.*, 1995) and *Streptococcus pyogenes* (Cleuziat *et al.*, 1992). PAPI from *Bacillus amyloliquefaciens* has been particularly well studied: its gene has been cloned, sequenced and expressed in *Escherichia coli*, and the protein product has been purified. *B. subtilis*, *S. pyogenes* and *P. fluorescens* were Southern blotted and only one signal was detected, indicating that the genes are present as single copies (Awadé *et al.*, 1992a,b; Cleuziat *et al.*, 1992; Gonzalès and Robert-Baudouy, 1994). *B. subtilis* and *S. pyogenes* total RNA samples were Northern blotted: the mRNA sequences were around 700 bp in length. Table 1.3 shows prokaryotic PAPI sequences.

PAPI enzyme sequence was mapped against the human genome to localise the PAPI gene. The gene is located on the nineteenth chromosome at approximately nucleotide number 18,945, unlike the PAPII gene, located on chromosome twelve. Further analysis of human PAPI shows the base composition to be 164 A, 194 C, 216 G, and 133 T; the total count is approximately 710 base pairs.

In comparison to PAPII (see below), PAPI is a lot smaller than PAPII. PAPI comprises approximately 710 bp, while the PAPII comprises approximately 5670 bp, and the PAPI structure is almost eight times smaller than that of PAPII. To compare the homology of PAPI,II, two genomic structures were aligned together as in Figure 1.6. A certain amount of homology with PAPII begins at basepair 32 and continued until basepair 837; approximately 42% direct homology is observed between the two genomic sequences, suggesting that the two structures were at one point in time derived from a common gene (Mader, 2001).

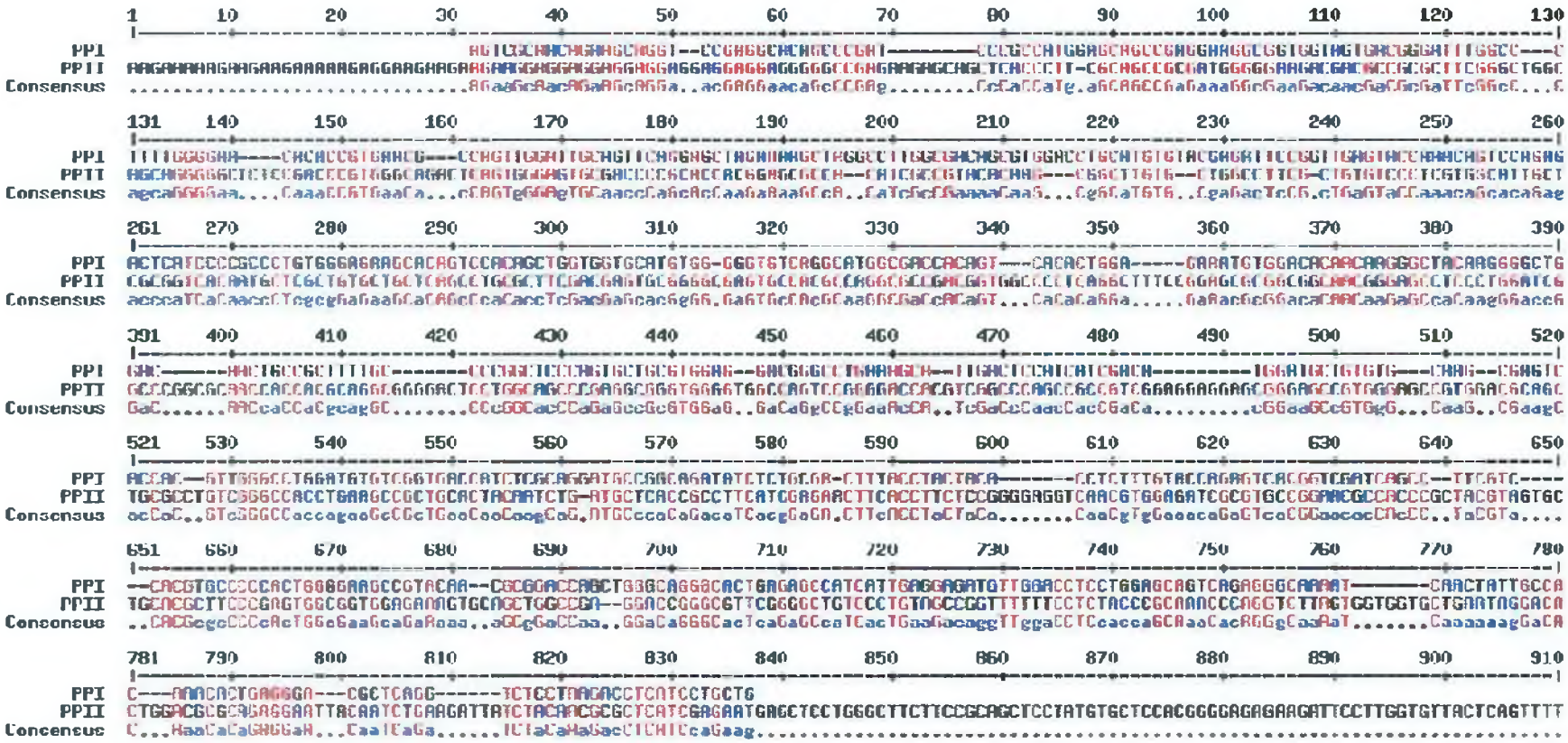

Figure 1.6. Comparison of the genetic structures of mammalian PAPI and PAPII. Base homology is indicated by a red colour. The aligned and common genomic bases are coloured in red and the uncommon bases are coloured in blue and black. (http://prodes.toulouse.inra.fr/multalin).

Cloning of human PAPI

E.coli strain (XL-10 Gold) containing plasmid pRV5 encoding PAPI, was used in this work, the cloning strategy for pRV5 was described in detail by Vaas (PhD thesis, DCU, 2005) and is outlined in figure 1.7. An *Eco*R1/*Hin*dIII restriction enabled the entire *rHsa-pap1*-6xHis fusion to be transferred from pRV3 to pPC225, which had been opened with *Eco*R1/*Hin*dIII. The *Eco*R1/*Hin*dIII restriction produced a band corresponding to the expected 680 bp fragment containing the *rHsa-pap1*-6xHis fusion. *Eco*RV, *Nco*1, *Eco*R1 and *Hin*dIII single restrictions produced bands corresponding to the expected 5235 bp linearised plasmid.

The exact sequence of pRV5 was subsequently verified by commercial DNA sequencing by MWG Biotechnology. The *rHsa-pap1*-6xHis fusion (680 bp) is excised from pRV3 (by restriction with *Eco*RI and *Hin*dIII) and ligated into pPC225 (previously opened with *Eco*R1 and *Hin*dIII). The resulting construct, pRV5, has *rHsa-pap1*-6xHis fusion under control of P*tac* promoter.

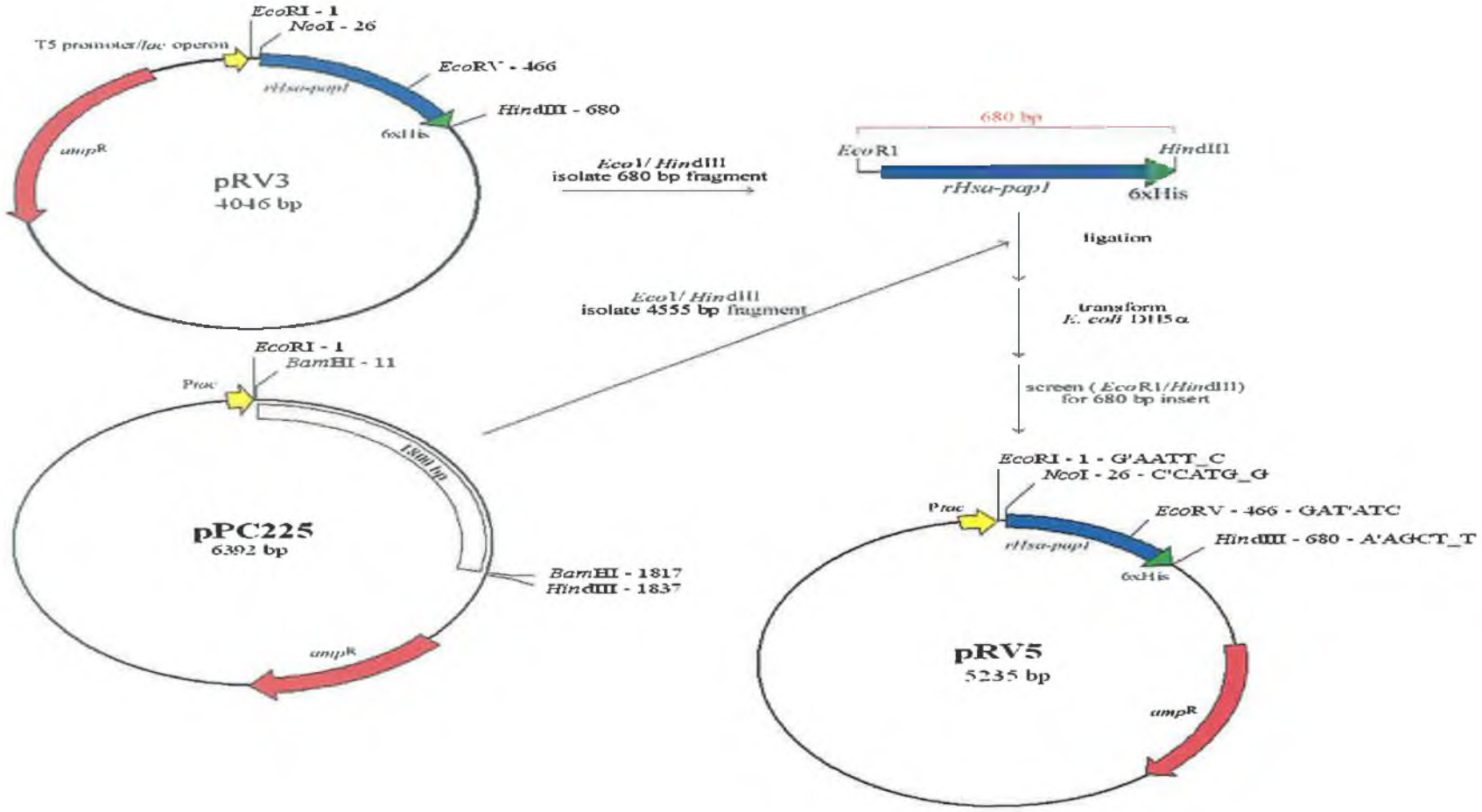

Figure 1.7 Cloning strategy for pRV5. Figure reproduced from P-R Vaas (PhD thesis, DCU, 2005) by permission.

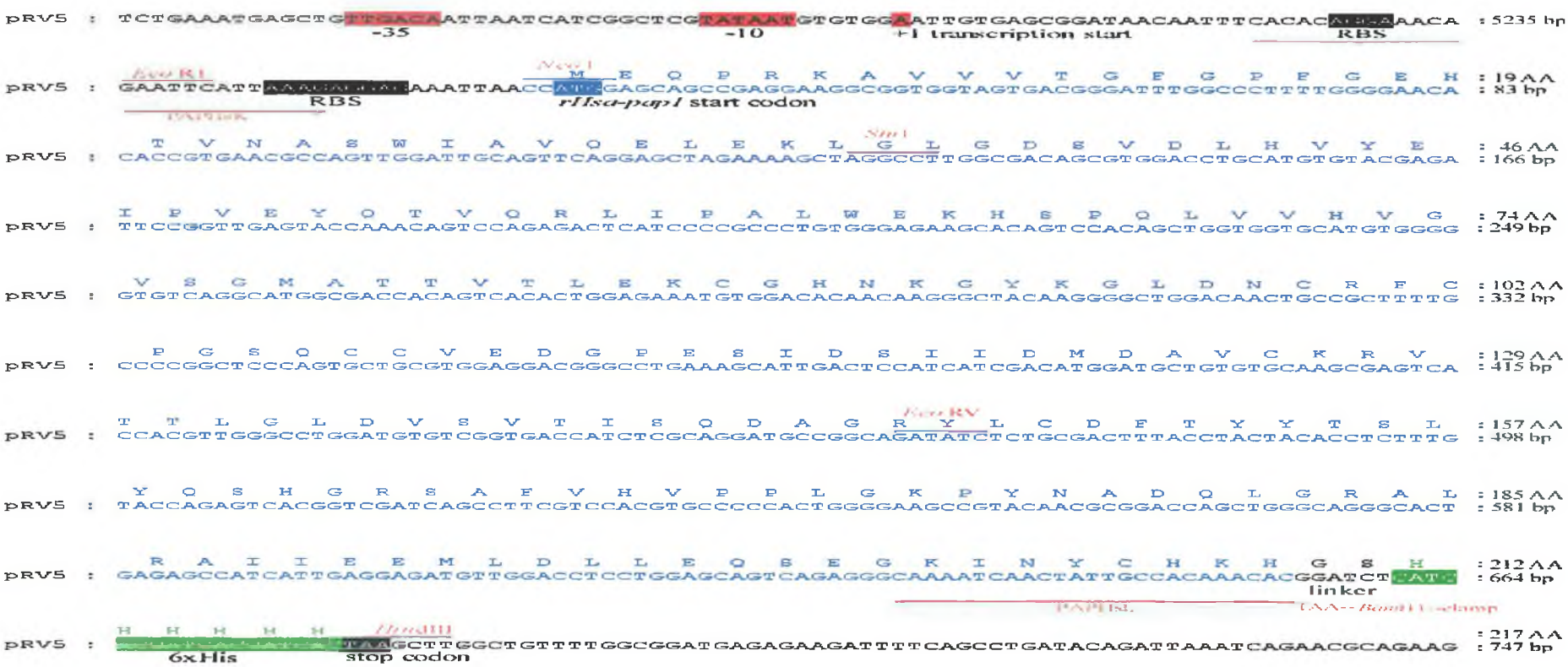

Figure 1.8 pRV5 sequence detail

The *rHsa-pap1* (blue) and P*tac* promoter (red) regions of pRV5 are shown in detail. The translation of *rHsa-pap1* is shown in blue above the ORF. The 6xHis tag sequence is shown in green, joined to *rHsa-pap1* by a Gly-Ser linker. Two ribosome binding sites (RBS, black) are shown. The first RBS upstream from the *rHsa-pap1* start codon was subcloned from pRV3 while the second RBS was present on pPC225 associated with the P*tac* promoter. Restriction enzymes and primers PAPHsK & PAPHsL are marked in red. Figure reproduced from P-R Vaas (PhD thesis, DCU, 2005) by permission.

1.4 Pyroglutamyl Peptidase II

Unlike PAPI, PAPII (EC 3.4.19.6) is a membrane-bound, zinc-dependent anchored ectoenzyme, mainly located in the CNS and is known as a highly specific enzyme for TRH and very closely related compounds. It belongs to clan MA, family M1, of the MEROPS database. (http:// Merops. Sanger. ac.uk) PAPII activities have been founded in rabbit, pig brain, rat brain and pituitary, bovine brain and human brain. It is a dimer of two identical 116 kDa subunits with a relatively large molecular mass (230kDa). PAPII has a broad pH optimum in the neutral range, and has its active site directed toward the extracellular space, where TRH would be located when involved in neurotransmission. PAPII is inhibited by chelating agents (e.g. 1,10-phenanthroline, 8-hydroxyquinoline and EDTA) but not by sulfhydryl blocking agents or the specific PAPI inhibitor, pGlu diazomethyl ketone. PAPII is primarily located in the CNS, where it is believed to play a predominant role and where it is almost exclusively associated with neurons, presumably on postsynaptic membranes (Gallagher *et al.*, 1997). Current evidence strongly indicates that PAPII is the principal enzyme responsible for terminating the actions of neuronally released TRH by removing the L-pGlu residue. (O'Connor and O'Cuinn 1985; Charli *et al.*, 1998) PAPII identified as metallopeptidase clan MA, family M1, as MEROPS database. Inhibition of PAPII specifically increases recovery of TRH released from brain tissue. (Charli *et al,* 1987)

The genes for rat and human PAPII were cloned (Schauder *et al.* 1994; Schomburg *et al.*, 1999) and the sequences of human and rat PAPII show a high degree of conservation (96% identical residues).

Northern blot analysis of the genomic sequence shows the highest transcript levels in the brain. The PAPII gene was localised to the long arm of human chromosome 12.

Southern analysis suggests that the gene is present as a single copy of DNA in many vertebrates and shows that PAPII is a specific neuropeptidase or neuromodulator that has been highly conserved among species. A serum form of PAPII has been reported, which has the same degree of specificity for TRH and identical biochemical characteristics as the membrane-bound form (Cummins and O'Connor 1998).

A study (Schmitmeier *et al.*, 2002) supports the hypothesis that both forms of PAP II are derived from the same gene, whereby the serum enzyme is generated by proteolytic cleavage of the membrane-bound form in the liver.

1.5 Serum Thyroliberinase (ST).

Serum Thyroliberinase (E.C 3.4.19.6) was partially purified from porcine, (Taylor *et al.*, 1978) and rat serum (Bauer *et al.*, 1979). Presently, the source of serum enzyme is unknown but earlier study by (Scharfman *et al.*, 1990;1991) points to the liver as the potential source. Serum enzyme was not inhibited by sulfhydryl-blocking reagents but inhibited by metal chelators, it shares many features with PAPII: it is optimally active at neutral pH, and has a molecular mass of 260 kDa. (Bauer *et al.*, 1981) have demonstrated that this enzyme cleaves the pyroglutamyl bond of TRH. However, it did not cleave other pGlu substrates such as LHRH, unlike PAPII. Hence researchers named this new enzyme "thyroliberinase". (Cummins and O'Connor 1998) It is assumed that PAPII and Thyroliberinase are products of the same gene. Serum enzyme may be

involved in regulatory mechanisms. Degradation of TRH by serum thyroliberinase, during its transport via the hypophyseal portal vasculature to the anterior pituitary, might represent a functional control element regulating TRH availability to receptors on target trophic cells. It may also play a role in body weight regulation (Cummins and O'Connor 1998). Schmitmeier *et al.* (2002) claimed fragment analysis of the serum ST revealed that the peptide sequences correspond to the cDNA deduced amino-acid sequences of the membrane-bound brain PAPII.

Table 1. 4 Comparison of Pyroglutamyl Peptidase types

Enzyme type	**PAP I**	**PAP II**	**Thyroliberinase**
Source	Mammalian and bacterial	Mammalian and bacterial	Mammalian
Type	Cysteine protease	Metalloproteases	
Location in body	Mainly in CNS	Primarily CNS and in other tissues	In liver
pH Optimum	6.5-8.5	7.0	7.0
Requirements	Thiol reducing agent (DTT),EDTA	Metal ion	TRH, Metal ion
Molecular mass	22-60 kDa	~230kDa	~260kDa
Specificity	Biologically active peptides, pGlu-X (X= amino acid)	TRH and TRH analogues	TRH
Inhibitors	Sulfhydryl-blocking reagents, pGCK.	Metal Chelators, CHPNA.	Metal Chelators, Thyroid Hormones.
Form	Monomeric	Dimeric	Unknown
Chromosome	19	12	Same as PAPII gene

1.6 PAPI wild type, and mutants F16Y, Y147F, as candidates for study

Proteases have a variety of important roles in the body. The use of proteases in biotechnology is an area of rapid growth and development. However, the uses of enzymes have some disadvantages in that they are easily denatured and inactivated and, therefore, lose their catalytic activity.

PAPI may have use in protein sequencing and/or in processing of peptides, and possibly in enzymatic peptide synthesis for the attachment of N-terminal pGlu residues. A thorough understanding of its stability and catalytic properties would be needed for any such applications.

The aim of this project is to study the recombinant human enzyme PAPI stability together with two of its mutants, F16Y and Y147F, which had previously been prepared by other workers.

In this thesis, PAPI was fully investigated with regards to its stability at elevated temperatures (Results; section 2.8), and in presence of organic solvents (Results; section 2.9). The kinetic parameters were also determined (Results; section 2.7). The stability and catalytic characteristics of PAPI mutants F16Y and Y147F were also investigated.

Chapter two

Materials and Methods

2.1 EQUIPMENT

Centrifugations were performed using an ALC Multispeed PK 121 bench centrifuge (r = 12cm, max speed 4300 rpm), or a Beckman centrifuge with rotor JA-14 (r = 10cm, max speed 14,000 rpm), or rotor JA-20 (r = 6 cm, max speed 20,000 rpm) (PAPI isolation). Gel electrophoresis was performed using a Biorad Mini Gel Box with ATTO vertical electrophoresis system and Biorad power pack 1000. Enzyme and protein assays were perfomed using a Perkin Elmer LS-50 Luminescence Spectrometer, Unicam UV2 uv/ visible spectrophotomer and a Labsystems Multiskan MS microplate reader

2.2 MATERIALS

E.coli strain (XL-10 Gold) containing plasmid pRV5 encoding PAP1 and the mutants F16Y and Y174F were gifts from the Laboratory of Dr B.O'Connor, School of Biotechnology and National Centre for Sensor Research, DCU.
Chemicals (reagent grade unless otherwise noted) used in these studies are listed below.

Bachem, (UK) Ltd.

Pyroglutamylaminomethylcoumarin (PGlu-AMC), Pyroglutamyl pentachlorophenol (Pyr-O-pcp)

Bio soft (Cambridge, UK) supplied the Enzfitter programme used for analysis of results.

Fisher Scientific UK Ltd., Loughborough, England.

Acetic acid glacial, acetone, acetonitrile HPLC grade, dimethylformamide HPLC grade (DMF), diaminoethanetetra-acetic acid (EDTA), ethanol 100% (v/v), glycerol, hydrochloric acid (HC1, 37% (v/v)), sodium chloride (NaCl), sodium hydroxide (NaOH), tetrahydrofuran HPLC Grade (THF), Tris-(hydroxymethyl) aminomethane (Tris).

Pierce Chemical Company, Illinois, USA.

BCA (Bicinchoninic acid) Protein Assay Kit, GelCode® Blue Stain Reagent.

Sigma-Aldrich Chemical Company (Tallaght, Dublin 24)

His-Select nickel affinity gel, 7-amino-4-methylcoumarin (AMC), Acrylamide/bis-Acrylamide 30% (w/v) solution, albumin bovine serum (BSA), ammonium persulphate, Bradford reagent, brilliant blue R, bromophenol blue, dialysis tubing (3.3cm x 2.1cm), dimethylsulphoxide HPLC grade (DMSO), DL-dithothreitol (DTT), Potassium dihydrogen phosphate (KH_2PO_4), Dipotassium phosphate (K_2HPO_4), sodium dodecyl sulfate (SDS), Sigma Marker™ low range (m.w. 6,500- 66,000), SigmaMarker™ wide range (m.w. 6,500-205,000) molecular weight markers, protein reagent (biuret), N, N,N',N' -tetramethylene-ethylenediamine (TEMED), tetracycline, Copper (II) sulphate, Ampicillin, IPTG, Imidazole, Glycine, EDTA, Dimethyl Suberimidate (DMS), N-Ethylmaleimide (NEM).

Oxoid (Basingstoke, Hampshire, UK)

Yeast Extract, Tryptone

METHODS

2.3 Purification

2.3.1 Preparation of Solutions:

Preparation of potassium phosphate buffer (50mM), pH 8.0

Dipotassium phosphate (K_2HPO_4, 50mM, 5.75g) was dissolved in distilled water, transferred to a 500 ml volumetric flask and made up to the mark with distilled water.

Potassium dihydrogen phosphate (KH_2PO_4, 50mM, 3.40g/500ml) was prepared similarly.

The acid component was used to adjust the pH of the base component to pH 8.0. The pH 8.0 solution was dispensed into a clean bottle, capped, and autoclaved at 121°C, 15 lb/in^2, 20 minutes.

Following cooling, it was stored at 4°C until required for use.

2.3.2 Production of LB (Luria-Bertani) Broth:

Three litre quantities of broth were prepared.

Ingredients per	Litre:
Tryptone	10g
Yeast Extract	5g
Sodium Chloride	10g

The above weighed ingredients were placed into a 1000ml conical flask. Approximately 800ml distilled water was added and the ingredients stirred, using a magnetic stirrer. The solution was transferred to a 1000ml volumetric flask and brought up to the mark with distilled water.

Aliquots (500ml) of the medium were transferred into six 1000ml conical flasks.

Bungs were inserted, tinfoil and autoclave tape placed around the necks of the conical flasks and the flasks autoclaved at 121°C, 15 lb/in^2, for 20 minutes. Following cooling, the media were stored at 4°C until required for use.

2.3.3 Inoculation of recombinant *E. coli* overnight culture.

Sterile LB broth (10mI) was dispensed aseptically into sterile universals

The appropriate volume of antibiotic (ampicillin: 100mg/ml stock, used at 10µl /10ml LB broth) was added aseptically into the broth.

One recombinant *E. coli* isolate was aseptically inoculated into each universal, which was labelled and incubated at 37°C overnight.

2.3.4 Production of Recombinant *E. coli* Suspension.

The appropriate quantity of antibiotic (ampicillin: 100mg /ml = 100µl /100ml LB medium) was aseptically added to LB growth broth. Broth (100ml) was aseptically inoculated with 3ml of overnight culture. The flasks were labelled and incubated at 37°C for a minimum of 5 hours. Growth of *E. coli* cells was monitored by aseptically taking samples and measuring the apparent absorbance at 600nm. Once the cells had entered exponential phase (A_{600} 0.3-0.5), production of the recombinant protein was induced by addition of 0.05M IPTG (500 µL of 10mM IPTG per 100ml broth). Cells were allowed to produce recombinant protein for 5 hours or overnight. Cells were then centrifuged, (6000rpm 10 min, 10cm radius). The supernatant was decanted off, and the cell pellet labelled and stored at 4°C until required.

2.3.5 Isolation and purification of recombinant PAP1.

Pellet washing and cell disruption steps.

If cells were frozen, they were removed from the freezer and thawed adequately. The pellet was re-suspended in 10ml of Potassium Phosphate Buffer (50mM, pH 8.0). If necessary, the solution was mixed by repeatedly drawing and discharging 10ml aliquots with the aid of a pi-pump and pipette.

Once the pellet had been totally re-suspended, the sample was sonicated (2.5 pulses.s^{-1}, 220 W, amplitude 40, for 15 min) to allow the periplasmic proteins to enter the buffer. The solution was kept on ice to prevent heating and to minimise proteolytic damage.

The lysate suspension was then centrifuged to remove the cells. The supernatant was retained in a separate universal.

2.3.6 Purification of recombinant protein via Ni^{2+} column chromatography

Ni^{2+} resin (1ml) was added to the universal containing protein lysate suspension from the previous stage, which was attached to a suitable shaking apparatus (The Belly Dancer, shaking value set at 7).

The Ni^{2+} resin was allowed to mix and interact with the recombinant protein for one hour before being carefully poured into a suitably sized clean column. The resin was allowed to sink to the bottom of the column. The remaining mixture was run through, taking care to ensure that the resin never ran dry. The run off was collected and labelled.

Potassium phosphate buffer (50mM, pH 8.0, 10ml) was run through the column three times; each time the run-off was collected and stored in a labelled container. Next, wash buffer (50mM potassium phosphate, pH 8.0, containing

20mM imidazole, 20ml) was run through the column three times; each time the run-off was collected and stored in a suitably labelled container.

Elution buffer (50mM potassium phosphate, pH 8.0, containing 200mM imidazole, 20ml) was then run through the column three times; each time the run-off was collected and stored in a labeled container. The required protein solution (containing native PAPI, or mutants F16Y and Y147F, activity) is generally located in fraction one or two.

2.4 SDS Polyacrylamide gel electrophoresis

The procedure used was based on that of Laemmli *et al* (1970)

2.4.1 Gel Preparation

Glass covers were cleaned, dried and assembled, ensuring seals were accurately placed.

Separating gel was prepared as outlined below:

Separating Gel

Distilled Water	1560µL
1.5M Tris-HCl, pH 8.8.	1625µL
Acrylamide/bis-acrylamide (30% /0. 8%, w/v)	3250µL
20% (w/v) SDS	32.5µL
10% (w/v) Ammonium persulphate.	32.5µL
TEMED.	3.25µL

The liquid gel was added slowly into the assembled gel apparatus, carefully and at an angle to prevent air bubble formation.

After pouring, the gel was layered with 70% v/v ethanol and allowed to set.

Once the gel was fully set, the ethanol was poured off and the stacking gel was prepared as outlined below and carefully added. It too was allowed to set.

Stacking Gel

Distilled Water	1538µL
0.5M Tris-HCl, pH 6.8.	625µ
Acrylamide/bis-acrylamide (30%/0.8%, w/v)	335µL
20% (w/v) SDS	12.5µL
10% (w/v) Ammonium persulphate.	12.5µL
TEMED.	2.5µL

Once the gel had set, it was stored at 4°C overnight to allow the acrylamide to cross-link fully and settle.

Running Buffer (5X) Preparation.

This buffer was prepared as a 5X concentrate as outlined below.

Tris Base	15g
Glycine	72g
SDS	5g

This mixture was diluted to 1 L with distilled water and its pH adjusted to 8.3.

2.4.2 Sample Buffer (5X) Preparation.

This buffer was prepared as a 5X concentrate as outlined below.

Distilled Water	1000µL
0.5M Tris-HC1	1250µL
Glycerol	5000µL
10% (w/v) SDS	2000µL
0.5% (w/v) Bromophenol Blue	250µL
2-Mercapoethanol.	500µL

Sample (25μL) was added to 5μL sample buffer, previously prepared as above in an Eppendorf tube.

The tube contents were then boiled for three minutes and allowed to cool.

Running of SDS PAGE

The clips and outer plastic seal were removed from the gel assembly and the gel was inserted, correctly orientated, into the housing.

The outer trough was half filled with running buffer and any entrapped air bubbles were removed. The inner trough was filled to the top with running buffer.

The prepared samples and markers were carefully injected into the different lanes, and the location of each sample noted. Molecular weight markers in the range of 205,000 – 6,500 daltons were used.

The top of the housing was attached and the electrodes connected to the power pack. The setting was adjusted to 25 mA constant current. The gel was allowed to run until the dye line reached the end of the gel.

Power was then turned off and the electrodes removed. The gel was carefully removed from the plates and placed into a large weighing boat. It was then flooded with distilled water to remove SDS. The weigh boat containing the gel was then placed on a Belly Dancer shaking device (at a rotating setting of 4) for ten minutes. This wash process was repeated three times.

After the wash, approximately 20ml of staining solution was added and the gel again placed on the Belly Dancer. If staining took place overnight, the weighing boat was covered with tinfoil to prevent evaporation.

Following staining, the gel was again washed with distilled water three times and after a period of time (24 hours) bands became clearly visible, and were examined and photographed.

Table 2.1. Molecular weights of Sigma marker proteins

Protein	**Mw (Da)**
Myosin	205,000
β-Galactosidase	116,000
Phosphorylase	97,000
Fructose-6-phosphate kinase	84,000
Albumin, Bovine Serum	66,000
Glutamic Dehydrogenase	55,000
Ovalbumin	45,000
Glyceraldehyde-3- phosphate Dehydrogenase	36,000
Carbonic Anhydrase	29,000
Trypsinogen	24,000
Trypsin Inhibitor	20,000
α -Lactalbumin	14,000

2.5 PROTEIN DETERMINATION

2.5.1 BCA Protein assay.

This procedure is based on a method of Smith et al. (1985).

Working BCA reagent was prepared by mixing one part copper sulphate with fifty parts bicinchoninic acid solution (both from BCA kit, Pierce Chemicals)

The working solution (200µL) was dispensed into wells of a 96-well microplate. Dialysed samples (25µL) from the nickel affinity column (Run through, Wash and Elution samples) were added in triplicate to wells.

A standard dilution range (0 - 2mg/ml) was constructed using 2mg/ml BSA stock solution.

Reaction was allowed to occur at 37°C for 30 minutes.

The resulting colour was then read at 560nm in an automatic plate reader.

From these data, a standard curve was plotted and used to calculate the protein concentration of the various unknown samples (Run through, Wash and Elution).

The concentration of PAPI were calculated using the equation:

$Y = 0.0012x$. (See Figure 3.2.1).

2.5.2 Biuret assay

The biuret assay was used to quantify the protein concentration in samples of 2-10mg/ml. Samples with a protein concentration > 10mg/ml were diluted with 50mM potassium phosphate, pH 8.0, to achieve a protein concentration within the above limits. The assay was performed on a 96 well microplate by combining enzyme sample (25µl) with biuret reagent (200µl) and incubating the mixture at 37°C for 30 minutes.

The absorbance of the resulting colour was read at 560nm on a plate reader.

A standard curve prepared in the range 2-10 mg/ml was used to calculate the protein concentration of the various samples.

The concentration of PAPI were calculated using the equation:

$Y = 0.0321x$. (See Figure 3.2.2).

2.6 ENZYME ASSAYS

2.6.1 Fluorescence Quantification of 7-amino-4-methyl-coumarin (AMC):

AMC Standard Curves

AMC (10mM; 17.52 mg/10ml) in 100% (v/v) DMSO was diluted to 100µM AMC using 50mM potassium phosphate, pH 8.0. This stock solution was stored in a dark glass container at 4°C to minimize any fluorescence. Lower AMC concentrations were prepared by dilution using 50mM potassium phosphate, pH 8.0 to form standard curves of 0-10µM. All curves were prepared as follows:

25µl 50mM potassium phosphate, pH 8.0

100µl AMC (concentration 0-10 µg/ml)

100µl 1.5M acetic acid

Fluorimetric analysis of these samples was achieved using a Perkin Elmer LS-50 fluorescence spectrometer set at excitation and emission wavelengths of 370nm and 440nm, respectively. The excitation slit width was maintained at 10nm while the emission slit width was adjusted according to the fluorescent intensity observed. Each concentration was assayed in triplicate and the mean fluorimetric intensity was calculated.

2.6.2 Quantitative fluorimetric measurement of PAP1 activity.

Substrate Preparation:

Stock solutions for use in the assay mixture were EDTA (200mM in distilled water), DTT (200mM in distilled water) and pGlu-AMC (10mM in potassium phosphate buffer, pH 8.0).

The working assay solution was prepared by dilution of the above stock solutions as follows.

DTT	50µL (final concentration 10mM)
EDTA	10µL (final concentration 2mM)
pGlu-AMC	100µL (final concentration 0.5mM)
Potassium phosphate buffer pH 8.0	825µL (final concentration 50mM)

A range of dilutions (0,10,20, - 100 %, v/v) of PAP1 was prepared from the 0.45 mg/ml PAPI stock solution.

Each enzyme dilution was placed into separate wells on the fluorometer microplate (25µL triplicate aliquots) and 100µL of the assay solution was then added to each well.

The microplate was incubated at 37°C for 30 minutes, after which time 100µL of 1.5M acetic acid was added to each well to arrest enzyme activity.

The plate was then inserted into the fluorometric plate reader and the fluorescent intensity was recorded for each enzyme concentration. The average of the triplicate was calculated for each dilution. Off scale readings were ignored.

The specific enzyme activity is calculated from Equation $Y = 0.0012x$.

One unit of activity is defined as the amount of enzyme which releases 1 nanomole of AMC per minute at 37°C (unit = $nmol.min^{-1}$)

From the standard curve: [AMC] in reaction sample is Flu/225µl $= X\ \mu M$

Reaction volume is 125×10^{-6} L $= X\ \mu mol.L^{-1}$

Therefore, AMC released $= \frac{X\,(125 \times 10^{-6})}{30\ min}\ \mu moles.min^{-1}$

Reaction uses 25×10^{-6} L enzyme

Therefore, AMC released by 1ml enzyme $= \frac{X\,(125 \times 10^{-6})}{30(25 \times 10^{-6})}\ \mu mol.min^{-1}$

$$= \frac{X\,(125 \times 10^{-6})(1000)}{30(25 \times 10^{-6})(1000)}\ nmol.min^{-1}.ml^{-1}$$

$$= \frac{X}{6}\ units.ml^{-1}$$

$$= \frac{Flu}{6\,m}\ units.ml^{-1} \quad (m = 37.46)$$

(m = slope of AMC standard curve)

When expressing units as µmoles.min^{-1}, this formula changes to

Flu /1000x6m units.ml^{-1}

2.6.3 Linearity of Pyroglutamyl Peptidase (PAPI) assay with respect to time.

Purified PAPI was diluted with 50mM potassium phosphate buffer, pH 8.0. The enzyme was assayed in triplicate for different times with 0.5mM pGlu-AMC as described in Section 2.6.2. A plot of fluorescence intensity versus time was constructed.

2.6.4 Linearity of Pyroglutamyl Peptidase (PAPI) assay with respect to enzyme concentration.

Purified PAPI was diluted with 50mM Potassium Phosphate buffer, pH 8.0, to achieve enzyme concentrations ranging from 0-100% v/v of the initial 0.45 mg/ml stock PAPI solution. The enzyme at these different concentrations was assayed in triplicate with 0.5mM pGlu-AMC as described in Section 2.6.2. All assays were carried out in triplicate. A plot of fluorescence intensity versus enzyme concentration (%) was constructed.

2.7 KINETIC ANALYSIS

2.7.1 K_m and V_{max} determination for PAPI with pGlu-AMC

pGlu-AMC (10mM in 5ml 100% DMSO) was diluted to 0.5mM with 50mM potassium phosphate buffer, pH 8.0. This solution was further diluted in buffer to a range of pGlu-AMC concentrations. Purified PAPI was assayed at each substrate concentration, as described in Section 2.6.2. The Michaelis-Menten constant (K_m) and maximum velocity value (V_{max}) were determined using Michaelis-Menten plot analysis (Enzfitter Programme, Biosoft, Cambridge, UK).

2.7.2 K_m and V_{max} determination for F16Y and Y147F with pGlu-AMC

A similar procedure to that in 2.7.1 above was followed for each of the mutants F16Yand Y174F`.

2.7.3 Active Site titration

This procedure is based on a method of Turk et al. (1993) using N-Ethylmaleimide instead of E-64. (NEM, 2mM stock solution dissolved in ultra-pure water, brought to l0ml final volume) was diluted to a 1mM working solution using ultra-pure water. Lower NEM concentrations 0-2.5µM were prepared by dilution of the working solution with ultra-pure water. A titration of activated PAPI with NEM was prepared. At each point, 25µl of purified PAPI (diluted 1/70 with 50mM potassium phosphate buffer, pH 8.0, was mixed with an equal volume of 0-2.5µM NEM, brought to a total volume of 100 µ1 with 50mM potassium phosphate buffer, pH 8.0, and incubated at 37°C for 15 minutes. Residual activity was then determined as described in Section 2.6.2. All assays were carried out in triplicate. A plot of fluorescent intensity versus NEM concentration was plotted and the operational molarity of PAPI determined

2.7.4 Active Site titration for F16Y and Y147F

A similar procedure to that in 2.7.3 above was followed for each of the mutants F16Yand Y147F.

2.8 TEMPERATURE STUDIES

2.8.1 Temperature profile

2.8.1.1 Temperature profile of PAPI (wild type).

Samples of purified PAPI (1ml volumes) at a concentration of 0.445mg/ml in 50mM potassium phosphate buffer pH 8.0 were incubated for 10 minutes over a range of temperatures between 30°C and 80°C. The samples were cooled rapidly on ice for 1 minute and remaining enzyme activity was assayed as described in Section 2.6.2. Blank controls were prepared, where 50mM potassium phosphate, pH 8.0, was substituted for enzyme PAPI. All assays were carried out in triplicate. A plot of % residual activity against temperature (°C) was constructed and the T_{50} (half-inactivation temperature) determined by inspection.

2.8.1.2 Temperature profile of F16Y and Y147F.

The temperature profiles of mutants F16Y and Y147F were determined similarly.

2.8.2 THERMOINACTIVATION

2.8.2.1 Thermoinactivation of PAPI (wild type)

PAPI samples at a concentration of 0.445mg/ml (i.e. standard assay concentration) in 50mM potassium phosphate buffer, pH 8.0, were maintained at a constant 60°C in a heated waterbath. At appropriate time intervals, aliquots were taken from the incubating solution, cooled rapidly on ice and the remaining PAPI activity assayed as described in Section 2.6.2. Blank controls were prepared, where 50mM potassium phosphate, pH 8.0, was substituted for PAPI. A plot of % residual activity versus time (minutes) was calculated from the initial

activity of the sample. Data were fitted to a first-order exponential decay using the Enzfitter programme (Bio soft, Cambridge, UK) in order to estimate the rate constant (k) and, hence, the half-life ($t_{1/2}$).

2.8.2.2 Thermoinactivation of F16Y and Y147F

A similar procedure was used for F16Y and Y174F mutants of PAPI, except that the incubation temperature was 70°C for both of these mutants.

2.9 ORGANOTOLERANCE STUDIES

2.9.1 PAPI Stability in organic solvent

The PAPI samples at a concentration of 0.445mg/ml in 50mM potassium phosphate buffer, pH 8.0, were incubated for 1 hour at room temperature with various solvents (ACN, DMF, DMSO, THF, methanol, ethanol) prepared in buffer to achieve final solvent concentrations ranging from 0-90% (v/v). The enzyme/solvent solution was adjusted to a final volume of 1ml with 50mM potassium phosphate pH 8.0. Blanks containing no enzyme were also set up for each solvent, at each solvent concentration. The samples were then assayed under normal conditions using the fluorimetric enzyme activity assay (Section 2.6.2). All assays were carried out in triplicate. A plot of activity versus solvent concentration (%) was constructed. Samples of enzyme/solvent were made up as follows:

Table 2.2: Preparation of enzyme/solvent solution (v/v)

% Solvent (v/v)	Vol. of Solvent (µl)	Vol. of Buffer (µl)	Vol. of Enzyme (µl)
0	0	900	100
10	100	800	100
20	200	700	100
30	300	600	100
40	400	500	100
50	500	400	100
60	600	300	100
70	700	200	100
80	800	100	100
90	900	0	100

2.10 CHEMICAL MODIFICATION

2.10.1 Enzyme Activity of PAP1 modified with dimethyl suberimidate (DMS).

The modification protocol was based on that of de Renobales and Welch (1980). Purified PAPI was diluted 1/50 with 50 mM potassium phosphate, pH 8.0 (3ml). A stock solution of DMS (2.5mg/ml) was diluted 1/50 in 50mM potassium phosphate buffer, pH 8.0 (3ml). DMS was mixed with PAPI (6 ml total volume); control PAPI and PAPI/DMS were incubated at room temperature for 30 minutes and a thermal profile was determined for each of PAPI and PAPI/DMS, as in Section 2.8.1.1. A plot of % residual activity versus temperatures was plotted for each of PAPI and PAPI/DMS.

2.11 EFFECT OF ADDITIVES ON PAPI ACTIVITY

2.11.1 Effect of ammonium sulphate on PAPI activity

Purified PAPI (0.45mg/ml) was diluted 1/50 with 50 mM potassium phosphate, pH 8.0, (0.009mg/ml final concentration). A stock solution of $(NH_4)_2SO_4$ (0.5 M final concentration) was prepared and was mixed (1:1 v/v) with PAP1. A thermal profile was determined as in Section 2.8.1.1. A plot of % residual activity versus temperatures was plotted for each of PAPI and PAPI/$(NH_4)_2SO_4$.

2.11.2 Effect of trehalose and xylitol on the enzyme PAPI

Purified PAPI (0.45mg/ml) was diluted 1/50 with 50 mM potassium phosphate, pH 8.0. Trehalose (0.5 M final concentration) was prepared in potassium phosphate buffer, pH 8.0. Trehalose was mixed with PAP1 (1:1 v/v) and subjected to a thermal profile, as described in Section 2.8.1.1, followed by

measurement of residual activity (Section 2.6.2). The effect of 0.5M xylitol on PAP1 stability was determined similarly.

2.11.3 Effect of 10 % and 50% v/v glycerol on PAP1 stability.

Purified PAPI was diluted 1/50 with 50 mM potassium phosphate pH 8.0. Glycerol (10% v/v and 50% v/v final concentrations) was prepared in potassium phosphate buffer pH 8.0. Glycerol was mixed with PAPI (1:1 v/v). Control PAPI and PAPI with 10% v/v and 50% v/v glycerol were each subjected to thermal profile (Section 2.8.1.1) procedures.

Chapter Three: RESULTS

Purification of Pyroglutamyl Peptidase PAP1 and of mutants F16Y and Y147F

3.0 RESULTS – PYROGLUTAMYL PEPTIDASE I (PAPI)

The assay for PAPI activity is a fluorescent one. The quantity of AMC released is an index of enzyme activity. All of the graphs illustrate data points that represent the average of triplicate fluorescence intensity or absorbance readings (n = 3), minus the blank measurement.

3.1 ASSAY DEVELOPMENT

3.1.1 AMC Standard Curves

AMC standard curves were prepared in the absence of pGlu-AMC as outlined in Section 2.6.1. Plots of fluorescence intensity versus AMC concentration (micromol) were constructed and the slope of the lines calculated. Figure 3.1.1 represents a typical AMC standard curve (excitation 370nm, slit width 10nm; emission 440nm, slit width 2.5nm). The effect on fluorescence intensity of including crude and purified PAPI and PAPI with organic solvent in the assay mixture was observed. Figures 3.1.3 and 3.1.2 are plots of fluorescence intensity versus AMC concentration (micromol) for each curve.

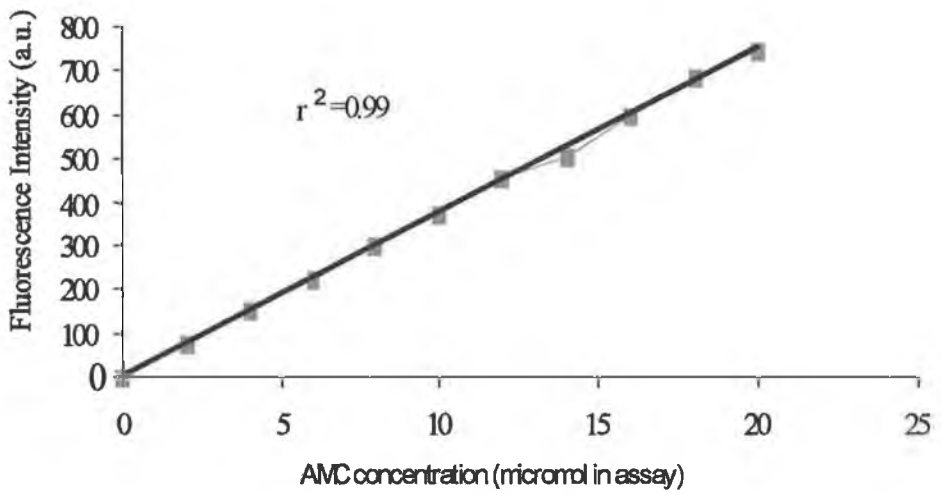

Figure 3.1.1. AMC Standard Curve

Plot of fluorescence intensity (excitation 370nm, slit width 10nm; emission 440nm, slit width 2.5nm) versus free AMC concentration (micromol) in buffer. a.u = arbitrary units as indicated on Perkin Elmer LS-50 instrument (Division of a.u. by the slope of the line (37.46) converts fluorescence values to μmol AMC)

3.1.2 AMC standard curve with 10% (v/v) DMF

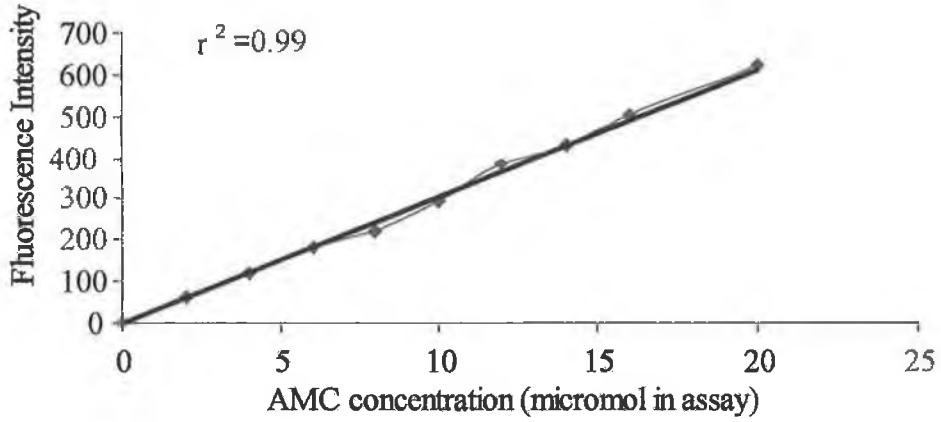

Figure 3.1.2: AMC standard curve with 10% (v/v) DMF

Plot of fluorescence intensity (excitation 370nm, slit width 10nm; emission 440nm, slit width 2.5nm) versus AMC concentration in 10% v/v DMF (Division of a.u. by the slope of the line (30.79) converts fluorescence values to µmol AMC)

3.1.3 AMC Standard Curve for crude and purified PAP1

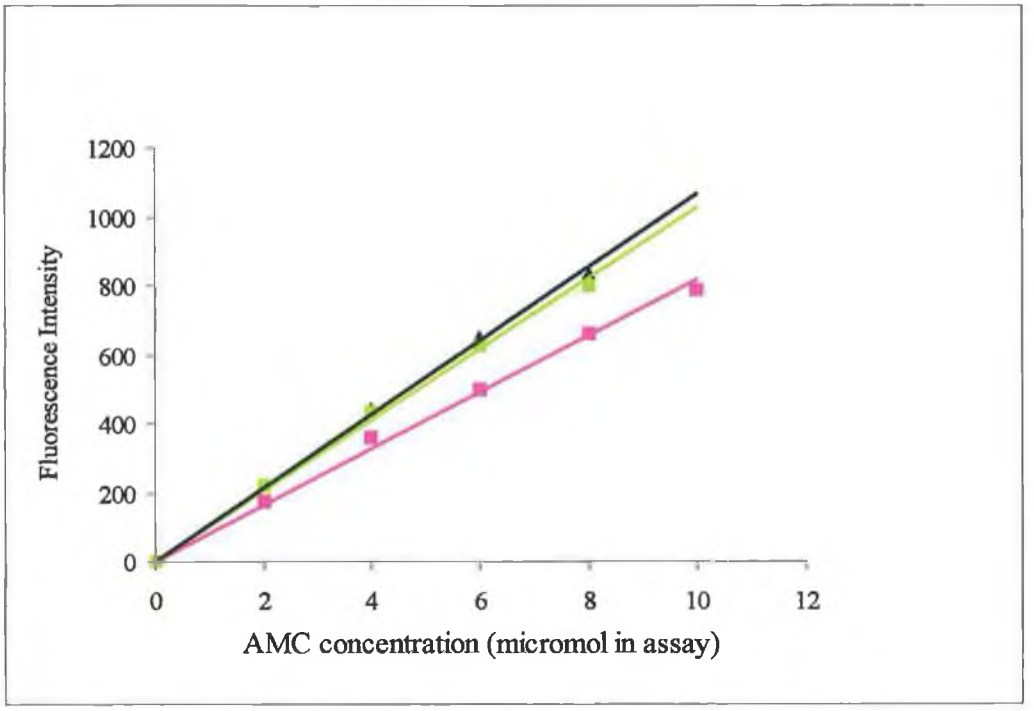

Figure 3.1.3. AMC Standard Curve for crude and purified PAP1

Plot of fluorescence intensity (excitation 370nm, slit width 10nm; emission 440nm, slit width, 2.5nm) versus free AMC concentration (micromol), in buffer (▲). The curves for crude (■) and purified PAPI preparation (■) are also shown. Division of a.u. by the slopes of the lines (X and Y for crude and pure PAPI, respectively) converts fluorescence values to μmol AMC.

3.1.4 AMC Standard Curve showing effects of culture medium and of imidazole

Plots of fluorescence intensity versus micromol AMC were also constructed for buffer potassium phosphate, pH 8.0, imidazole and bacterial culture medium. The slopes of the lines were similarly calculated (Figure 3.1.4). These AMC standard curves allow one to relate fluorescence intensity of pGlu-AMC assay mixtures to concentration of AMC product under all the conditions employed in this research

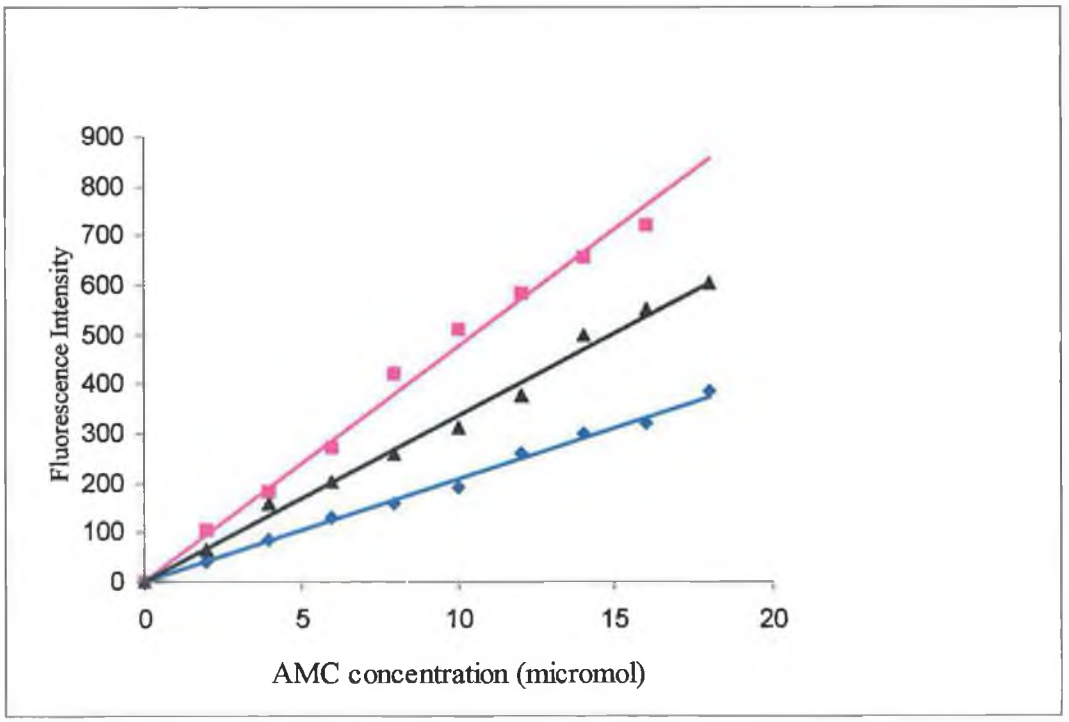

Figure 3.1.4. AMC Standard Curve showing effects of culture medium and of imidazole

Plot of fluorescence intensity (excitation 370nm, slit width 10nm; emission 440nm, slit width 2.5nm) versus free AMC concentration (micromol), for culture medium (♦), imidazole (■), and purified PAPI (▲). Division of a.u. by the slopes of the lines (X, Y and Z for medium, imidazole and pure PAPI, respectively) converts fluorescence values to μmol AMC.

Table 3.1. slopes of AMC standard curves

Sample	r^2	Slope
50mM potassium phosphate pH 8.0 buffer	0.99	37.46
200mM Imidazole	0.99	20.75
(LB) Culture medium	0.99	47.58
Crude PAPI	0.99	81.49
Purified PAPI	0.99	102.78

3.1.5 Linearity of PAPI assay with respect to time

The enzyme's activity was assayed using the substrate pGlu-AMC. The assay was optimised with respect to time as described in Section 2.3.6. A linear graph ($r^2 = 0.99$) for change in fluorescence versus time was observed Figure (3.1.5) up to 30 minutes.

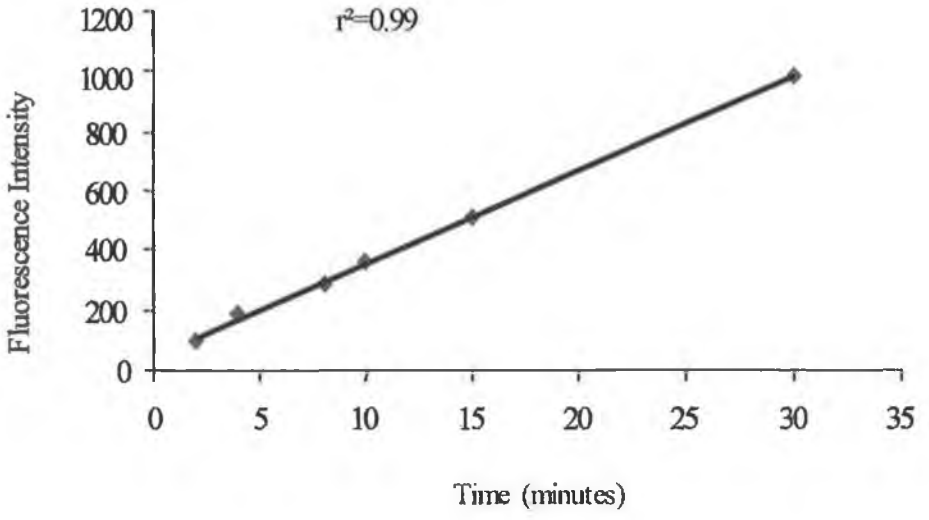

Figure 3.1.5: A graph of the change in fluorescence intensity (excitation 370nm, slit width 10nm; emission 440nm, slit width 2.5nm) versus time (minutes) for PAP1 activity in 50mM potassium phosphate buffer, pH 8.0, to optimise the time of assay.

3.1.6 Linearity of assay with respect to PAPI concentration

The assay was optimized with respect to enzyme concentration and examined as outlined in Section 2.6.4. Figure 3.1.6 illustrates that the assay is linear (r^2=0.99) for change in fluorescence versus enzyme concentration.

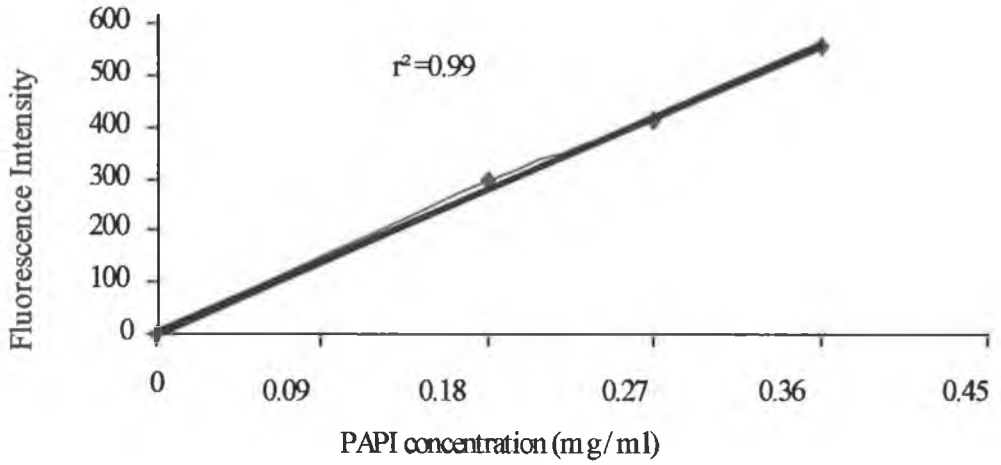

Figure 3.1.6: A graph of the change in fluorescence intensity (excitation 370nm, slit width 10nm; emission 440nm, slit width 2.5nm) versus concentration of PAPI for enzyme's activity in 50mM potassium phosphate buffer, pH 8.0. The protein concentration representing 100% activity is 0.45 mg/ml.

3.2 PROTEIN DETERMINATION

Bovine serum albumin (BSA) standard curves were prepared, as outlined in Section 2.5. Plots of protein absorbance at 560nm versus BSA concentration (mg/ml) are shown in Figure 3.2.1 and 3.2.2 for standard BCA and Biuret assays. PAPI concentration was estimated to be 0.45mg/ml in the purified sample.

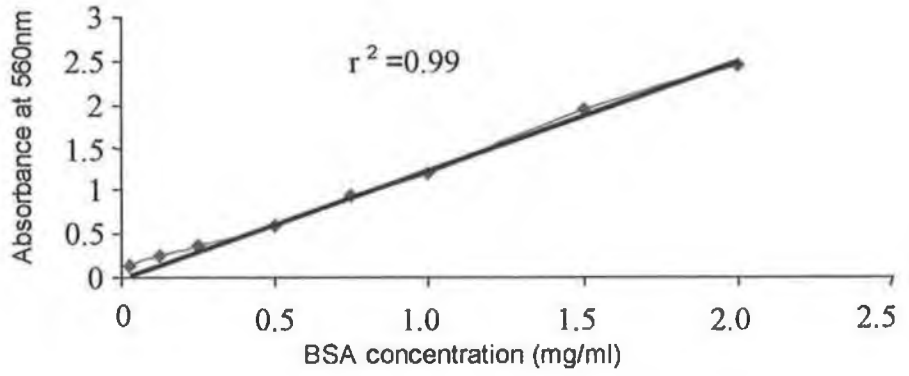

Figure 3.2.1: BCA Protein Standard Curve

Plot of absorbance at 560nm versus bovine serum albumin (BSA) concentration (mg/ml).

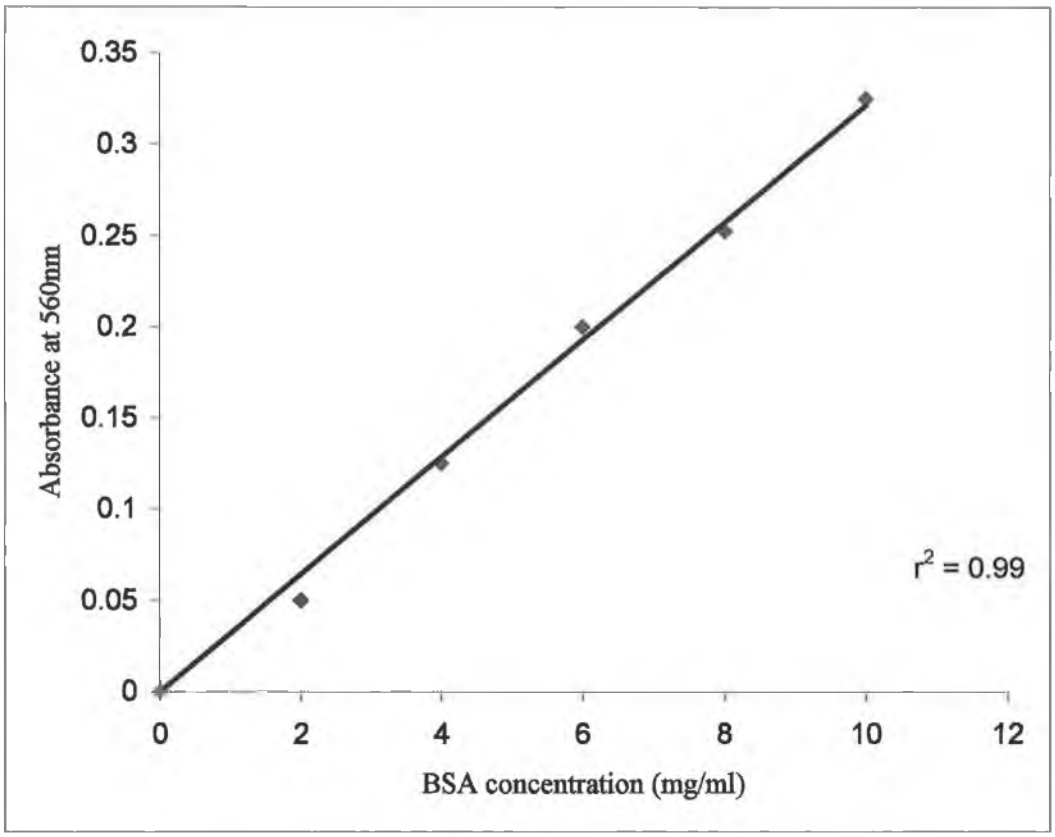

Figure 3.2.2. Biuret Protein Standard Curve

Plot of absorbance at 560nm versus protein concentration (mg/ml) using the Biuret method

3.3 PURIFICATION

3.3.1 Purification of pyroglutamyl peptidase (PAP1)

Pyroglutamyl peptide (PAPI) was over expressed in *E. coli* grown in 3 litres of LB culture medium containing the antibiotic ampicilin (Section 2.3).

Recombinant protein production was induced by IPTG addition to the broth at the exponential phase of the *E. coli* growth cycle (A_{600} 0.3-0.6) and expression of the protein was allowed to continue for 5 hours. The culture was then centrifuged at 6000 rpm for 10 minutes using a Beckman centrifuge JA-14 rotor (r = 10 cm). The sample was resuspended in 10ml 50mM potassium phosphate buffer, pH 8.0. The protein was released from the cell by sonication and subsequently purified from the lysate by nickel affinity chromatography as described in Section 3.3.3.

A PAPI activity peak was observed and the elution profile from this column is shown in Figure 3.3.1. PAPI containing fractions were combined, mixed with 40% v/v final concentration glycerol and stored at 4°C until required. A similar expression and purification technique was used for both mutants, F16Y and Y147F.

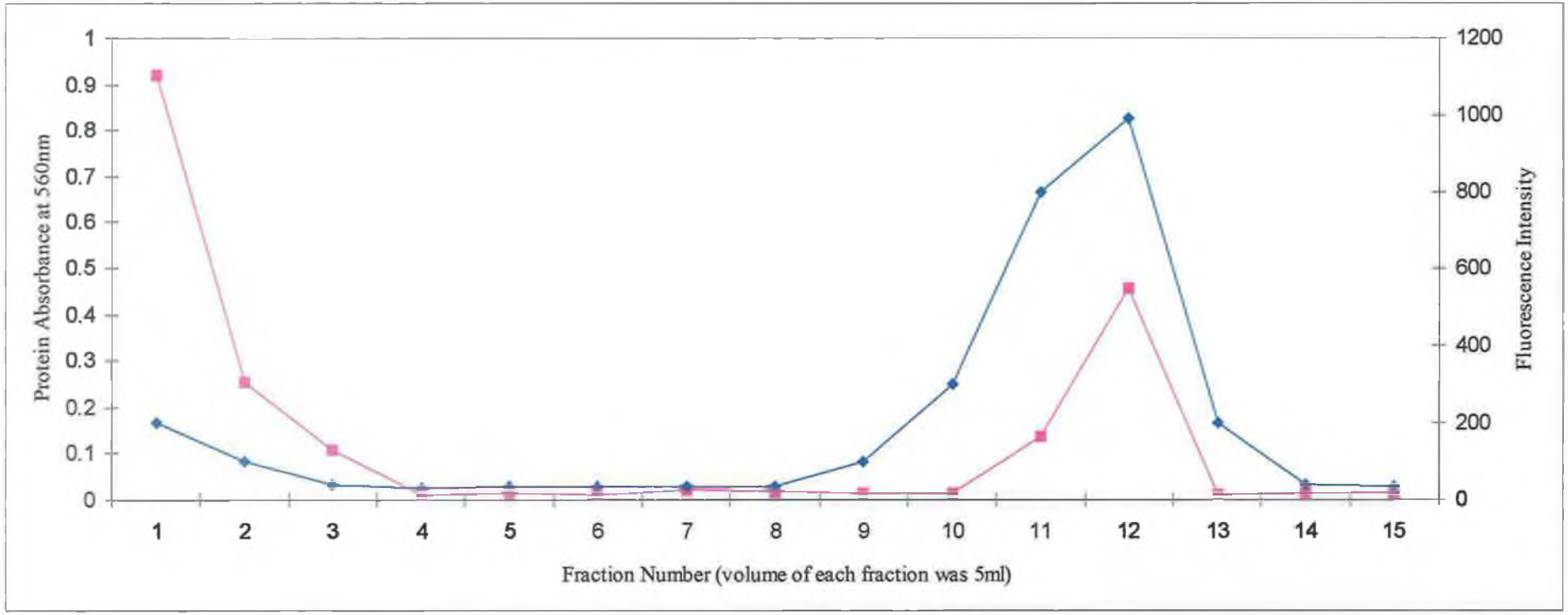

Figure 3.3.1: Nickel affinity purification of pyroglutamyl peptidase PAPI (Fraction 11-12). Fluorescence intensity (excitation 370nm, slit width 10nm; emission 440nm, slit width, 2.5nm) indicates PAPI activity. (■) Protein absorbance, (♦) AMC Fluorescence.

The following table shows the purification data for Pyroglutamyl Peptidase I. Activity (U) is defined as nanomol/min/ml.

Purification Table 3.2:

Stage of operation	Total protein conc (mg)	Total Activity ($U.mg^{-1}$)	Recovery (%)	Specific Activity ($U.mg^{-1}$)	Purification Factor
Resuspended cells	19800	1215	100	0.06	1
Ni^{2+} column	2250	765	63	0.34	5.67

3.3.2 Purification of mutants F16Y and Y147F.

Similar expression and purification techniques were used for both mutant F16Y and Y147F (1.5 litres *E.coli* culture grown in LB medium, as described in Section 3.2). F16Y and Y147F activity peaks were observed and the elution profiles from nickel affinity chromatography columns are shown in Figure 3.3.2.A and Figure 3.3.2.B, respectively. Mutant fractions were combined, mixed with glycerol 40% (v/v) final concentration and stored at 4°C until required.

A: Purification of F16Y mutant

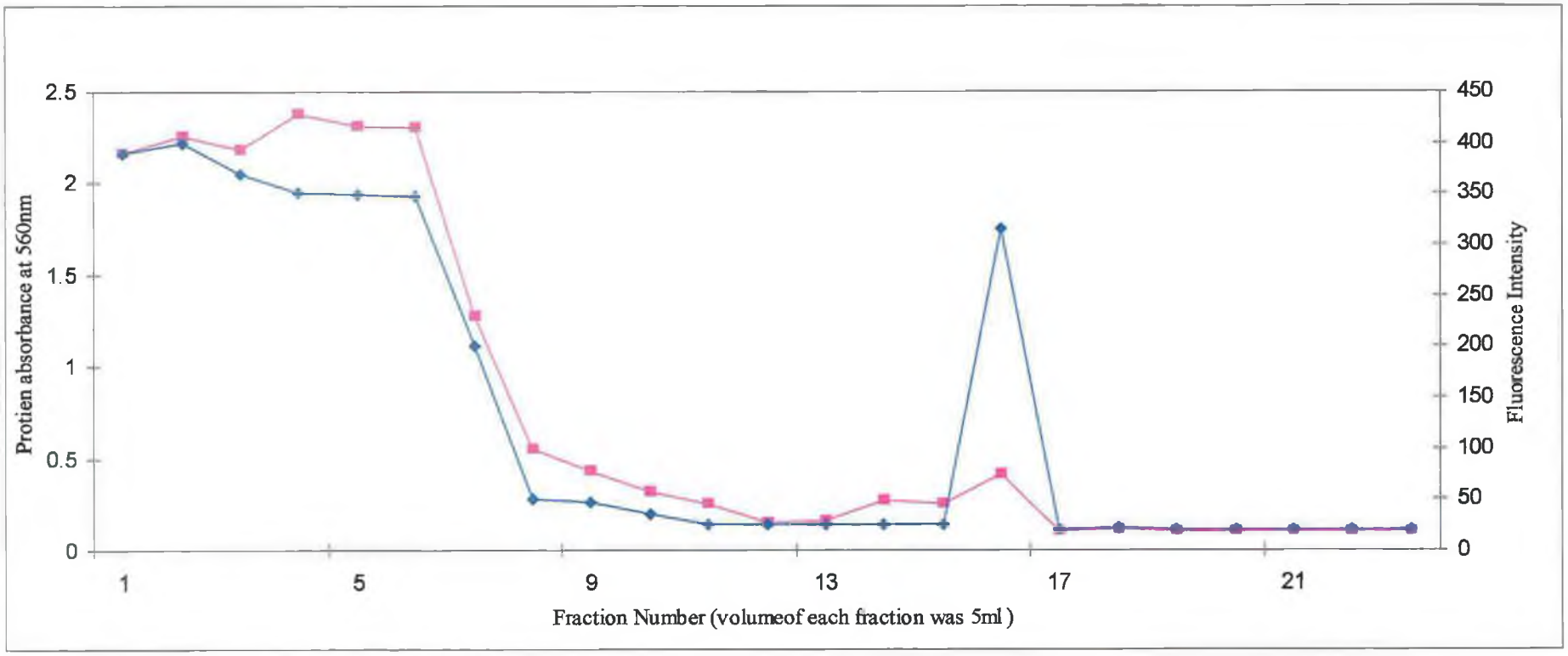

Figure 3.3.2.A Nickel affinity purification of mutant F16Y (Fraction 16). Fluorescence intensity (♦) (excitation 370nm, slit width 10nm; emission 440nm, slit width, 2.5nm) indicates F16Y activity. (■) Protein concentration. Specific activity of purified F16Y was 0.008 U/mg; U is defined as nanomoles/min/ml.

B: Purification of Y147F mutant

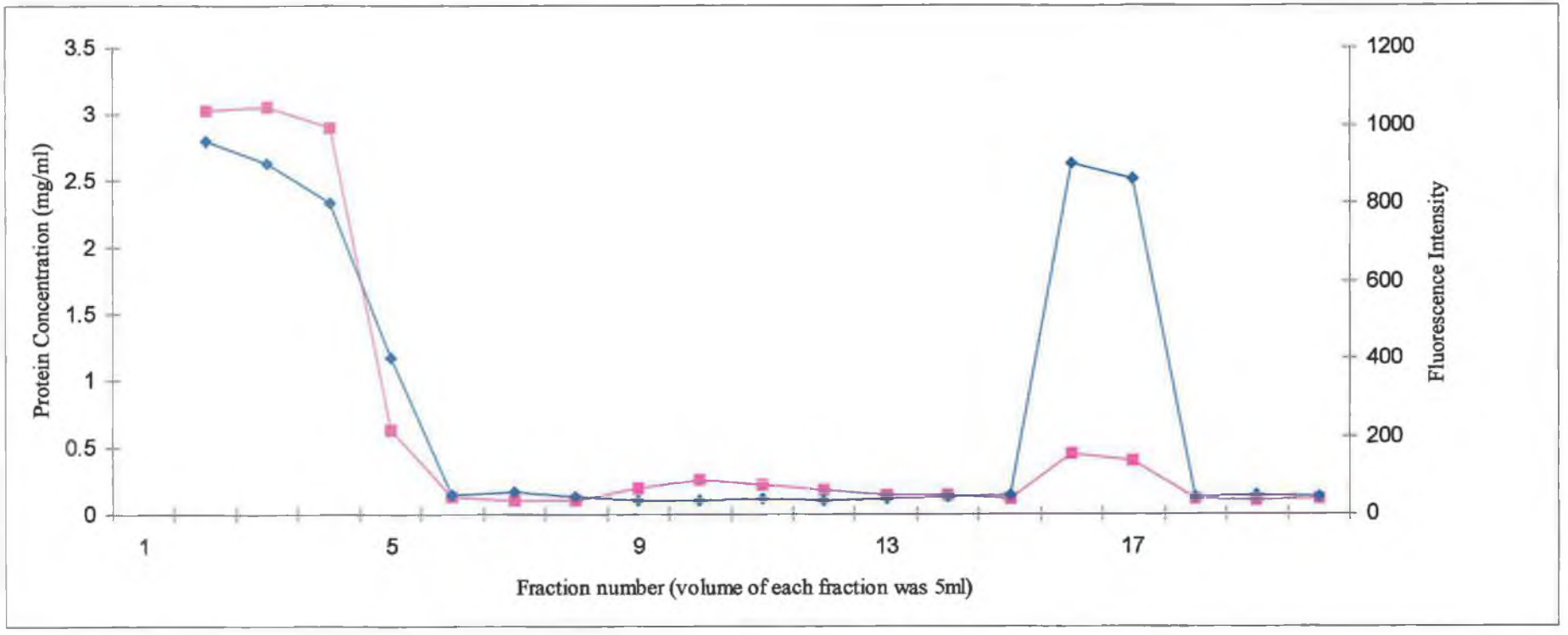

Figure 3.3.2.B: Nickel affinity purification of mutant enzyme Y147F (Fraction 16-17). Fluorescence intensity (♦); (excitation 370nm, slit width 10nm; emission 440nm, slit width, 2.5nm) indicates Y147F activity. (■) Protein concentration.

Specific activity of purified Y147F was 0.83 U/mg; U is defined as nanomoles/min/ml.

3.3.3 SDS (Polyacrylamide Gel Electrophoresis

SDS polyacrylamide gel electrophoresis was performed, as described in section 2.4. The stained gel showed that pyroglutamyl peptidase I (30µl per well) migrated as a single band on SDS-PAGE with a relative molecular weight range of 23-24 kDa; see Figure 3.3.3.

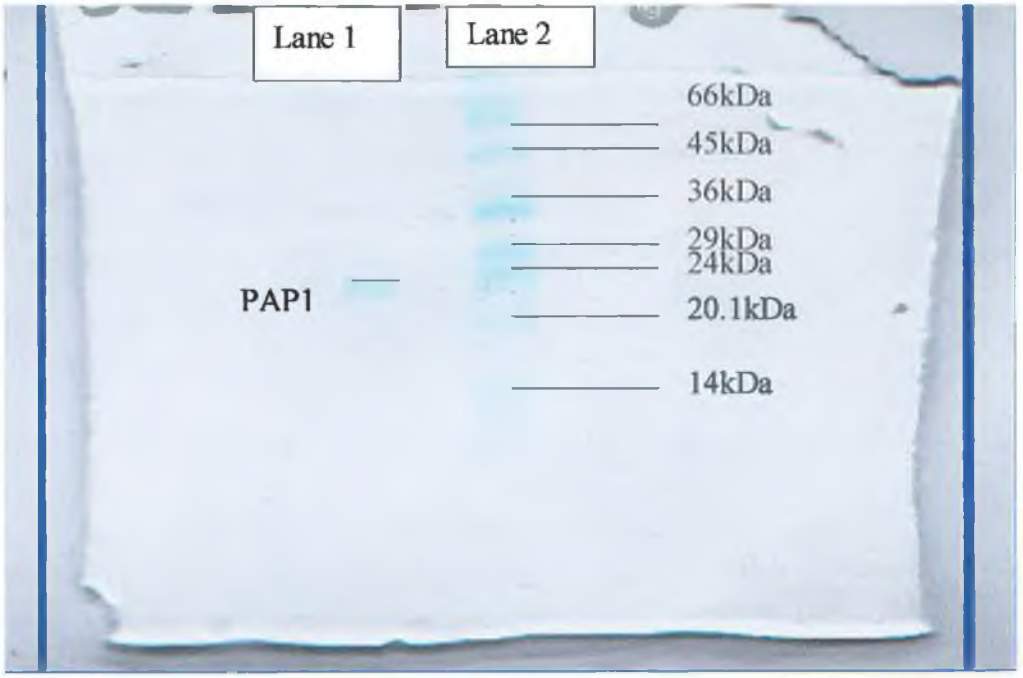

Figure 3.3.3: SDS-PAGE of PAPI.

The molecular weight low range markers on the right (lane2) were (from top) bovine serum albumin (66 kDa), egg albumin (45 kDa), glyceraldehyde-3-phosphate dehydrogenase (36 kDa), carbonic anhydrase (29 kDa), bovine trypsinogen (24 kDa), soybean trypsin inhibitor (20.1 kDa) and alpha-lactalbumin,bovine milk (14,200). The wells between the sample and molecular weight markers were empty.

F16Y and Y147F each give a single band in a similar location.

Chapter Four : RESULTS

Studies on Pyroglutamyl Peptidase (PAPI)

4.0 STUDIES ON PYROGLUTAMYL PEPTIDASE (PAPI)

4.1 Introduction

Pyroglutamyl peptidase (PAPI) is an omega exopeptidase, which cleaves pyroglutamic acid from the N-terminus of peptides. The amide substrate, pGlu-AMC when hydrolyzed by PAPI releases AMC, which is monitored fluorometrically, making this a sensitive and suitable substrate.

Recombinant PAPI was investigated with regards to temperature and solvent stability prior to chemical modification of the enzyme. A temperature profile was determined and the apparent half-inactivation temperature (T_{50}) estimated. The effect of organic solvents on PAPI was investigated with a range of solvents at various concentrations and the half-inactivation concentration (C_{50}) determined for DMSO and methanol. The steady state kinetics of wild type and mutants F16Y and Y147Y were studied.

4.2 PAPI KINETICS

4.2.1 Active Site Titration of PAPI

Active pyroglutamyl aminopeptidase (0.45mg/ml stock concentration diluted 1/50 for assay) was determined, as described in section 2.7.3. Figure illustrates the titration of PAPI with NEM. The concentration of active enzyme was determined from this plot, where the intercept on the x-axis (best line fit) is equal to the concentration of active enzyme. The enzyme was determined to have an operational molarity of 0.8μM.

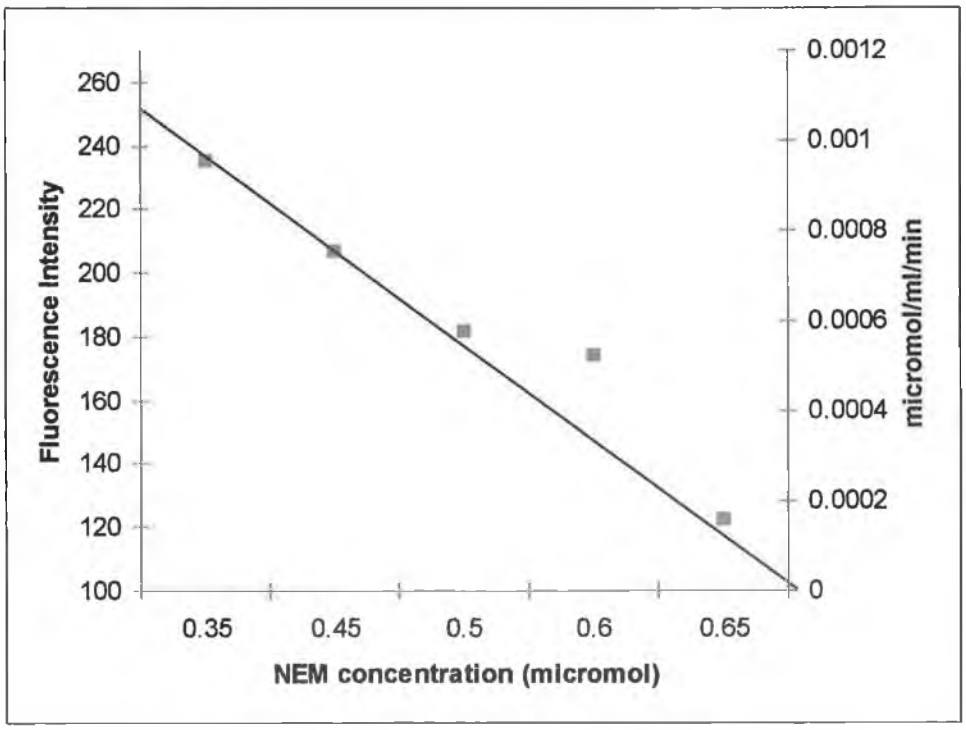

Figure 4.2.1: Titration of PAPI with NEM

Plot of Fluorescent Intensity (excitation 370nm, slit width 10nm; emission 440nm, slit width 2.5nm) and activity (μmol/ml/min) versus NEM concentration (μM) ("micromol" refers to fluorescence intensity converted to micromol AMC).

4.2.2 K_m , V_{max} and k_{cat} determination for pGlu-AMC with PAPI (wild type)

Michaelis-Menten kinetics were determined for native PAPI as described in Section 2.7.1. The enzyme displayed normal Michaelis-Menten kinetics, giving a K_m value of 0.132 ± 0.024 mM, V_{max} = 0.0013 ± 0.0001 μmol.ml^{-1}.min^{-1} (Enzfitter: Biosoft, Cambridge, UK). Values of k_{cat}/K_m and k_{cat} were calculated from the equation $V_{max}/[E] = k_{cat}$, where [E] is the active enzyme concentration (Section 4.2.1 above): k_{cat} was 2.68x10^{-5} (s^{-1}), while k_{cat}/K_m was 0.202 (s^{-1}.M^{-1}).

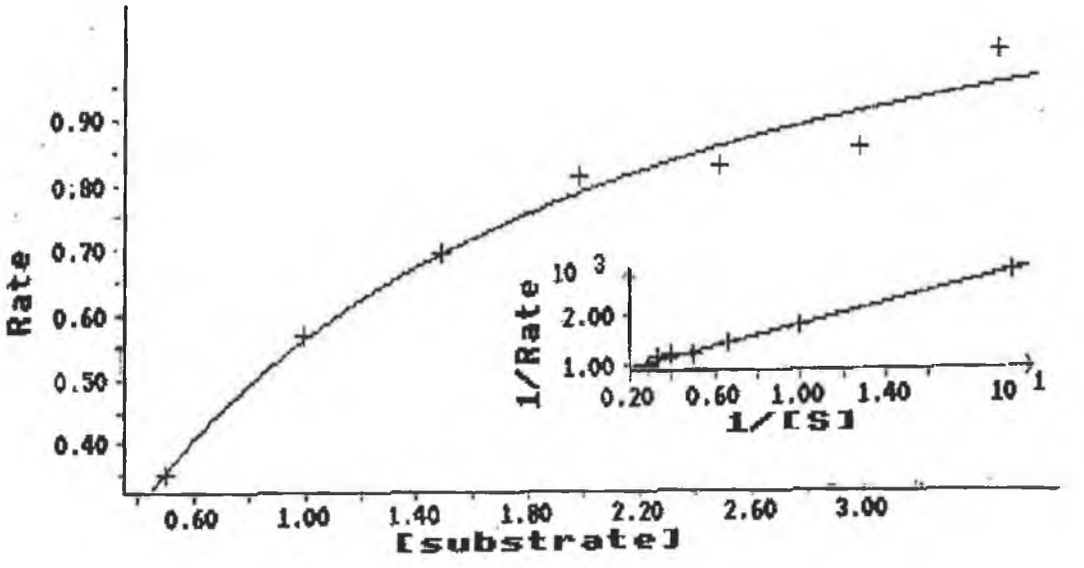

Figure 4.2.2: Michaelis-Menten plot for PAPI.

[Substrate] = mM pGlu-AMC.

Rate = arbitrary fluorescence units (multiply by flu/6000 m, where m = 37.46, to convert to μmol AMC/min using a standard curve (Figure 3.1.1).

Inset : ln plot of the same data.

4.3 TEMPERATURE STUDIES

4.3.1 Temperature Profile

A temperature profile of PAPI was performed at 30°C, 40°C, 50°C, 60°C, 70°C and 80°C, as described in Section 2.8.1.1. The enzyme was incubated at the appropriate temperature for 10 minutes in a waterbath.

The temperature profile (Figure 4.3.1) showed that the PAPI did not retain full activity above 45°C. The half-inactivation temperature (T_{50}, value where observed activity was 50% of maximal) was estimated by inspection to be 60°C ± 1°C.

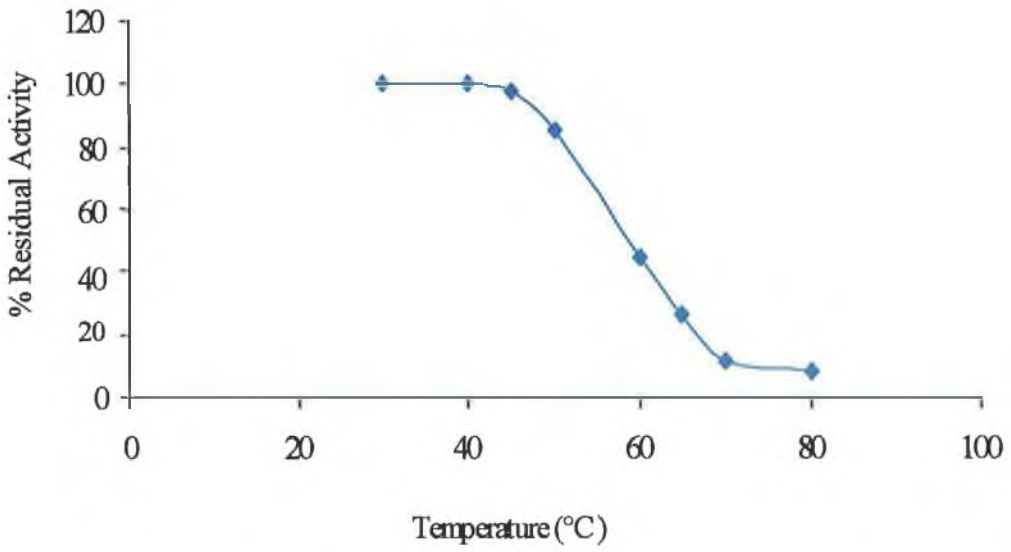

Figure 4.3.1 : A temperature profile of PAPI.

Plot of % residual activity versus temperature (°C). Activity is represented as a percentage of the 30°C value.

4.3.2 PAPI thermoinactivation assay

The kinetics of thermoinactivation of PAPI were studied at 60 °C (T_{50}) over a 45 minute period as described in Section 2.8.2.1. The results of % residual activity versus time plots were analysed using the computer programme, Enzfitter (Biosoft, Cambridge, UK). Data were fitted to the first order exponential decay equation and visual observation shows that the fit is a good one.

The *k* value was 0.046 ± 0.002 min^{-1} and half-life ($t_{1/2}$) was calculated to be 15 minutes.

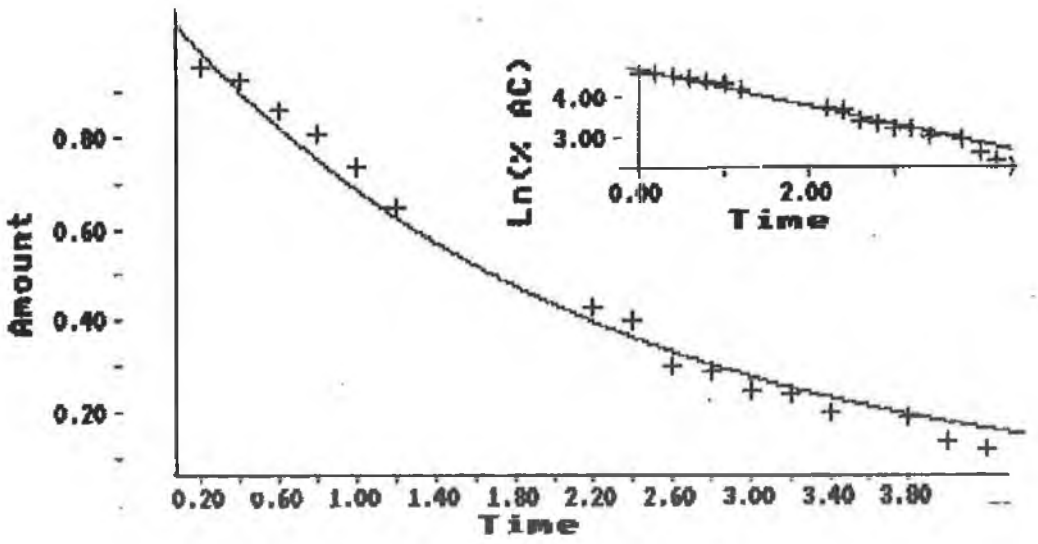

Figure 4.3.2: Thermoinactivaction of PAPI at 60 °C.

Plot of % residual activity versus time (minutes). Residual activity is represented as a percentage of the t = 0 value. "Amount" = % residual activity.

Inset: plot of ln (Activity) versus time.

4.4 ORGANOTOLERANCE

4.4.1 Solvent stability studies

The organotolerance of native PAPI was determined using the substrates pGlu-AMC in potassium phosphate buffer, pH 8.0, as described in Section 2.9.1.1, for the following water-miscible organic solvents: DMF, DMSO, THF, ACN, acetone, methanol and ethanol. The effects of these solvents on PAPI activity are illustrated in Figures 4.4.4.1 to 4.4.4.3, in which % residual activity versus concentration of solvent is plotted. The half-inactivation concentration (C_{50}) was determined where possible. Methanol and DMSO were the least injurious solvents for PAPI activity.

Table 4.1.

C_{50} Values for PAPI in organic solvents

Solvent	C_{50}
Dimethyl sulphoxide	10 ± 0.5 (%, v/v)
Methanol	12 ± 0.5 (%, v/v)

4.4.1.1 Tetrahydrofuran (THF) and dimethyl formamide (DMF)

This solvent had a notably adverse effect on PAPI activity. It can be see from the results that the activity of the enzyme declined to about 10% of aqueous activity at 10% (v/v) THF and remained at this low level at higher THF concentrations. No recovery or stimulation of activity was observed at any THF concentration. The results of DMF with PAPI were similar to those with THF. At 10% (v/v) DMF, activity was 26% of that in aqueous buffer, while at 20% (v/v) DMF the

activity was 10%. Above 20% (v/v), only a flat baseline activity (<10%) of PAP1 was apparent.

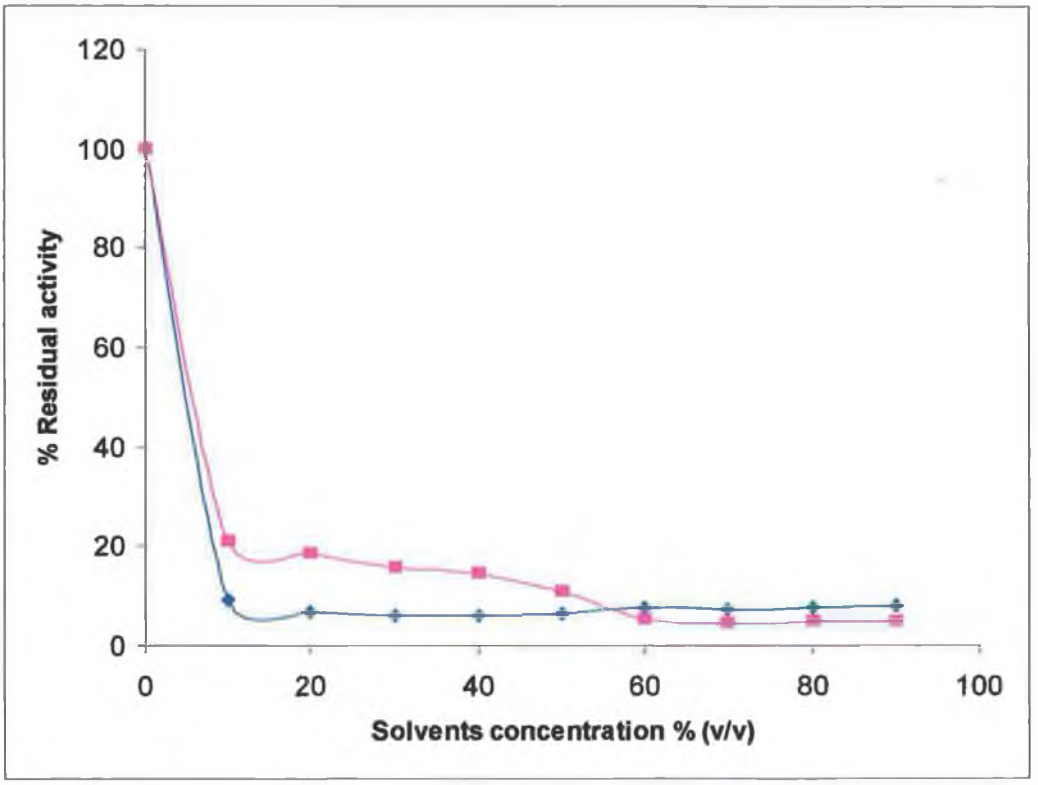

Figure 4.4.1.1 **: Residual PAP1 activity (%) versus (♦)THF and (■)DMF** concentration (%, v/v)

4.4.1.2 Acetonitrile and acetone

With ACN, reduced PAPI activity was observed at 10% (v/v) solvent concentration, where the residual activity was 21% of that in aqueous buffer. Activity ranged from 10-20% at 10-50% v/v ACN and from 60%-90% (v/v) concentration, PAPI activity was 10% or less.

The results with PAPI were quite similar to those with other solvents. At 10% (v/v) concentration, residual activity was 33% and above 50% (v/v) concentration, no significant PAPI activity remained.

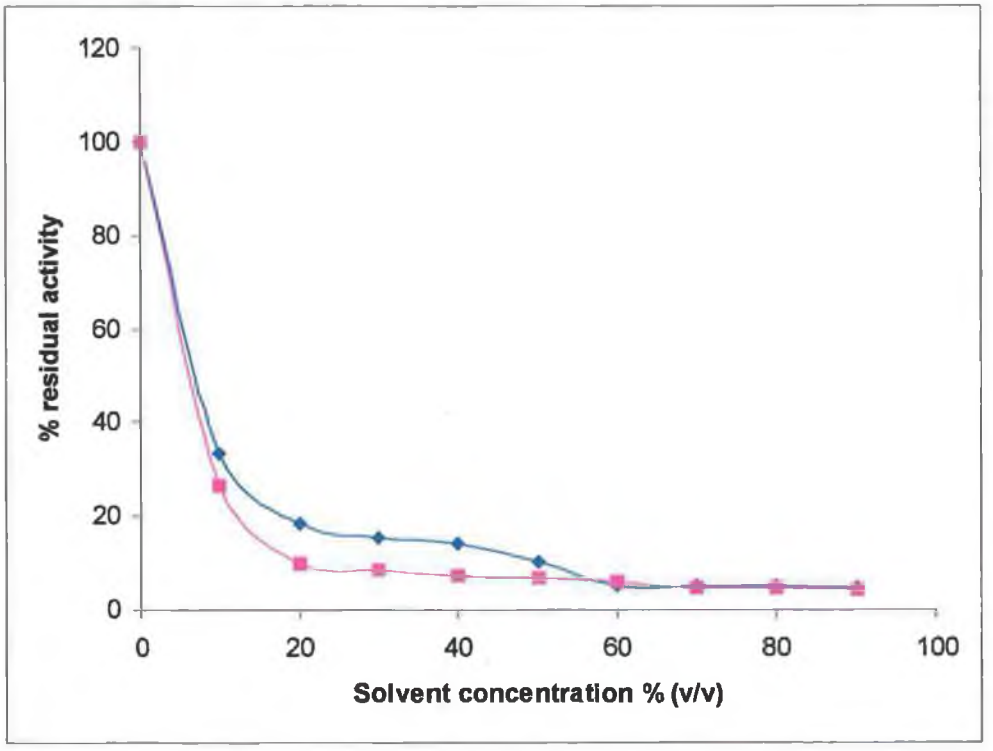

Figure 4.4.1.2: Residual PAPI activity (%) versus (■) ACN and (♦) Acetone concentration (% v/v)

4.4.1.3 Methanol, Ethanol and DMSO

PAPI in the presence of methanol retained considerable activity in comparison with other solvents. It can seen from the results that the greatest values occur at 10% (v/v) and 20% (v/v) concentrations, where the residual activity is 56% and 37%, respectively, of that in aqueous buffer. PAPI in 10-20% (v/v) methanol performs better than in the other solvents at equivalent concentration.

Activity ranged from 26% - 10% at MeOH concentration 30% - 60% v/v. From 70%-90% (v/v) concentration, insignificant PAP1 activity remained.

For PAPI treated with ethanol, 10% and 20% (v/v) concentrations reduced activity to 40 % and 29 % of that in aqueous buffer, respectively. At 40% (v/v) concentration and greater, virtually no activity remained.

DMSO at 10% (v/v) and at 20% (v/v) concentration reduced PAPI activity to 50% of its level in aqueous buffer. Activities at 20% v/v and at 30% v/v DMSO were 43% and 40% of the aqueous level. From 40% (v/v) concentration upwards, very little activity (< 10%) remained.

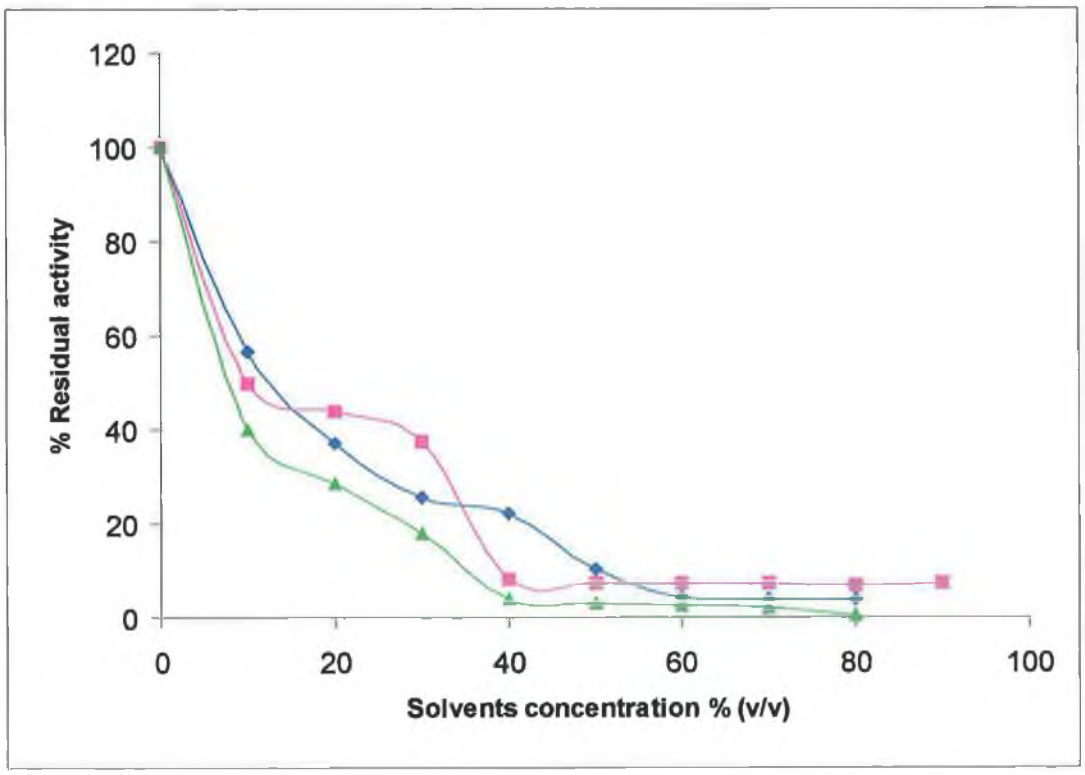

Figure 4.4.1.3: Residual PAPI activity (%) versus (♦) Methanol, (▲) Ethanol and (■) DMSO concentration (%, v/v).

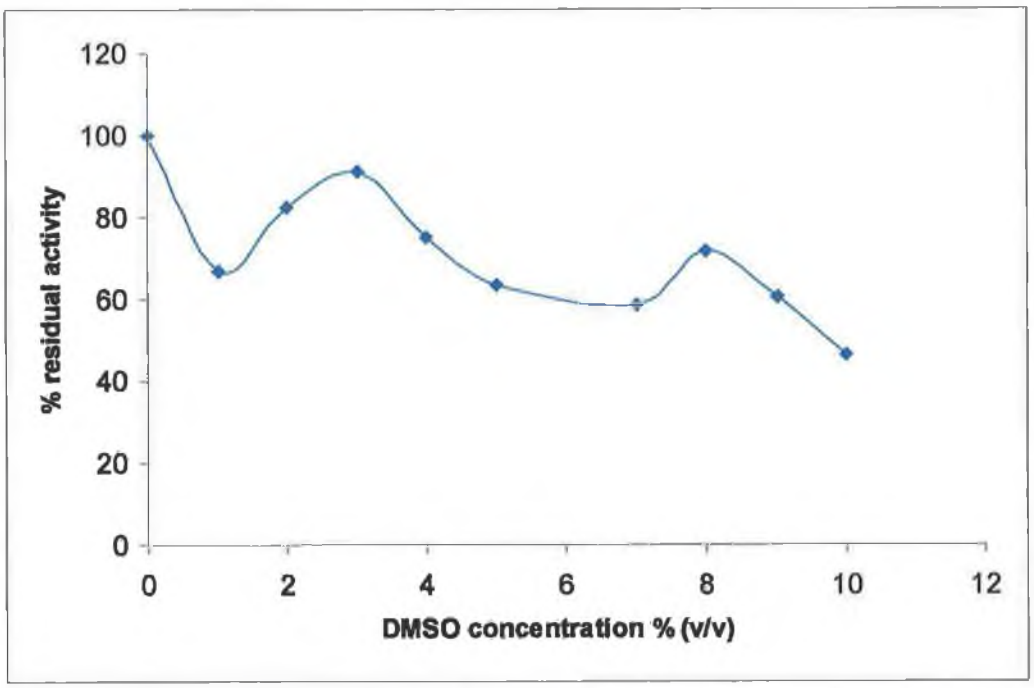

Figure 4.4.1.4 : : Residual Activity of PAPI (%) in presence of DMSO, 0-10% v/v.

4.4.1.5. A COMPARISON OF ORGANIC SOLVENTS FOR PAPI AT 10 AND 20 % (v/v) CONCENTRATIONS

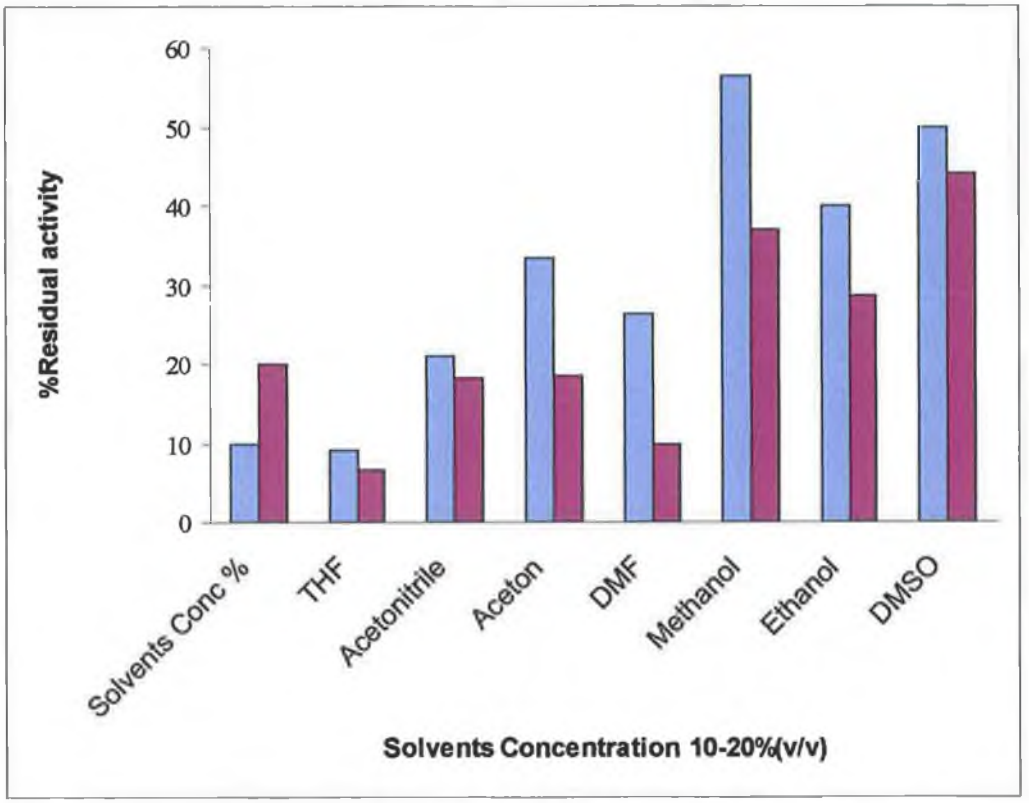

Figure 4.4.1.5: Effect of solvents (10 and 20% v/v) on PAPI

Plot of % residual activity versus 10/20 (% v/v) solvents concentration.

(■) Solvents concentration 10 % (v/v), (■) solvents concentration 20 % (v/v)

4.5 CHEMICAL MODIFICATION

4.5.1 Crosslinking with dimethyl suberimidate (DMS)

Modification of PAPI with the bifunctional crosslinking reagent DMS was performed as described in Section 2.10. Activity of native and modified PAPI was determined. Amidase activity of PAPI was 100% at 30°C, while modified PAPI decreased to 20% at 30°C. The DMS modification did not stabilize the remaining activity. It was decided not to use this reagent further because of the low activity of modified PAPI.

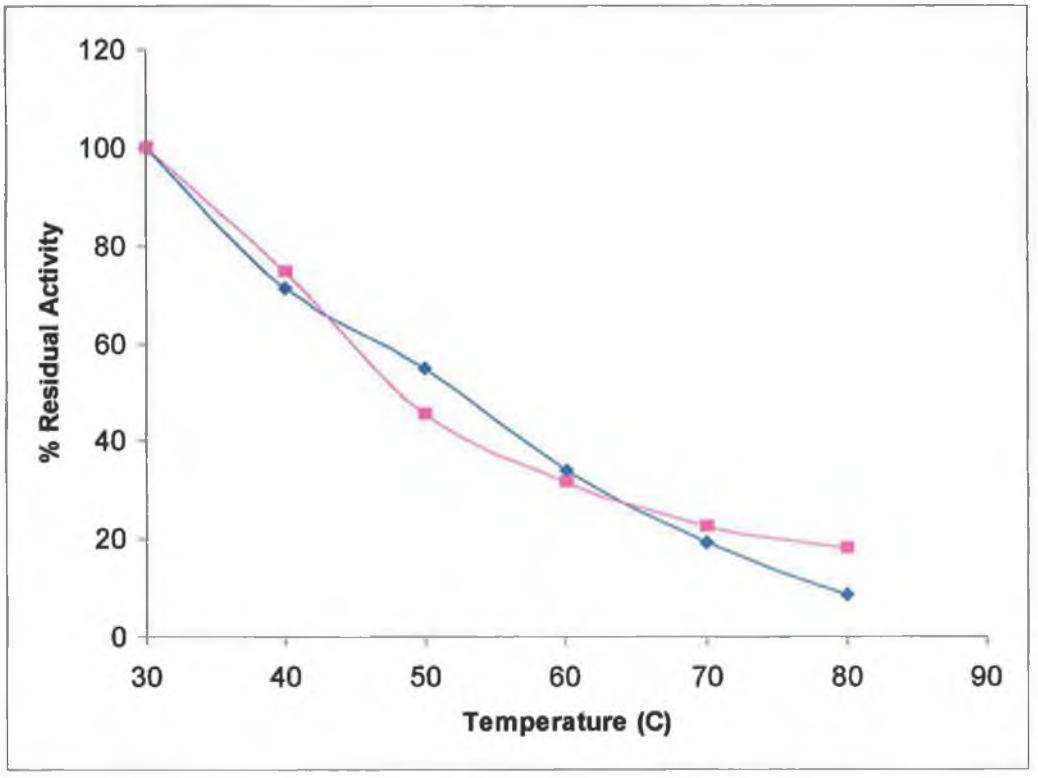

Figure 4.5.1. Effect of DMS on the enzyme PAPI

Plot of % residual activity versus temperature (°C) of modified PAPI (■), and native PAPI (♦). Activity is represented as a percentage of the 30°C level for each one (untreated PAPI and PAPI post-modification).

4.6 EFFECTS OF STABILIZING ADDITIVES ON PAPI

4.6.1 Effect of ammonium sulphate on enzyme PAPI

The effect of ammonium sulphate on the stability of purified PAPI, using pGlu-AMC as substrate, was investigated, as outlined in Section 2.11.1. A decrease in enzymatic activity was observed at 0.5 M ammonium sulphate concentration (35% less activity than in buffer) and activity of PAPI/$(NH_4)_2 SO_4$ was inhibited by 50% at 45°C, while native PAPI was 50% active at 50°C, a higher temperature. Ammonium sulphate had no stabilising or protective effect on PAPI at any of the temperatures tested, contrary to expectation.

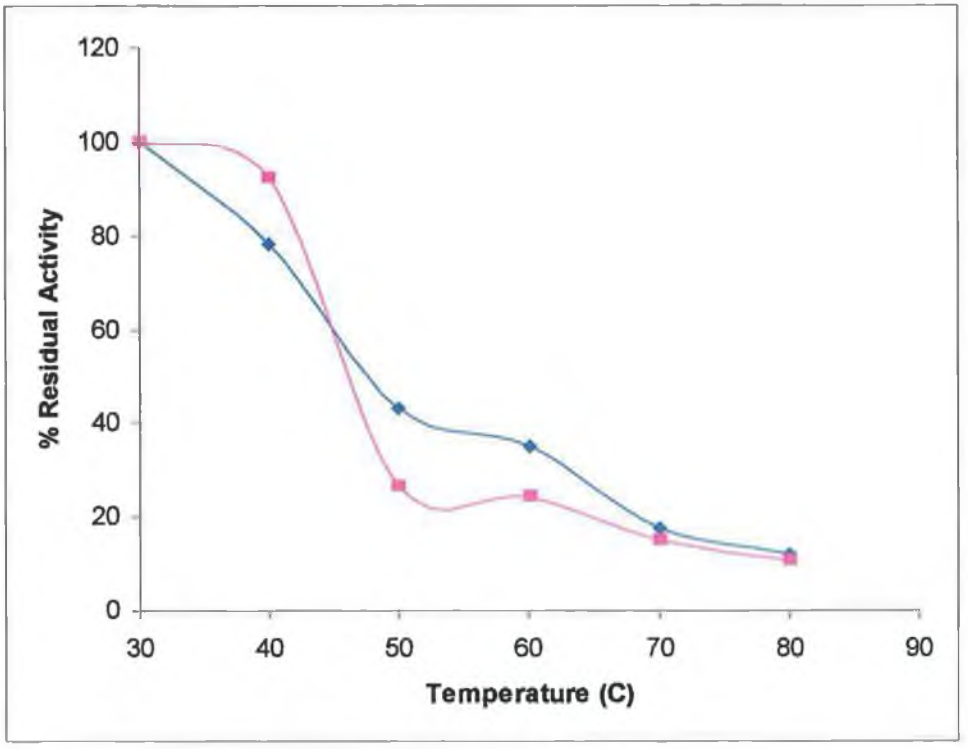

Figure 4.6.1: Effect of ammonium sulphate on the enzyme PAPI

Plot of % residual activity versus temperature (°C), (♦) is native PAPI in 50mM potassium phosphate, pH 8.0; (■) is PAPI with ammonium sulphate. Activity is represented as a percentage of the 30°C value of each PAPI fraction.

4.6.2 Effect of Trehalose on enzyme PAP1

The effect of 0.5M trehalose on PAPI activity when incubated at various temperatures in potassium phosphate buffer, pH 8.0, resulted in a marginal stabilisation of PAPI activity: the activity of PAPI without trehalose was 50% at 45°C while PAP1/0.5M trehalose was 50% active at 50°C, a higher temperature.

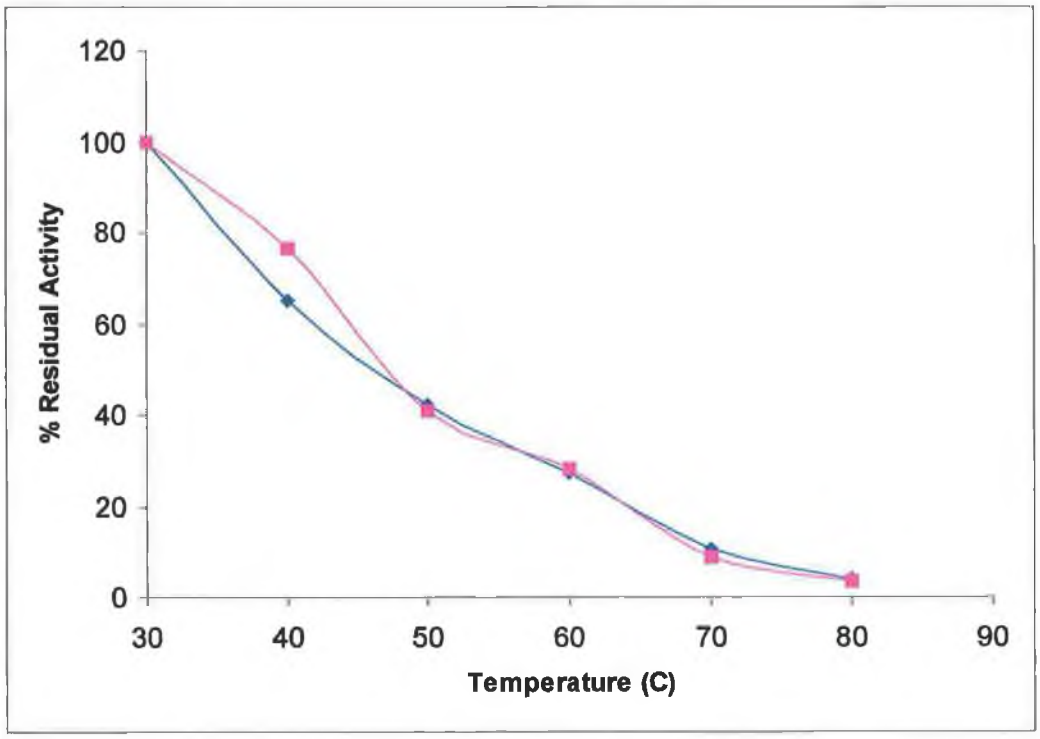

Figure 4.6.2: Effect of Trehalose on enzyme PAPI

Plot of % residual activity versus temperature (°C) of PAPI with 0.5M Trehalose. (♦) PAPI with out trehalose and (■) PAPI with 0.5M trehalose. Activity is represented as a percentage of that at 30°C in each case

4.6.3 Effect of xylitol on enzyme PAPI

Similarly to Section 4.6.2 above, xylitol was included at a concentration 0.5M in the PAP1-buffer mixture. Xylitol addition resulted in a significant increase in PAPI activity at 30°C and 40°C. PAPI with xylitol retained 50% activity at 60°C while, without xylitol, PAPI retained 50% of its 30°C activity at 45°C.

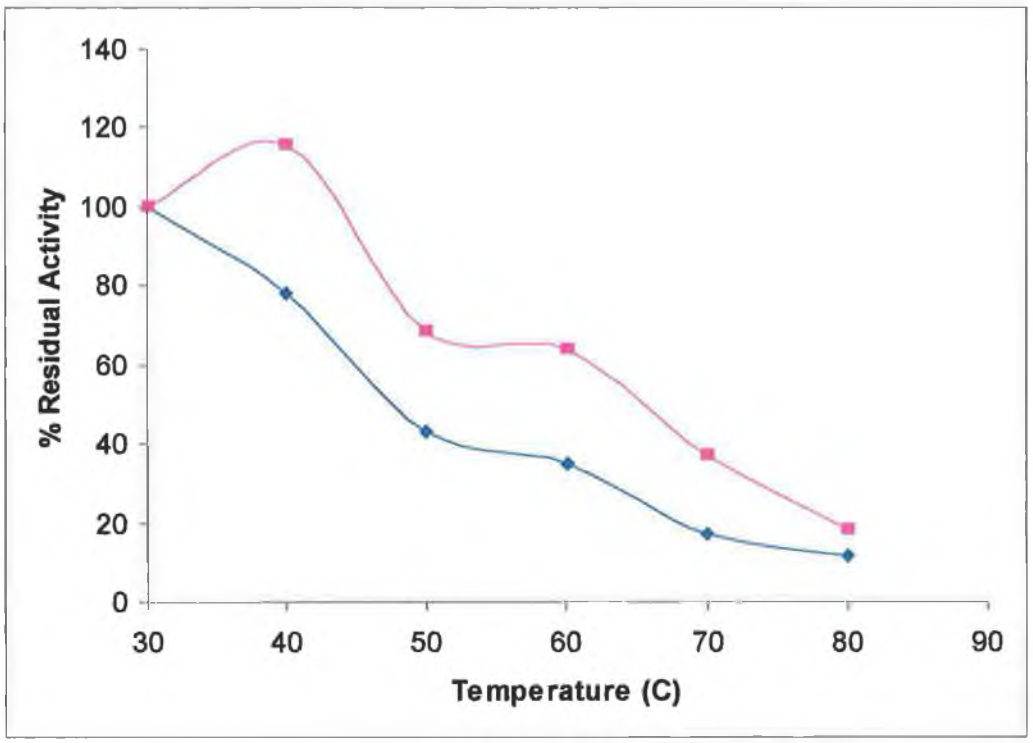

Figure 4.6.3. Effect of Xylitol on PAP1

Plot of % residual activity versus temperature (°C), (♦) is PAP1 without xylitol and (■) is PAPI with xylitol. Activity is represented as a percentage of the 30°C value of each case.

4.6.3.1 Thermoinactvation assay of Xylitol on PAPI

The kinetics of thermoinactivation of Xylitol on PAPI (diluted 1/50 in buffer) were studied at 60°C as described in Section 2.8.2.1. The results of these experiments were analysed using the computer programme Enzfitter.

Data were fitted to the first order exponential decay equation and visual observation shows that the fit is a good one.

The *k* value for Xylitol on PAPI at 60°C was 0.05 ± 0.002 min^{-1} and half- life ($t_{1/2}$) was calculated to be 13.9 minutes while the *k* value of PAPI in buffer at 60°C was 0.08 ± 0.003 min^{-1} and half-life ($t_{1/2}$) was calculated to be 9 minutes.

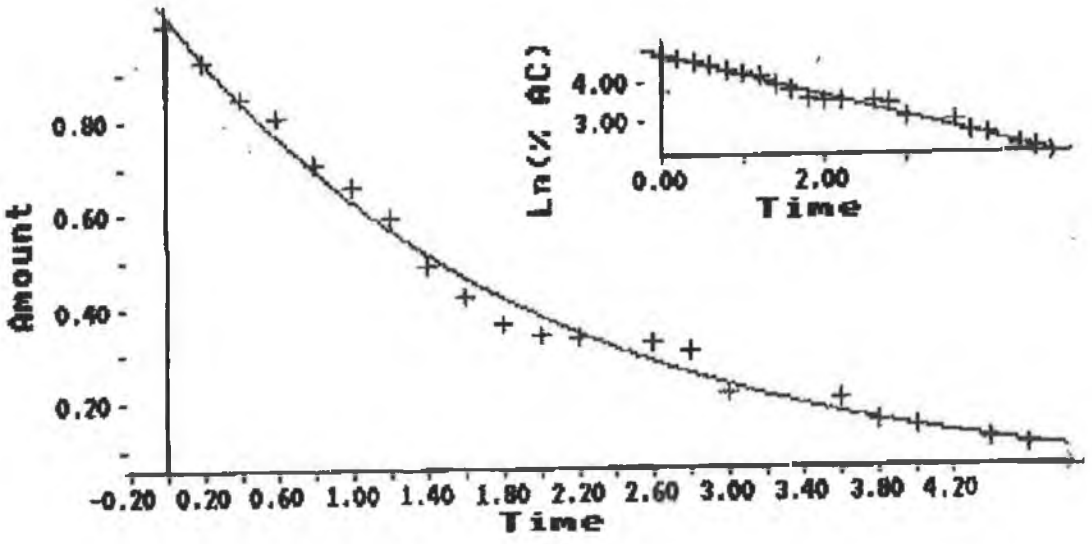

Figure 4.6.3.1: Thermoinactivaction of PAPI with Xylitol at 60°C

Plot of % residual activity versus time fitted to the first order exponential decay equation using the Enzfitter programme.

Amount: (% residual activity) versus time in minutes.

Inset: ln (% residual activity) versus time in minutes.

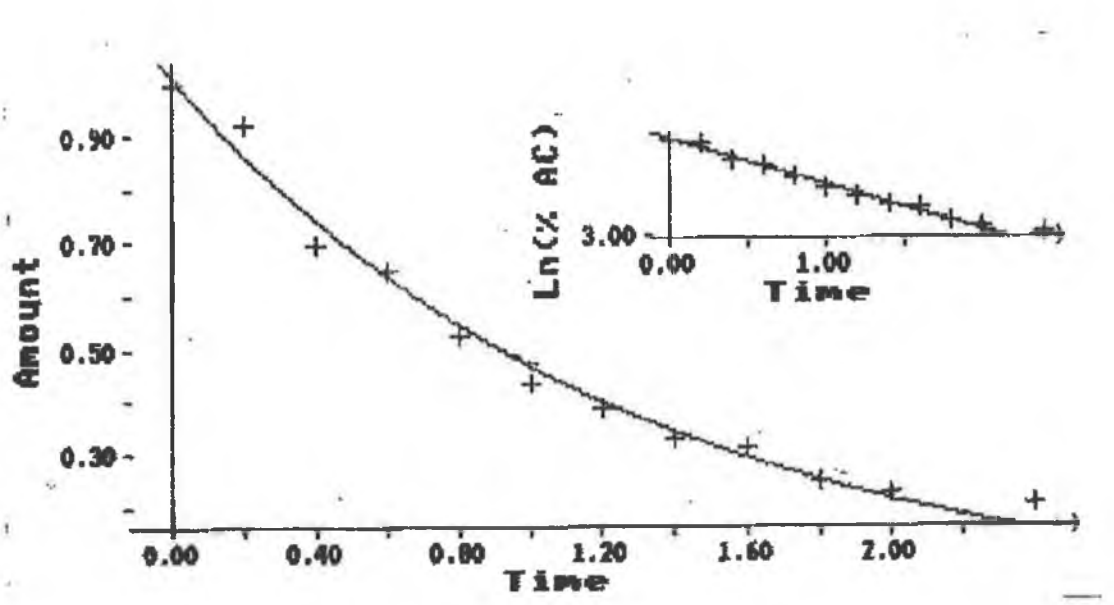

Figure 4.6.3.2: Thermoinactivaction of PAPI without xylitol 60°C

Plot of % residual activity versus time fitted to the first order exponential decay equation using the Enzfitter programme.

Amount : (% residual activity) versus time in minutes.

Inset : ln (% residual activity) versus time in minutes.

4.6.4 Effect of 10 and 50% (v/v) glycerol on PAPI

The effect of glycerol at 10 and 50 % (v/v) concentration on PAPI thermal stability was investigated, as outlined in Section 2.11.3. A decrease in enzymatic activity was observed on glycerol addition and activity of PAPI was further inhibited with increasing glycerol concentration. PAPI activity was inhibited by glycerol: PAPI displayed 50% activity at 10% (v/v) glycerol and only 18% at 50% (v/v) glycerol. Except for a marginal effect above 60°C at an inhibitory 50% (v/v), Glycerol had no protective or stabilising effect on PAPI at elevated temperatures.

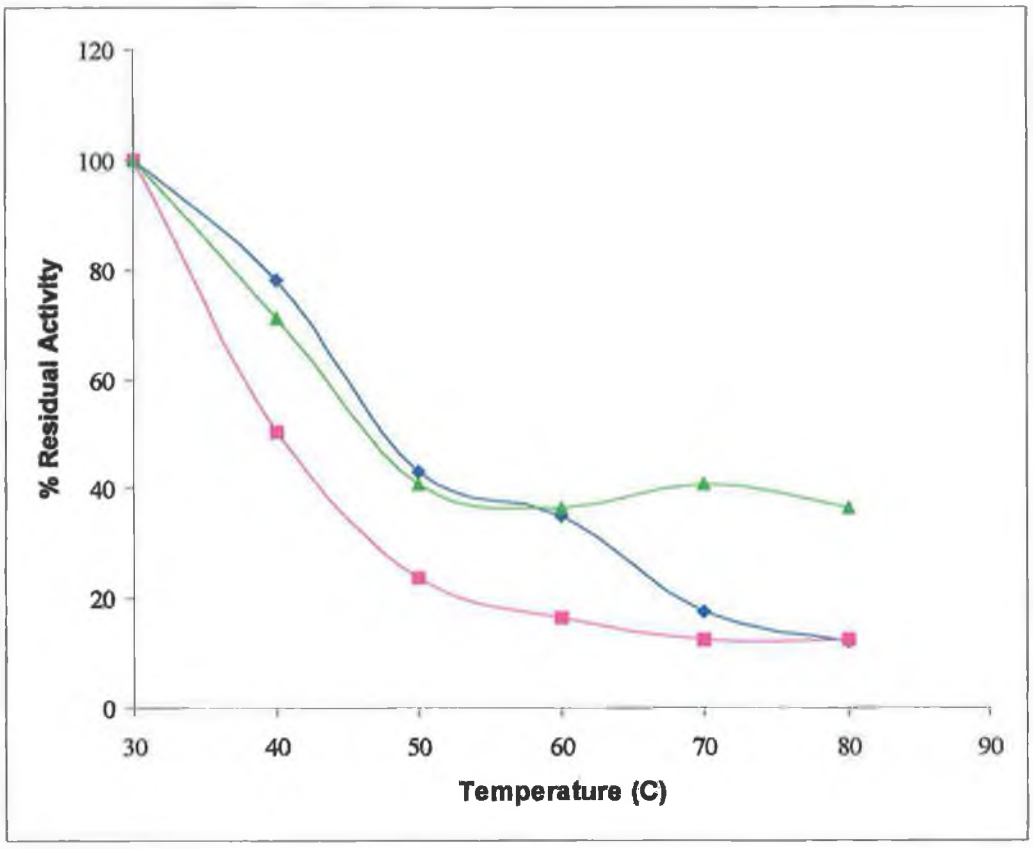

Figure 4.6.4. Effect of glycerol 10 and 50 % (v/v) on the enzyme PAPI

Plot of % residual activity versus temperature (°C), (♦) is native PAPI, (■) is PAP1 with 10% (v/v) glycerol; (▲) is PAPI with 50 % (v/v) glycerol. Activity is represented as a percentage of the 30°C value of each case.

4.7 A COMPARISON OF THE EFFECTS OF AMMONIUM SULPHATE, SUGAR DERIVATIVES AND GLYCEROL ON PAPI

Figures 4.7.1 and 4.7.2 illustrate that only the sugar alcohol, xylitol, was suitable as a stabiliser of pyroglutamyl peptidase (PAPI) activity.

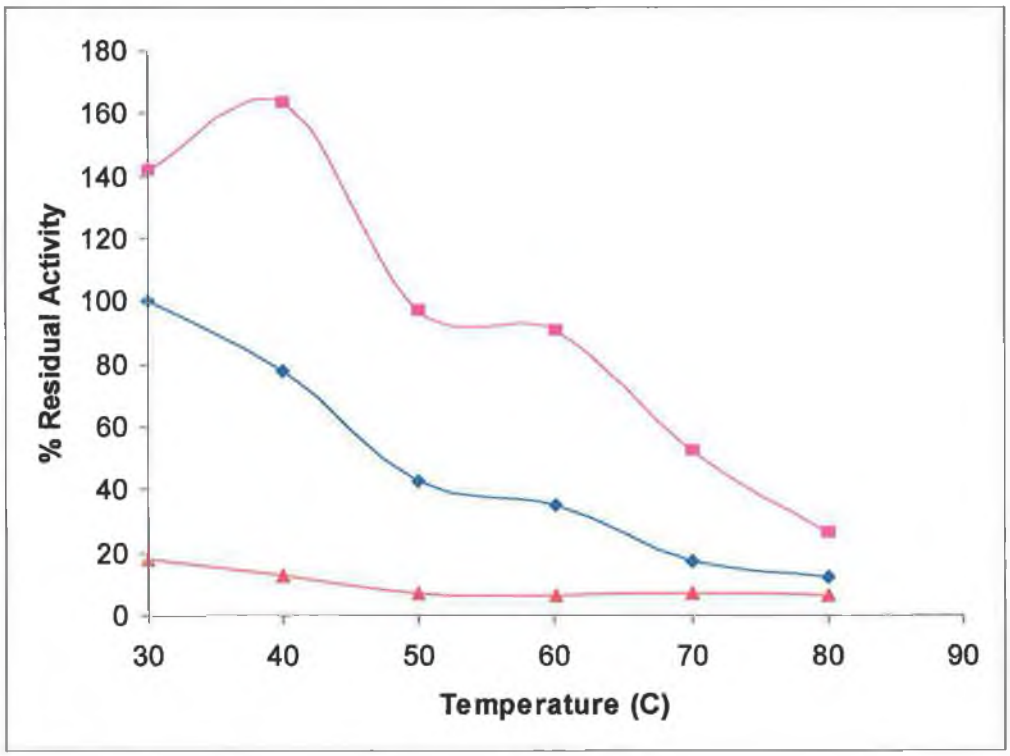

Figure 4.7.1: Comparison of the effects of sugar derivatives and glycerol on PAPI

Plot of % residual activity (%) versus temperature (°C), (♦) is native PAPI, (▲) is PAPI with 50 % (v/v) glycerol; (■) is PAPI with 0.5M xylitol. Activity is represented as a percentage of the 30°C value of native PAPI with no additives.

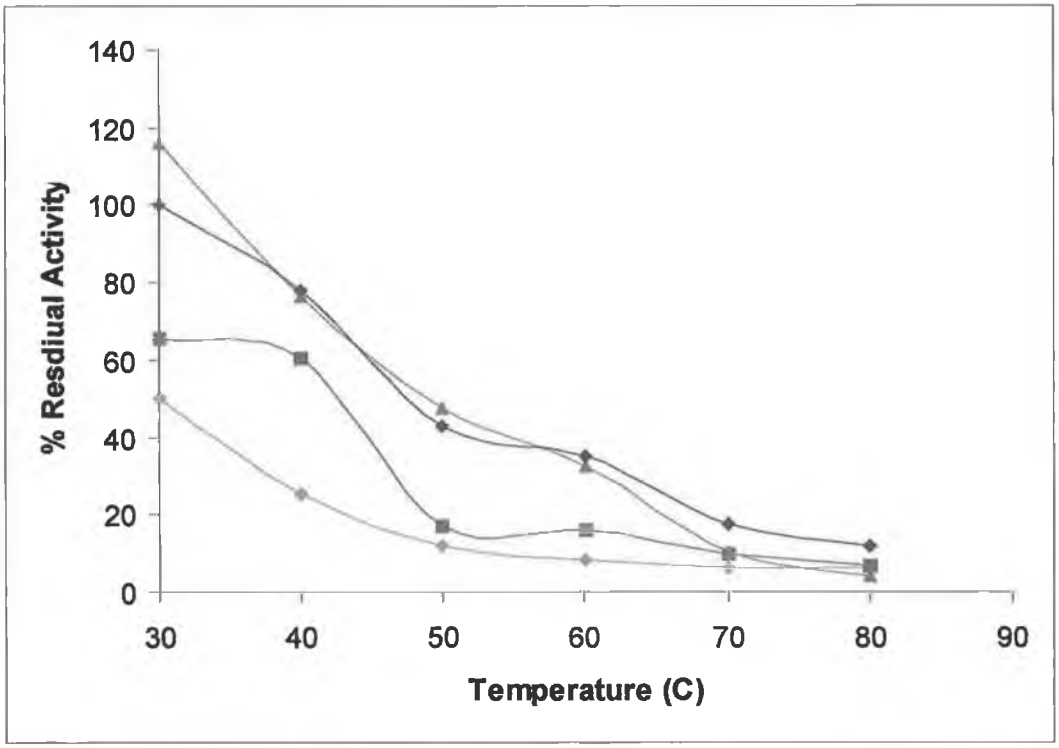

Figure 4.7.2: A comparison of the effects of ammonium sulphate, trehalose and glycerol on PAPI

Plot of residual activity (%) versus temperature (°C), (♦) is native PAPI, (♦) is PAPI with 10% (v/v) glycerol, (▲) is PAPI with trehalose and (■) is PAPI with $(NH_4)_2 SO_4$. Activity is represented as a percentage of the 30°C value of native PAPI with no additives.

CHAPTER FIVE : RESULTS

Studies on mutants F16Y and Y174F

5.0 STUDIES ON MUTANTS F16Y AND Y147F

5.1 Introduction

Mutants F16Y and Y147F of PAPI were investigated and their temperature profiles determined. The apparent half-inactivation temperatures (T_{50}) were estimated and compared with wild type PAPI. Thermoinactivations at a constant 70°C were also undertaken. The steady state kinetics of mutants F16Y and Y147F were determined and the K_m and k_{cat} values compared with native PAPI.

5.2 STABILITY AND KINETICS OF F16Y

BCA standard curves (Section 2.5.1) indicated that the protein concentration of F16Y was 0.325mg/ml.

5.2.1 Temperature Profile

A temperature profile of both PAPI (0.12 mg/ml, diluted 1/80 to final volume 3ml using potassium phosphate buffer pH 8.0 including 0.12 mg/ml bovine serum albumin to ensure a constant protein concentration of 0.12mg/ml) and F16Y (0.12mg/ml) was performed as described in Section 2.8.1.1. The enzymes were incubated at the appropriate temperature for 10 minutes in a waterbath. The half-inactivation temperature, T_{50} (where observed activity was 50% of maximal), was estimated by inspection to be 51°C ± 1°C for F16Y while for PAPI it was 54°C ± 1°C.

Note that here, PAPI wild type T_{50} was determined at a different concentration from that in chapter 4.

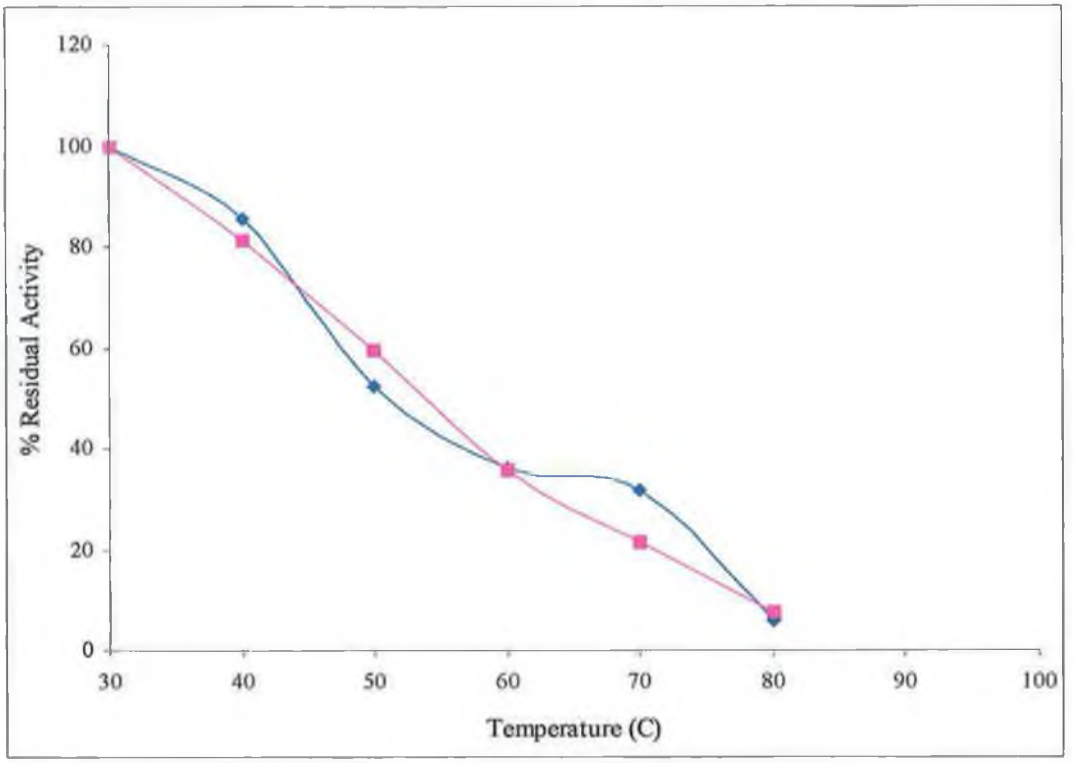

Figure 5.2.1: A temperature profile of wild type PAP1 and the mutant F16Y. Plot of % residual activity versus temperature (°C). Activity is represented as a percentage of the 30°C value for each one. (■) is native PAPI (0.12mg/ml diluted 1/80); (♦) is mutant F16Y (0.12mg/ml).

5.2.2 F16Y thermoinactvation assay

The kinetics of thermoinactivation of F16Y (0.325 mg/ml final concentration) were studied at 70°C because this is a convenient temperature to study wild type with both mutants over a 30 minute period, as described in Section 2.8.2.1. The results of these experiments were analysed using the computer programme Enzfitter (Biosoft, Cambridge, UK). Data were fitted to the first order exponential decay equation and visual observation shows that the fit is a good one. The *k* value for F16Y at 70°C was 0.026 ± 0.002 min^{-1} and half- life ($t_{1/2}$) was calculated to be 27 minutes.

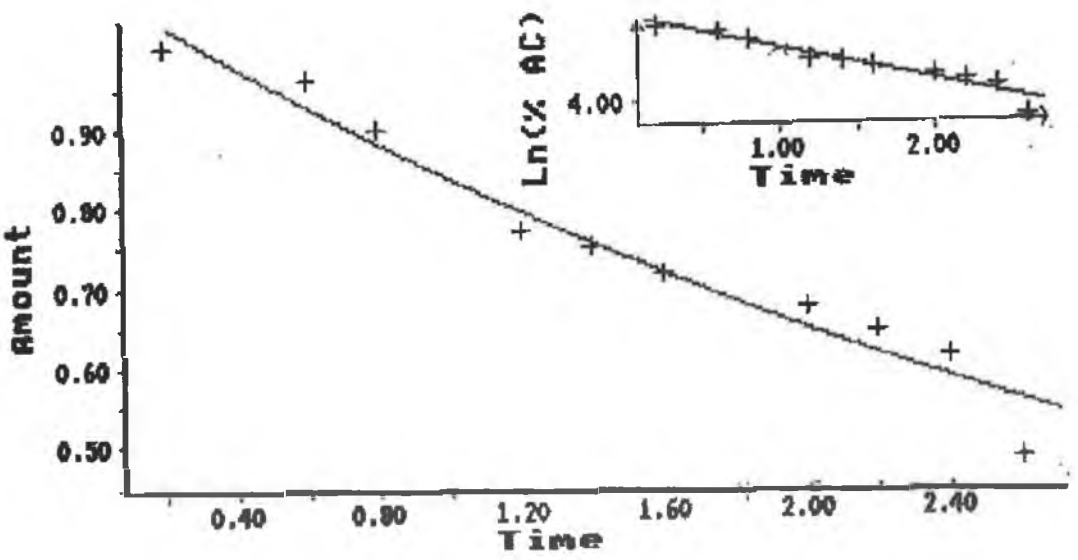

Figure 5.2.2: Thermoinactivaction of the F16Y mutant of PAPI at 70 °C

Plot of % residual activity versus time fitted to the first order exponential decay equation using the Enzfitter programme. Amount: (% residual activity) versus time in minutes. Inset: ln (% residual activity) versus time in minutes.

5.2.3 Active Site Titration of F16Y

Active site concentration of F16Y was determined similarly to PAPI (Sections 2.7.3, 2.7.4). Figure 5.2.3 illustrates the titration of F16Y with NEM. The concentration of active enzyme was determined from this plot, where the intercept on the x-axis (best line fit) is equal to the concentration of active enzyme. The enzyme was determined to have an operational molarity of 0.8 μM.

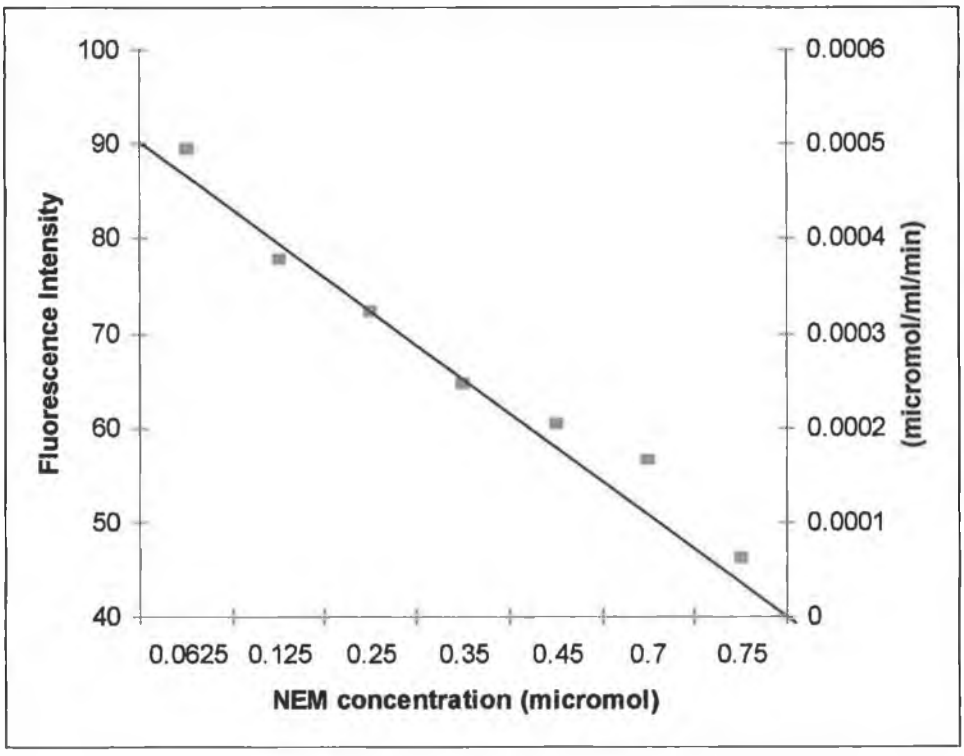

Figure 5.2.3: Titration of F16Y with NEM

Plot of Fluorescent Intensity (excitation 370nm, slitwidth l0nm; emission 440nm, slitwidth 2.5nm) and activity (μmol/ml/min) versus NEM concentration (μM) ("micromol" refers to fluorescence intensity converted to micromol AMC).

5.2.4 K_m, V_{max} and k_{cat} determination for F16Y mutant

Michaelis-Menten kinetics were determined for the mutant F16Y as described in Section 2.7.2. F16Y displayed normal Michaelis-Menten kinetics, giving K_m values of 0.162 ± 0.020 mM and V_{max} 0.003 ± 0.0002µmol/min/ml (Enzfitter programme). Using the result of the active site titration (above, section 5.2.3), k_{cat} (5.75×10^{-5} s^{-1}) and k_{cat}/K_m(0.355 $s^{-1}.M^{-1}$) were calculated.

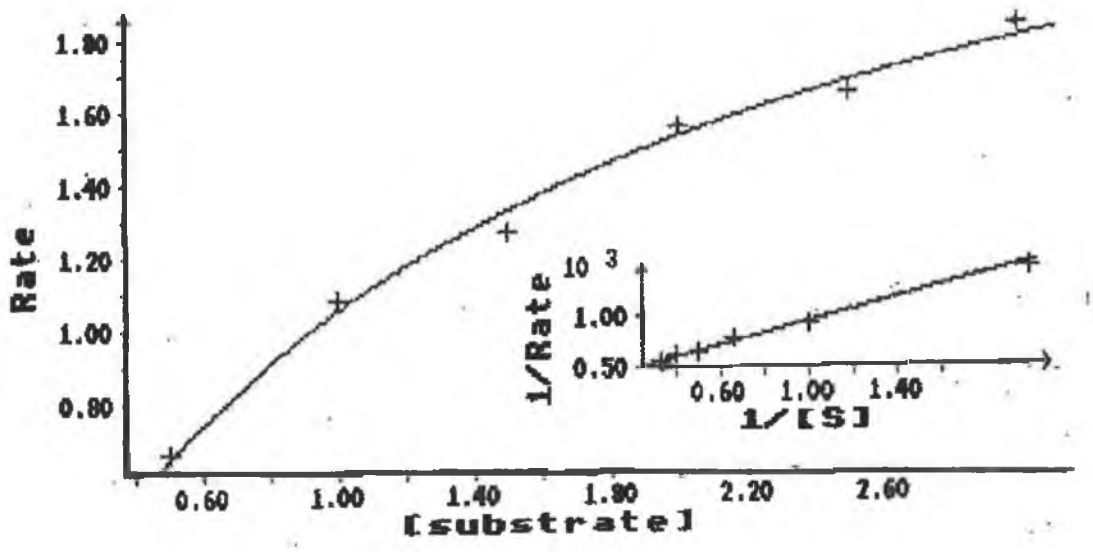

Figure 5.2.4: Michaelis-Menten plot for F16Y.

[Substrate] = mM pGlu-AMC. Rate = arbitrary fluorescence units (multiply by flu/6000 m, where m = 37.46 to convert to µmol AMC/min using a standard curve such as Figure 3.1.1) Inset: Lineweaver-Burk plot of the same data.

5.3 STABILITY AND KINETICS OF Y147F

Protein concentration of Y147F, estimated using the equation of the protein standard curve as described in Section 2.5.1, was 0.354mg/ml.

5.3.1 Temperature Profile

Temperature profiles of both wild type PAPI (0.12 mg/ml stock solution, diluted 1/60 to final volume 3ml using potassium phosphate buffer, pH 8.0, containing 0.12mg/ml bovine serum albumin to ensure a constant protein concentration), and Y147F (0.12 mg/ml stock, diluted similarly), were performed, as described in Section 2.8.1.1. The temperature profile (Figure 5.3.1) showed that the Y147F was more stable than wild type and F16Y. The half-inactivation temperature, T_{50} (where observed activity was 50% of maximal), was estimated by inspection to be 63°C ± 1°C for PAPI and 78°C ± 1°C for Y147F. Note that here, PAPI wild type T_{50} was determined at a different concentration from that in chapter 4.

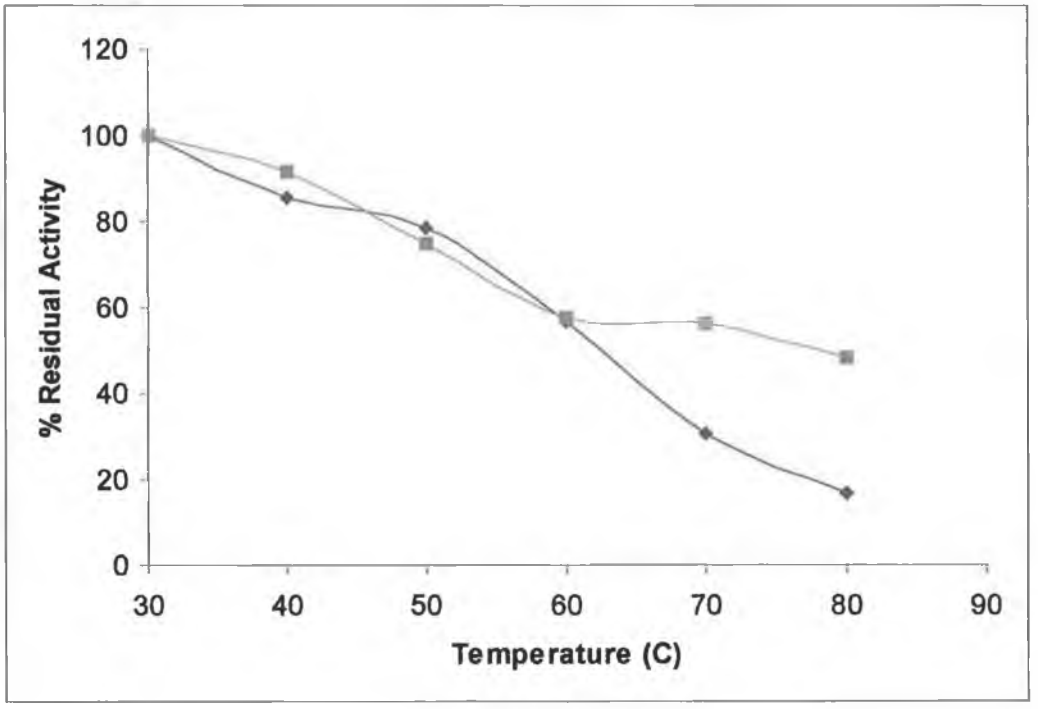

Figure 5.3.1: Temperature profiles of PAPI wild type and Y147F mutant.

Plot of % residual activity versus temperature (°C). Activity is represented as a percentage of the 30°C value of each one. (♦), Native PAPI; (■) mutant Y147F. Concentration of both Y147F and PAPI was 0.12mg/ml, diluted 1/60 in 50mM potassium phosphate buffer, pH 8.0, containing 0.12 mg/ml BSA to ensure a constant protein concentration.

5.3.2 Y147F thermoinactivation assay

The kinetics of thermoinactivation of Y147F (0.12 mg/ml stock solution diluted to 1/80 in 50mM potassium phosphate buffer, pH 8.0, to final volume 5ml were studied at 70°C over 80 minutes, as described in Section 2.8.2.2. The results were plotted for Y147F and for PAPI. The *k* value for Y147F was 0.028 ± 0.001 min^{-1} and half-life ($t_{1/2}$) was calculated to be 25 minutes, while the *k* value for PAPI was 0.079 ± 0.003 min^{-1} and half- life ($t_{1/2}$) was calculated to be 9 minutes.

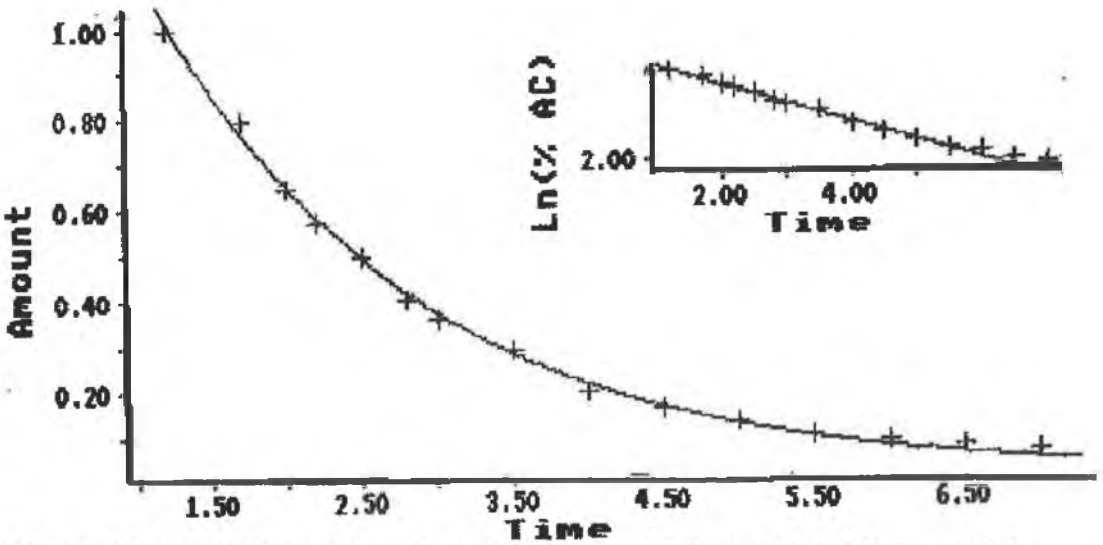

Figure 5.3.2 (A): Thermoinactivaction of the PAPI mutant Y147F at 70°C.

Plot of % residual activity versus time, fitted to the first order exponential decay equation using the Enzfitter programme. Amount: % Residual Activity versus time (minutes). Inset : ln plot of the same data.

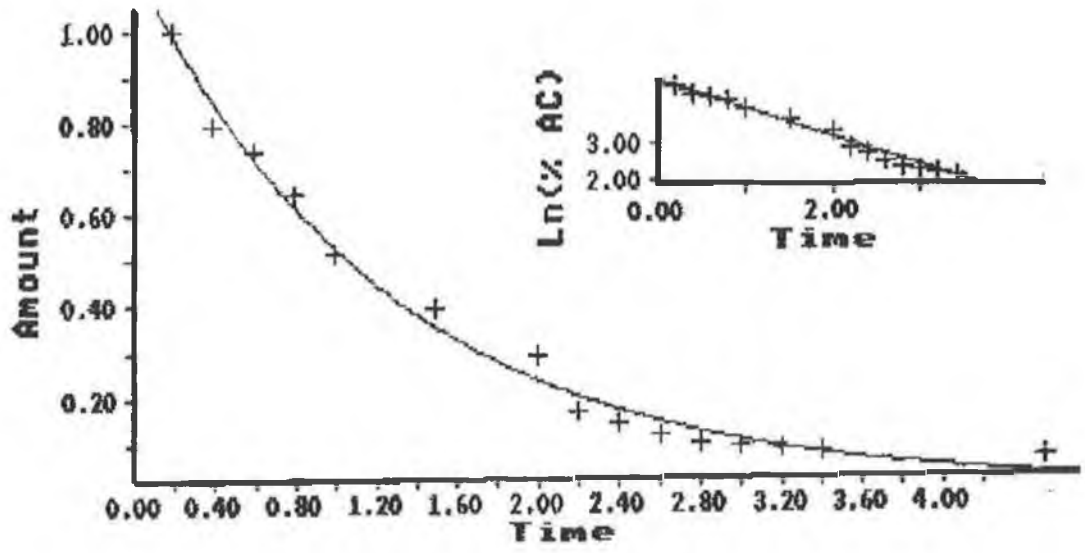

Figure 5.3.2(B): Thermoinactivaction of wild type PAPI at 70°C.

Plot of % residual activity versus time, fitted to the first order exponential decay equation using the Enzfitter programme. Amount: % Residual Activity versus time (minutes). Inset: ln plot of the same data.

5.3.3 Active Site Titration of Y147F

Active site concentration of Y147F (diluted 1/50 in buffer) was determined similarly to PAPI (Section 2.7.4). Figure 5.3.3 illustrates the titration of Y147F with NEM. The concentration of active enzyme was determined from this plot, where the intercept on the x-axis (best line fit) is equal to the concentration of active enzyme. Y147F was determined to have an operational molarity of 1.04 µM.

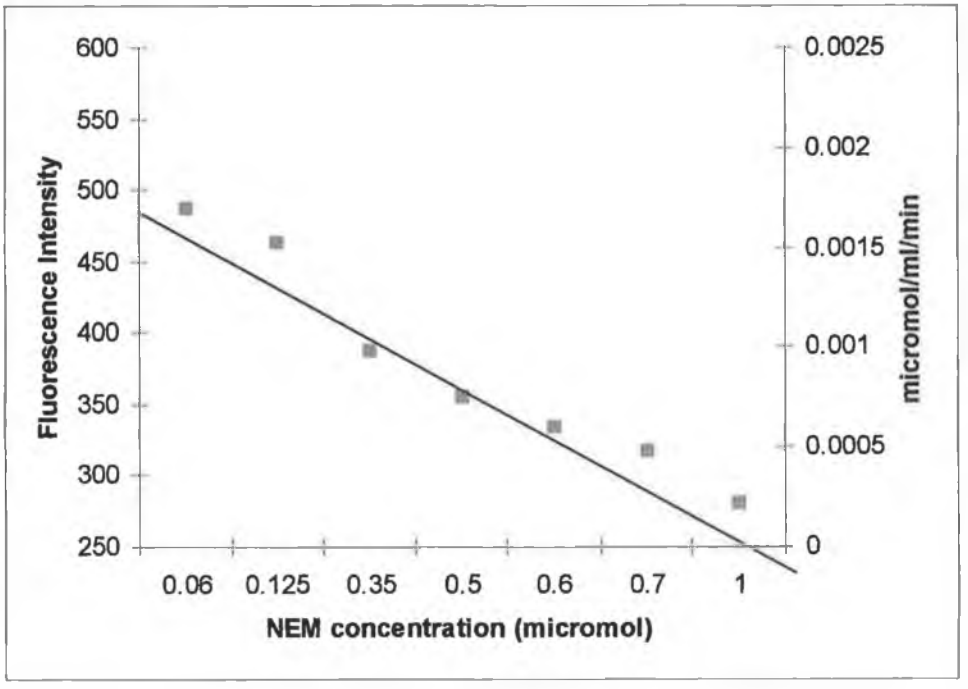

Figure 5.3.3: Titration of Y147F with NEM

Plot of Fluorescent Intensity (excitation 370nm, slitwidth 10nm; emission 440nm, slitwidth 2.5nm) and activity (µmol/ml/min) versus NEM concentration (µM) ("micromol" refers to fluorescence intensity converted to micromol AMC).

5.3.4 K_m , V_{max} and k_{cat} determination for PAPI mutant Y147F

Michaelis-Menten kinetics were determined for Y147F similarly to PAP1 and F16Y. Mutant Y147F displayed normal Michaelis-Menten kinetics, giving K_m and V_{max} values of 0.115 ± 0.019 mM and 0.0015 ± 0.0002 µmol/min/ml respectively (Enzfitter programme). From V_{max} and the result of the active site titration (Section 5.3.3 above), values for k_{cat} (2.45×10^{-5} s^{-1}) and k_{cat}/K_m (0.212 $s^{-1}.M^{-1}$) were calculated.

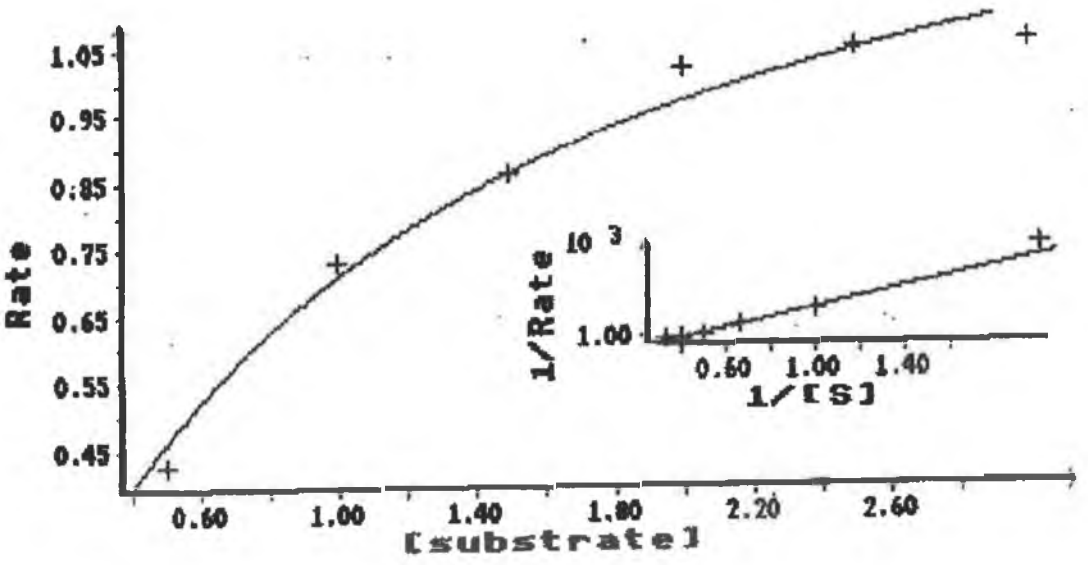

Figure 5.3.4: Michaelis-Menten plot for Y147F with substrate pGlu-AMC.

Rate = arbitrary fluorescence units (multiply by flu/ 6000m, where m = 37.46, to convert to µmol AMC/min using a standard curve such as Figure 3.1.1)

Inset: ln plot of the same data.

5.3.5 A Comparison of the half-life ($t_{1/2}$) for PAP1, F16Y and Y147F.

A thermoinactivation study was performed at 70°C for PAP1, Y174F and F16Y. Due to differences in activity levels, PAPI and Y147F (both stock concentrations 0.12mg/ml) were diluted 1/80 in 50mM potassium phosphate buffer pH 8.0, and 0.325mg/ml working solution for F16Y. The assays were performed as described in Section 2.8.2.1. *k* value of PAPI was 0.079 ± 0.003 (min^{-1}), and of Y147F 0.028 ± 0.001 (min^{-1}), while that of F16Y 0.026 ± 0.002 (min^{-1}).

The half-lives ($t_{1/2}$) for PAPI, F16Y and Y147F at 70°C were calculated from the corresponding *k*-values using the computer programme Enzfitter.

Table 5.1. Comparison of PAPI, F16Y and Y147F.

	Wild-type PAPI	Mutant Y147F	Mutant F16Y
Protein concentration (mg/ml)	0.0015	0.0015	0.325
T_{50}	63°C ± 1 °C	78 °C ± 1°C	51 °C ± 1 °C
k (min^{-1})	0.079 ± 0.0032	0.028 ± 0.001	0.026 ± 0.002
Half-life ($t_{1/2}$), 70°C	9 minutes	25 minutes	27 minutes
K_m (mM)	0.132 ± 0.024	0.115 ± 0.019	0.162 ± 0.020
V_{max} (µmol/min/ml)	0.0013 ± 0.0001	0.0015 ± 0.0002	0.003 ± 0.0002
NEM (µM)	0.8	1.04	0.8
k_{cat} (s^{-1})	$2.68x10^{-5}$	$2.45x10^{-5}$	$5.75x10^{-5}$
k_{cat}/K_m ($s^{-1}.M^{-1}$)	0.202	0.212	0.355

The mutant Y147F was more stable than wild type PAP1, while mutant F16Y was less stable. Among the kinetic parameters, only k_{cat} for F16Y was notably different from wild type PAPI (2-fold greater than wild type).

Chapter 6
Discussion and Conclusion

6.0 Discussion

This work focused on the study of PAPI and two mutants F16Y and Y147F. PAPI from human brain and mutants have previously been cloned, characterized and over expressed in *E. coli* grown in LB culture medium. This source of material is readily available and cheap to produce.

Assay methods

In this work, fluorimetric assays were used to estimate PAPI catalytic activity. Fluorimetric assays generally offer increased safety, sensitivity and specificity compared with the older β-naphthylamide compounds estimated by spectrophotometry. The substrate used to detect amidase activity of PAPI and mutants was pGlu-AMC. This substrate releases a fluorophore product as a direct result of enzymatic hydrolysis. In this case PAPI hydrolysis of the substrate pGlu-AMC releases AMC, which can be estimated fluorometrically. pGlu AMC does not hydrolyse in the absence of the enzyme.

Fluorimetric assay of free AMC shows that the optimum excitation wavelength is 370nm and, for emission, 440nm.The assay's sensitivity can be increased by widening of the excitation and emission slit width used. At an excitation wavelength of 370nm the 10nm width is best for both excitation and emission, and it is recommended to maintain the same excitation and emission slit width for all assays.

Free AMC standard curves were constructed as outlined in Section 2.6.1. A little quenching was observed in the presence of culture medium or solvents. Figures 3.1.5 and 3.1.6 demonstrate the effect of buffer, crude PAPI culture medium and

purified PAPI. The linear fluorescence with AMC concentration allowed for accurate quantification of enzyme activity (see figure 3.1.3).

The fluorimetric assay was used to determine percentage residual activity for both temperature profile and thermoinactivation experiments.

Purification

The aim of protein purification is to isolate one particular protein from all other proteins in the starting material. Crude PAPI was produced by *E. coli* grown in LB culture medium and, following its release by sonication, was purified by nickel affinity chromatography. (This method exploits the His_6 tag on the cloned protein.) The elution profile (Figure 3.3.1) demonstrates that a single peak of PAPI activity was separated (over two fractions) in elution buffer. Purity of PAPI was assessed by SDS polyacrylamide gel electrophoresis (SDS PAGE). The sample was shown not to contain any other species: only one protein band was observed for PAPI (Figure 3.3.3), showing that the enzyme is pure. SDS PAGE separates proteins based primarily on their molecular weights (Laemmli, 1970) and is routinely used for determination of protein purity (Bollag *et al.*, 1996). SDS (PAGE) was also employed in the estimation of the molecular mass of purified PAPI. Sigma markers (66-14 kDa) were used and molecular mass of PAPI determined to be in the range 23-24 kDa (Figure 3.3.3). The molecular weight previously obtained for PAPI from human brain was 23.138 kDa (Dando *et al.*, 2003). The native molecular weight (no SDS present) for this enzyme was not determined.

Heat stability

The effect of assay temperature on PAPI activity was investigated as outlined in Section 2.8.1.1. Samples were incubated for 10 minutes at the appropriate temperature, then placed on ice prior to re-warming and assay at 37°C; this ensured true measurement of the remaining PAPI activity. PAPI catalytic activity declined above 45°C and very little activity remained at 70°C. Its T_{50} was 60°C and, at this temperature (at concentration 0.45 mg/ml, diluted 1/80), its *k* value was 0.046 ± 0.002 min^{-1}, giving a half-life of 15 minutes.

For a stability comparison of native PAPI and its mutants F16Y and Y147F, a temperature profile was carried out. At the same concentration (0.12 mg/ml, diluted 1/80), mutant Y147F was more stable: T_{50} for native PAPI was 63°C and the *k* value was 0.079 ± 0.003min^{-1}, while the respective values for mutant Y147F were 78°C and 0.028 ± 0.001 min^{-1} at 70°C. For F16Y (less active, used at 0.325mg/ml with no further dilution), T_{50} was 51°C and *k* was 0.026 ± 0.002 min^{-1} at 70°C. The mutations changes are small: the only difference between Phe and Tyr is that Tyr has a –OH on the benzene ring. Yet, this small change has a very stabilizing effect at position 147 but is destabilizing at position 16. Human PAPI expressed in Sf9 insect cells was stable at temperatures up to 40 °C for 4.5 h, but activity was almost completely lost within 30 min at 60°C. Maximal activity of the human recombinant enzyme was seen at 50°C in 10 min assays (Dando *et al.*, 2003). A similar pattern of temperature activities was described for B. amyloliquefaciens by Tsuru *et al.* (1978).

The temperature-activity profile of PAPI (from the hyperthermophilic archaeon *Thermococcus litoralis*) demonstrates a maximum at 70°C, slightly lower than the optimum growth temperature of *T. litoralis*. Although considerably more

thermostable than mesophilic enzymes, *T. litoralis* PAPI loses its activity rapidly at temperatures above 80°C. This is likely to be due to destruction of the critical cysteine in the active site. However, the enzyme still has a half-life of 1 hr at 70°C (Singleton *et al.*, 2000). The thermophilic *Pfu*PAPI exhibits optimum activity at 90°C (Ogasahara *et al.*, 2001).

Enzyme	R hu PAPI	Bov ser DPP IV	*T. litoralis* PAPI
Reference	This work	D Ruth, PhD thesis, DCU, 2004	Singleton et al. 2000
T_{50}	60°C	71°C	<80°C
k, min^{-1}	0.046 ± 0.002	0.071 ± 0.003	Not reported
$t_{1/2}$, min	15 (60°C)	10 (71°C)	60 (70°C) 75 (60°C)

It is interesting to compare the stability properties of PAPI with those of another neuropeptidase, the proline-specific dipeptidyl peptidase IV (DPP IV, EC 3.4.14.5). Bovine serum DPP IV demonstrated an increase in catalytic activity up to 62°C (maximal activity observed at 50°C, T_{50} at 71°C), as opposed to the expected thermal inactivation, and the enzyme has a half-life of 10 minutes at 71°C (D Ruth, PhD thesis, DCU, 2004). This is well above normal mammalian body temperature (37°C). Durinx *et al.* (2000) investigated the thermostability of human serum DPP IV over the range 25-80°C. They determined optimum temperature between 50-60°C. Similar results were obtained for porcine seminal plasma DPP IV (Ohkubo *et al.*, 1994), while Yoshimoto et al. (1978) reported an optimum temperature of 60°C for lamb kidney DPP IV, with 50% of activity retained up to 72°C.

Note that monomeric recombinant human PAPI is not glycosylated by *E. coli* but multimeric beef DPP IV is probably glycosylated. Sometimes glycosylation can influence protein stability.

Protein molecules are stable within a certain temperature range. However, the subtle balance between the folded and unfolded state can be disrupted by a number of factors such as temperature. The upper temperature for activity in enzymes appears to be governed by the limits of protein stability.

The rate of inactivation of an enzyme in solution increases rapidly with the temperature. In most cases, inactivation becomes virtually instantaneous at temperatures well below 100°C and in some cases below 70°C (Dixon and Webb, 1979). However, there are a number of enzymes that can withstand more extreme temperatures and remain catalytically active. Enzymes exist with optima above 100°C and some thermophilic enzymes have half-lives above 120°C (Daniel, 1996; Eichler, 2001).

Resistance to solvents

With regard to solvent tolerance, PAPI was tested in DMF, THF, ANC, DMSO, Acetone, Methanol and Ethanol over a range of (0-90 %) concentration and was not stable in most solvents (Figures 4.4.1.1, 4.4.1.2 and 4.4.1.3). All solvents used in this work are hydrophilic (mix freely with water), not hydrophobic. The half-inactivation concentrations (C_{50}) for DMSO and methanol were 10% and 12%, respectively (Figure 4.4.1.5) and they were the least injurious for PAPI activity. THF, on the other hand, is a strong denaturant which reduces catalytic activity; when PAPI was placed in it, no appreciable activity was observed.

In sharp contrast, the enzyme DPP IV was most stable in acetonitrile, where at 70% (v/v) the enzyme still retained up to 50% initial activity. Enzyme activity in DMSO steadily declined above 50% (v/v). DMF did not affect DPP IV catalytic activity up to 40% (v/v); however, further addition of solvent resulted in an abrupt decrease in enzyme activity (D Ruth, PhD thesis, DCU, 2004).

Michaelis-Menten kinetics

The number of active sites was determined for PAPI and mutants, using the assay described in Section 2.7.3 and 2.7.4. Michaelis-Menten constants (K_m) and V_{max} values were determined for wild type PAPI and mutants, as described in Section 2.7.1. Kinetic data were fitted by computer to the Michaelis-Menten and Lineweaver-Burk equations to produce K_m, V_{max} and k_{cat} values for native PAP1 and mutants with pGlu-AMC as substrate; Table 5.1 presents the calculated constants. The amidase activity showed a k_{cat}/K_m value for PAPI of 0.202 ($s^{-1} M^{-1}$) while the corresponding value for Y147F was 0.212 ($s^{-1} M^{-1}$) and was 0.355 ($s^{-1}M^{-1}$) for F16Y. These values are not significantly different. Many other PAPI mutants have been prepared (P-R Vaas, PhD thesis, DCU, 2005) but were not studied in this project.

In *B. amyloliquefaciens* PAPI, residues F10, F13, T45, Q71, I92, F142 and V143 form a hydrophobic substrate binding pocket (Ito *et al.*, 2001). The k_{cat} value of the F10Y mutant decreased 5.8-fold, and its K_m was 3.6-fold higher than wild type, but the two mutants F13Y and F142Y showed little change in kinetic parameters compared with PAPI. Catalytic efficiencies (k_{cat}/K_m) of the F13A and F142A mutants were 1000-fold less than that of wild-type, while F10A could not be purified (Ito *et al.*, 2001).

Chemical modification

In order to assess the effect on PAPI stability of chemical modification with dimethyl suberimidate (DMS), a temperature profile was carried out according to section 2.10.1.The temperature profile would suggest that this modification makes the enzyme *less* thermostable as compared to native PAPI at same concentration. Modification with DMS gave only 20% recovery of initial activity; due to this poor recovery, the reagent was not investigated further. This result was unexpected – DMS is a very mild protein modifying reagent and so should not inactivate the enzyme. DMS has effectively stabilized other enzymes: horseradish peroxidase (HRP) half-life increased 4-fold after DMS treatment (Ryan *et al.*, 1994). Also, DMS-modified alanine aminotransferase is more heat-resistant than native enzyme: the T_{50} of native enzyme was 46 min while that of DMS-modified alanine aminotransferase was 56 min (Moreno and O'Fagain, 1997). DMS usually reacts with protein lysine/ amino groups only and not with any other R-groups (Ji, 1983).

Effect of salt and polyols on PAPI activity

Ammonium sulphate was incubated with purified PAPI and the effect on heat stability measured as outlined in Section 2.11.1. The enzyme activity was significantly reduced at 0.5 M ammonium sulphate, with 35% less activity than in buffer. DPPIV activity was also significantly reduced by ammonium sulphate, with an 80% decrease at 1M ammonium sulphate compared with buffer alone (S Buckley, PhD thesis, 2001).

The effect of glycerol was investigated, as described in Section 2.11.3. A decrease in enzymatic activity was observed on glycerol addition and activity of

PAPI was further inhibited with increasing glycerol concentration. PAPI displayed 50% activity at 10% (v/v) glycerol and only 18% of its activity in buffer at 50% v/v glycerol. Glycerol had no protective or stabilising effect on PAPI at elevated temperatures.

It was hoped that PAPI would be stabilized against heat by the inclusion of xylitol or trehalose (Schein, 1990). Xylitol (0.5M) was included in the PAPI reaction mixture subjected to heat treatment. This additive led to increased activity at all temperatures tested, giving an apparent stabilization of PAPI activity (Fig. 4.6.3).

Thermoinactivation of PAPI at 60°C in the presence and absence of xylitol indicated a protecting effect: half-life was 60% longer with xylitol (14 min versus 9 min for PAPI alone).

Trehalose prevents proteins from denaturing at high temperature *in vitro*. Trehalose also suppresses the aggregation of denatured proteins, maintaining them in a partially- folded state from which they can be reactivated by molecular chaperones. The continued presence of trehalose, however, interferes with refolding, suggesting why it is rapidly hydrolysed following heat shock (Singer and Lindquist, 1998) Trehalose (0.5M) was mixed with PAPI but it was found not to stabilize PAPI.

Attempt to develop esterase assay

It would be interesting and instructive to measure PAPI's activity against pyroglutamyl esters, instead of amide substrates such as pGlu-AMC. The esterase/amidase ratio can be a good indicator of how well a given peptidase

might perform in peptide synthesis. pGlu pentachlorophenol is commercially available but has no fluorogenic or chromogenic group for convenient detection. Awawdeh and Harmon (2005) devised a spectrophotometric method to measure pentachlorophenol levels up to 1mM by means of its interaction with porphyrins, including *meso*-tetra(4-sulfonatophenyl)porphyrin. This compound was purchased and a standard curve for pentachlorophenol was prepared according to Awawdeh and Harmon (2005; data not shown). It was hoped that this method would provide a workable pyroglutamyl esterase assay for PAPI. Unfortunately, pGlu pentachlorophenol proved insoluble in phosphate buffer and, in light of PAPI's very poor tolerance of organic solvents, no attempt was made to use any alternative solvent system. No other pGlu ester was commercially available and attempts by an organic chemistry laboratory to synthesise a pGlu-AMC ester (at our request) were unsuccessful. Accordingly, attempts to measure PAPI esterase activity were abandoned.

6.1 Conclusion

Successful high-level expression and subsequent purification of recombinant human PAPI (from the gene cloned into *E.coli* grown in LB medium) was achieved with a final yield of 60%, and its stability, biochemical and kinetic characteristics were ascertained. Mutants F16Y and Y147F of PAPI were also analyzed.

The fluorimetric assay used to monitor enzyme activity allowed rapid determination of large number of samples, saved time and minimized use of reagents. The k_{cat}/K_m of native PAPI was determined to be 0.202 ($s^{-1} M^{-1}$) with pGlu-AMC as substrate.

The thermostability of brain PAPI proved considerably higher than would be expected for this enzyme, since mammalian pyroglutamyl peptidases normally exist at the physiological body temperature of 37°C. PAPI was catalytically active up to quite elevated temperatures, with a T_{50} value of 60 ± 1°C. Data fitted well to a single exponential decay and the apparent half-life ($t_{1/2}$) determined at 60°C was 15 minutes ($k = 0.046 \pm 0.002$ min^{-1}, protein concentration 0.45 mg/ml, diluted 1/80).

From a biotechnological aspect, there are numerous potential advantages in employing enzymes in organic as opposed to aqueous media. Organotolerance studies determined that PAPI was not stable in most solvents. Methanol and DMSO were the least injurious for PAPI activity and THF was deemed to be the most deleterious solvent to the enzyme. PAPI exhibited reduced tolerance in the present of organic solvents and, unless it can be stabilized by some means, does not seem to be suitable for use in organic solvents.

Modification of PAPI with DMS, a very mild reagent, was undertaken but gave only 20% recovery of initial activity and did not stabilize the enzyme.

The possible stabilizing effect of polyol additives was investigated and it was found that the enzyme's activity and stability increased with xylitol while trehalose, glycerol and ammonium sulphate did not stabilize PAPI. Xylitol, therefore, may be a better preservative for PAPI than glycerol, the additive currently used.

The project also involved investigating the stability and kinetic properties of PAPI mutants Y147F and F16Y. Mutant Y147F displayed a T_{50} of 78°C, notably higher than the wild type, and an apparent half-life ($t_{1/2}$) at 70°C of 25 minutes ($k = 0.028 \pm 0.001$ min^{-1}). For mutant F16Y, T_{50} was 51°C (less than wild type), and the apparent half-life ($t_{1/2}$) of an undiluted sample at 70°C was 27 minutes ($k = 0.026 \pm 0.002$ min^{-1}). The k_{cat}/K_m for Y147F was 0.212 $s^{-1}.M^{-1}$ and for F16Y was 0.355 $s^{-1}.M^{-1}$, both very close to the wild-type value (0.202 s^{-1} M^{-1}, above). A comparison of the half-lives of wild type PAPI and both mutants Y147F and F16Y performed at the same concentration and temperature showed that Y147F was more stable than wild type PAPI, while F16Y was less stable (Table 5.1). Mutants were not tested in organic solvents.

The original research objectives of investigating the stability properties and kinetics of native PAPI and two mutants have been achieved. This work now provides some interesting, significant and potentially useful results for other researchers working in the field of protein stability/ stabilization and enzyme catalysis.

Bibliography

7.0 Bibliography

7.1 Journal Bibliography:

Abe, K., Fukada, K. and Tokui, T. (2004) Marginal Involvement of Pyroglutamyl Aminopeptidase I in Metabolism of Thyrotropin-Releasing Hormone in Rat Brain. *Biological & Pharmaceutical Bulletin* **27**: 1197-1201.

Abe, K., Saito, F., Yamada, M. and Tokui, T. (2004) Pyroglutamyl Aminopeptidase I, as a Drug Metabolizing Enzyme, Recognises Xenobiotic Substrates Containing L-2-Oxothiazolidine-4-carboxylic Acid. *Biological & Pharmaceutical Bulletin* **27**: 113-116.

Abe, K., Watanabe, N., Kosaka, T., Yamada, M., Tokui, T. and Ikeda, T. (2003) Hydrolysis of Synthetic Substrate, L-Pyroglutamyl p-Nitroanilide is Catalyzed Solely by Pyroglutamyl Aminopeptidase I in Rat Liver Cytosol. *Biological & Pharmaceutical Bulletin* **26**: 1528-1533.

Alba, F., Arenas, C. and Lopez M.A. (1995) "Comparison of soluble and membrane-bound pyroglutamyl-peptidase I activities in rat brain tissues in the presence of detergents". Neuropeptides **29**: 103-107.

Albert, Z. and Szewczuk, A. (1972) Pyrrolidonyl peptidase in some avian and rodent tissues. Histochemical localization and biochemical studies. *Acta Histochemica* **44**: 98-105.

Alur, H.H., Desai, R.P., Mitra, A.K. and Johnston, T.P. (2001) Inhibition of a model protease - pyroglutamate aminopeptidase by a natural oligosaccharide gum from *Hakea gibbosa*. *International Journal of Pharmaceutics* **212**: 171-176.

Aoyagi, T., Hatsu, M., Imada, C., Naganawa, H., Okami, Y. and Takeuchi, T. (1992b) Pyrizinostatin: A New Inhibitor Of Pyroglutamyl Peptidase. *The Journal of Antibiotics* **45**: 1795-1796.

Aoyagi, T., Hatsu, M., Kojima, F., Hayashi, C., Hamada, M. and Takeuchi, T. (1992a) Benarthin: A New Inhibitor Of Pyroglutamyl Peptidase I. Taxonomy, Fermentation, Isolation and Biological Activities. *The Journal of Antibiotics* **45**: 1079-1083.

Armentrout, R.W. and Doolittle, R.F. (1969) Pyrrolidonecarboxyl Peptidase: Stabilization and Purification. *Archives of Biochemistry and Biophysics* **132**: 80-90.

Armentrout, R.W.(1969) Pyrrolidonecarboxylyl Peptidase from Rat Liver. *Biochimica et Biophysica Acta* **191**: 756-759.

Awadé, A., Cleuziat, Ph., Gonzales, Th. and Robert-Baudouy, J. (1994) Pyrrolidone Carboxyl Peptidase (Pcp): An Enzyme That Removes Pyroglutamic Acid (pGlu) From pGlu-Peptides and pGlu-Proteins. *Proteins: Structure, Function and Genetics* **20**: 34-51.

Awadé, A., Cleuziat, Ph., Gonzalès, Th. and Robert-Baudouy, J. (1992) Characterisation of the pcp gene encoding the pyrrolidone carboxyl peptidase of *Bacillus subtilis*. *Federation of European Biochemical Societies* **305**: 67-73.

Awadé, A., Gonzalès, Th., Cleuziat, Ph. and Robert-Baudouy, J. (1992) One step purification and characterisation of the pyrrolidone carboxyl peptidase of *Streptococcus pyogenes* over-expressed in *Escherischia coli*. *Federation of European Biochemical Societies* **308**: 70-74.

Awawdeh, M,. Harmon, M (2005) "Spectrophotometric detection of pentachlorophenol (PCP) in water using immobilized and water-soluble porphyrins" **20**: 1595-1601.

-B-

Barrett, A.J. and Rawlings, N.D. (2001) Evolutionary Lines of Cysteine Peptidases. *Biological Chemistry* **382**: 727-733.

Bauer, K. and Kleinkauf, H. (1980) Catabolism of Thyroliberin by Rat Adenohypophyseal Tissue Extract. *Journal of Biochemistry* **106**: 107-117.

Bauer, P. Nowak. (1979) Characterization of a Thyroliberin-Degrading Serum Enzyme Catalyzing the Hydrolysis of Thyroliberin at the Pyroglutamyl-Histidine Bond. *European Journal of Biochemistry* **99**: 239-246.

Bauer, K. (1976) "Regulation of degradation of thyrotropin releasing hormone by thyroid hormones" *Nature* (London) **259**: 591-593.

Bauer, P. Nowak, H. Kleinkauf, J. (1981) Specificity of a Serum Peptidase Hydrolyzing Thyroliberin at the Pyroglutamyl-Histidine Bond. *European Journal of Biochemistry* **118**: 173-176.

Bharadwaj, D., Roy, M.S., Saha, G. and Hati, R.N. (1992) Pyroglutamate aminopeptidase in rat submaxillary gland. *Indian Journal of Biochemistry* **29**: 442-444.

Browne, P. and O'Cuinn (1983) An evaluation of the role of a pyroglutamyl peptidase, a post-proline cleaving enzyme and a post-proline dipeptidyl amino peptidase, each purified from the soluble fraction of guinea-pig brain, in the degradation of thyroliberin *in vitro*. *European Journal of Biochemistry* **137**: 75-87.

Bollag, D.M., Rozycki, M.D. & Edelstein, S.J. (1996a). Hydrophobic interaction chromatography, *In: Protein Methods,* 2nd edition. New York: Wiley-Liss. 346-351.

-C-

Charli, JL, Mendez, M., Joseph-Bravo, P. and Wilk, S. (1987) Specific Inhibitors Of Pyroglutamyl Peptidase I And Prolyl Endopeptidase Do Not Change The *In Vitro* Release Of TRH Or Its Content In Rodent Brain. *Neuropeptides* **9**: 373-378.

Cleuziat, P., Awadé, A. and Robert-Baudouy, J. (1992) Molecular characterisation of pcp, the structural gene encoding the pyrrolidone carboxylyl peptidase from *Streptococcus pyogenes*. *Molecular Microbiology* **6**: 2051-2063.

Coyle, J.T., Donlad, L.P., Delong, M.R. (1983) "Alzheimers disease: a disorder of cortical cholinergic innervation" *Science*, **219**: 1151-1156.

Creighton, T. E. (1993) in " Proteins: Structures and Molecular Properties" 2nd ed, W. H. Freeman, New York, 417-433.

Cummins, P.M. and O'Connor, B. (1998) Pyroglutamyl peptidase: an overview of the three known enzymatic forms. *Biochimica et Biophysica acta* **1429**: 1-17.

Cummins, P.M. and O'Connor, B. (1996) Bovine Brain Pyroglutamyl Aminopeptidase (Type-1): Purification and Characterisation of a Neuropeptide-Inactivating Peptidase. *The International Journal of Biochemistry and Cell Biology* **28**: 883-893.

-D-

Dando, P.M., Fortunato, M, Strand, G.B., Smith, T.S. and Barrett, A.J. (2003) Pyroglutamyl-peptidase I: cloning, sequencing, and characterisation of the recombinant human enzyme. *Protein Expression and Purification* **28**: 111-119.

Daniel, R.M (1996). The upper limits of enzyme thermal stability. *Enzyme and Microbial Technology*, **19**: 74-79.

DeGandarias, J.M., Irazusta, J., Gil, J., Varona, A., Ortega, F. and Casis, L. (2000) Subcellular ontogeny of brain pyroglutamyl peptidase I. *Peptides* **21**: 509-517.

DeGandarias, J.M., Irazusta, J., Silio, M., Gil, J., Saitua, N. and Casis, L. (1998) Soluble and membrane-bound pyroglutamyl-peptidase I activity in the developing cerebellum and brain cortex. *International Journal of Developmental Biology* **42**: 103-106.

DeGandarias, J.M., Irazusta, J., Fernandez, D., Varona, A. and Casis, L. (1994) Developmental Changes of Pyroglutamate-peptidase I Activity in Several Regions of the Female and Male Rat Brain. *International Journal of Neuroscience* **77**: 53-60.

DeGandarias, J.M. De, Casis, O., Echevarria, E., Irazusta, J. and Casis, L. (1992) Pyroglutamil-peptidase I activity in the cortex of the cat brain during development. *International Journal of Developmental Biology* **36**: 335-337.

DeRenobales, M. & Welch, W. (1980) Chemical cross-linking stabilizes the enzymic activity and quaternary structure of formyltetrahydrofolate synthetase. *Journal of Biological Chemistry.*, **255:** 10460-10463.

Dixon, M. & Webb, E.C. (1979b). Effect of temperature, *In: Enzymes,* 3rd edition. New York: Academic Press Inc.164-182.

Doolittle, R.F. and Armentrout, R.W. (1968) Pyrrolidonyl Peptidase. An Enzyme for Selective Removal of Pyrrolidonecarboxylic Acid Residues from Polypeptides. *Biochemistry* **7**: 516-521.

Durinx, C., Lambeir, A-M., Bosmans, E., Falmagne, J-B., Berghmans, R., Haemers, A., Scharpé, S. & De Meester, I. (2000). Molecular characterization of dipeptidyl peptidase activity in serum: soluble CD26/dipeptidyl peptidase IV is responsible for the release of X-Pro dipeptides. *European Journal of Biochemistry,* **267**: 5608-5613.

-E-

Exterkate, F.A. (1977) Pyrrolidone Carboxylyl Peptidase in *Streptococcus cremoris*: Dependence on an Interaction with Membrane Components. *Journal of Bacteriology*. **129**: 1281-1288.

Eichler, J. (2001). Biotechnological uses of archaeal extremozymes. *Biotechnology Advances*, **19:** (4), 261-278.

-F-

Faivre-Bauman, A., Loudes, C., Barret, A., Tixier-Vidal, A. and Bauer, K. (1986) Possible Role Of Neuropeptide Degrading Enzymes On Thyroliberin Secretion In Fetal Hypothalamic Cultures Grown In Serum Free Medium. *Neuropeptides* **7**: 125-138.

Falkous, G., Shaw, P.J., Ince, P.G. and Mantle, D. (1995) Comparison of cytoplasmic and lysosomal proteolytic enzyme levels in spinal cord tissue from motor neurone disease and control cases. *6th International Symposium on ALS/MND*, Dublin, Ireland

Friedman, T.C., Kline, T.B. and Wilk, Sherwin (1985) 5-Oxoprolinal: Transition-State Aldehyde Inhibitor of Pyroglutamyl-Peptide Hydrolase. *Biochemistry* **24**: 3907-3913.

Fujiwara, K., Kitagawa, T. and Tsuru, D. (1981a) Inactivation of Pyroglutamyl Aminopeptidase by L-Pyroglutamyl Chloromethyl Ketone. *Biochimica et Biophysica Acta* **655**: 10-16.

-G-

Gallagher, S.P., O'Leary, R.M and O'Connor, B. (1997) "The Development of Two Fluorimetric Assays for the Determination of Pyroglutamyl Aminopeptidase Type-II Activity" *Analytical Biochemistry* **250**:1-9.

Gonzalès, T. and Robert-Baudouy, J. (1994) Characterisation of the pcp Gene of *Pseudomonas fluorescens* and of Its Product, Pyrrolidone Carboxyl Peptidase (Pcp). *Journal of Bacteriology* **176**: 2569-2576.

Griffiths, E.C. (1985) Thyrotropin Releasing Hormone: Endocrine And Central Effects. *Psychoneuroendocrinology* **10**: 225-235.

-H-

Hardie D.G , (1991) "Biochemical Messengers, Hormones, Neurotransmitters, and Growth Factors." London; New York: Chapman and Hall. (first edition)

He, W. and Barrow, C.J. (1999) The Aβ 3-Pyroglutamyl and 11-Pyroglutamyl Peptides Found in Senile Plaque Have Greater β-Sheet Forming and Aggregation Propensities *in Vitro* than Full-Length Aβ. *Biochemistry* **38**: 10871-10877.

-I-

Irazusta, J, Larrinaga, G., González, J., Gil, J., Meana, J. and Casis, L. (2002) "Distribution of prolyl endopeptidase activities in rat and human brain." Neurochemistry. International., **40**: 337-345.

Ito, K., Inoue, T., Takahashi, T., Huang, H S., Esumi, T., Hatakeyama, S. (2001) "The mechanism of substrate recognition of PAPI from *Bacillus amyloliquefaciens* as determined by X-ray crystallography and site-directed mutagenesis." *Journal of Biological Chemistry.*, **276**: 18557-18562.

-J-

Ji, T.H. (1983) Bifunctional reagents. In: Hirs, C.H.W & Timasheff, S.N., eds. Methods in Enzymology. NY: Academic Press, **91:** 580-609.

-K-

Kabashima, T., Li, Y., Kanada, N., and Yoshimoto, T. (2001) "Enhancement of the thermal stability of pyroglutamyl peptidase I by introduction of an intersubunit disulfide bond", *Biochimica et, Biophysica Acta Protein Struture and Molecular Enzymology.*, **1547**: 214-220.

Kawarabayasi Y, Sawada M, Horikawa H, Haikawa Y, Hino Y, Yamamoto S, Sekine M, Baba S, Kosugi H, Hosoyama A, Nagai Y, Sakai M, Ogura K, Otsuka R, Nakazawa H, Takamiya M, Ohfuku Y, Funahashi T, Tanaka T, Kudoh Y, Yamazaki J, Kushida N, Oguchi A, Aoki K, Kikuchi H. (1998) Complete

sequence and gene organization of the genome of a hyper-thermophilic archaebacterium, *Pyrococcus horikoshii* OT3. *DNA Research* **5**: 55-76.

Kim J.K., Kim S.J., Lee H.G., Lim J.S., Kim S.J., Cho S.H., Jeong W.H., Choe I.S., Chung T.W., Paik S.G., Choe Y.K. (2001) Molecular Cloning and Characterisation of *Mycobacterium bovis* BCG *pcp* Gene Encoding Pyrrolidone Carboxyl Peptidase. *Molecules and Cells* **12**: 347-352.

Kwiatkowska, J., Torain, B. and Glenner, G.G. (1974) A Pyrrolidonecarboxylate Peptidase from the Particulate Fraction of *Klebsiella cloacae*. *The Journal of Biological Chemistry* **249**: 7729-7736.

-L-

Laemmli, U.K. (1970) "Cleavage of structural proteins during the assembly of the head of bacteriophage T4". Nature (London), **227**:680-685.

Le Saux, O., Gonzales, T. and Robert-Baudouy, J. (1996) Mutational Analysis of the Active Site of *Pseudomonas fluorescens* Pyrrolidone Carboxyl Peptidase. *Journal of Bacteriology* **178**: 3308-3313.

Lauffart, B., McDermott, J.R., Biggins, J.A., Gibson, A.M. and Mantle, D. (1989) Purification and characterization of pyroglutamyl aminopeptidase from human cerebral cortex. *Biochemical Society Transactions* **17**: 207-208.

-M-

Mantle, D., Lauffart, B. and Gibson, A. (1991) Purification and characterisation of leucyl aminopeptidase and pyroglutamyl aminopeptidase from human skeletal muscle. *Clinica Chimica Acta* **197**: 35-46.

Mantle, D., Lauffart, B., McDermot, J. and Gibson, A. (1990) Characterisation of aminopeptidases in human kidney soluble fraction. *Clinica Chimica Acta* **187**: 105-114.

Mineyama, R. and Saito, K. (1998) Partial purification and some properties of pyroglutamyl peptidase from *Enterococcus faecalis*. *Microbios* **94**: 47-62.

Moreno, J., O' Fagain, C. (1997) " Activity and Stability of native and modified alanine aminotransferase in cosolvent systems and denaturants" **2**: 271-279.

Mudge, R.E. Fellows, (1973) Bovine pituitary pyrrolidonecarboxylyl peptidase, Endocrinology **93** :1428–1434.

-O-

O'Connor B., O'Cuinn G. (1985) Purification of a kinetic studies on a narrow specificity synaptosomal membrane pyroglutamate aminopeptidase from guinea-pig brain, *European Journal of Biochemistry.*, **150**: 47-52.

O'Cuinn, G., O'Connor, B. and Elmore, M. (1990) Degradation of Thyrotropin-Releasing Hormone and Luteinising Hormone-Releasing Hormone by Enzymes of Brain Tissues. *Journal of Neurochemistry* **54**: 1-13.

Odagaki, Y., Hayashi, A., Okada, K., Hirotsu, K., Kabashima, T., Ito, K., Yoshimoto, T., Tsuru, D., Sato, M. and Clardy, J. (1999) The Crystal Structure Of Pyroglutamyl Peptidase I from *Bacillus amyloliquefaciens* reveals a new structure for a cysteine protease. *Structure* **7**: 399-411.

Ogasahara, K., Khechinashvili, N., Nakamura, M., Yoshimoto, T. and Yutani, K. (2001) Thermal stability of pyrrolidone carboxyl peptidase from the hyperthermophilic Archaeon, *Pyrococcus furiosus*. *European Journal of Biochemistry* **268**: 3233-3242.

Ohkubo, I., Huang, K., Ochiai, Y., Takagaki, M. & Kani, K. (1994). Dipeptidyl peptidase IV from porcine seminal plasma: purification characterization, and N-terminal amino acid sequence. *Journal of Biochemistry,* **116**: 1182-1186.

Orlowski, M. and Meister, A. (1971), Enzymology of Pyrrolidone Carboxylic Acid, In: Boyer, P.D. (ed.), *The Enzymes, IV: Hydrolysis*, Academic Press, New York 123-151.

-P-

Patti, J.M., Schneider, A., Garza, N. and Boles, J.O. (1995) Isolation and characterisation of pcp, a gene encoding a pyrrolidone carboxyl peptidase in *Staphylococcus aureus*. *Gene* **166**: 95-99

Pierro, M. and Orsatti, M. (1970) On intestinal hydrolysis of pyrrolidonylpeptides. *Bollettino Della Societa Italiana Di Biologia Sperimentale* **45**: 1630.

Prasad, C. Mori, M., Pierson, W., Wilber, J., Ewards, R. (1983) "Developmental changes in the distribution of rat brain pyroglutamate aminopeptidase, a possible determinant of endogenous cyclo(His-Pro) concentrations" Neurochem. Res. **8**: 389-399.

Prasad, C. and Peterkofsky, A. (1976) Demonstration of Pyroglutamylpeptidase and Amidase Activities toward Thyrotropin-releasing Hormone in Hamster Hypothalamus Extracts. *The Journal of Biological Chemistry* **251**: 3229-3234

-R-

Ramírez, M., Sanchez, B. Alba, F.; Luna, J. .; Martínez, I.;. (1991) "Diurnal variation and left-right distribution of pyroglutamyl peptidase I activity in the rat brain and retina"Acta Endocrinologica., **125**: 570-573.

Robert-Baudouy, J., and Thierry, G. (1998) in *Handbook of Proteolytic Enzymes*. edited by Alan J. Barrett, Neil D. Rawlings, F. San Diego: Academic Press, 791–795.

Ryan, O., Smyth, MR and O' Fagain, C. (1994) " Thermostabilized chemical derivatives of horseradish peroxidase" Enzyme and Microbial Technology **16**: 501-505.

-S-

Sánchez, B., Alba, F.; Luna, J. D.; Martínez, I.; Ramírez, M. (1996) "Pyroglutamyl Peptidase I levels and their left –right distribution in the rat retina and hypothalamus are influenced by light-dark conditions". Brain Research, **731**: 254-257.

Scharfmann, S. Aratan-Spire, (1991) Ontogeny of 2 topologically distinct TRH-degrading pyroglutamate aminopeptidase activities in the rat-liver, Regulatory Peptides. **32**: 75-83.

Scharfmann, J.C. Ebiou, J.L. Morgat, S. Aratan-Spire (1990), Thyroid status regulates particulate but not soluble TRH-degrading pyroglutamate aminopeptidase activity in the rat-liver, Acta Endocrinologica.**123**:84-89.

Schauder, B., Schomburg, L., Kohrle, J. and Bauer, K. (1994) Cloning of a cDNA encoding an ectoenzyme that degrades thyrotropin-releasing hormone. *Proceedings of the National Academy of Sciences of the United States of America* **91**: 9534-9538.

Schein, G. H. (1990) Solubility as a function of Protein Struction and Solvent Components. *Biotechnology* **8**: 308-317.

Schmitmeier, S., Thole, H., Bader, A. and Bauer, K. (2002) Purification and characterization of the thyrotropin-releasing hormone (TRH)-degrading serum enzyme and its identification as a product of liver origin. *European Journal of Biochemistry* **269**: 1278-1286.

Schomburg, L., Turwitt, S., Prescher, G., Lohmann, D., Horsthemke, B. and Bauer, K. (1999) Human TRH-degrading ectoenzyme: cDNA cloning, functional expression, genomic structure and chromosomal assignment. *European Journal of Biochemistry* **265**: 415-422.

Singer and Lindquist (1998) Multiple effects of trehalose on protein folding in *vitro* and in *vivo*, Departments of Pathology and Molecular Genetics and cell Biology Howard Hughes Medical Institute University of Chicago **1**: 639-648.

Singleton, M.R. and Littlechild, J.A. (2001) Pyrrolidone Carboxylpeptidase from *Thermococcus litoralis*. *Methods in Enzymology* **330**: 394-403.

Singleton, M.R., Taylor, S.J.C., Parrat, J.S. and Littlechild, J.A. (2000) Cloning, expression, and characterization of pyrrolidone carboxyl peptidase from the archaeon *Thermococcus litoralis*. *Extremophiles* **4**: 297-303.

Singleton, M.R., Isupov, M.N. and Littlechild, J.A. (1999a) Crystallisation and preliminary X-ray diffraction studies of pyrrolidone carboxyl peptidase from the hyperthermophilic archaeon *Thermococcus litoralis*. Acta *Crystallographica* **D55**: 702-703.

Singleton, M., Isupov, M. and Littlechild, J. (1999b) "X-ray structure of pyrrolidone carboxyl peptidase from the hyperthermophilic archaeon *Thermococcus litoralis*" Structure, **7**: 237-244.

Smith, P.K., Krohn, R.I., Hermanson, G.T., Mallia, A.K., Gartner, F.H., Provenzano, M.D., Fujimoto, E.K., Goeke, N.M., Olson, B.J. & Klenk, D.C. (1985). Measurement of protein using bicinchoninic acid. *Analytical Biochemistry* , **150**: 76-85.

Sokabe, M., Kawamura, T., Sakai, N., Yao, M., Watanabe, N. and Tanaka, I. (2002) X-ray crystal structure of pyrrolidone-carboxylate peptidase from hyperthermophilic *Pyrococcus horikoshii. Journal of Structural and Functional Genomics* **2**: 145-154.

Sullivan, J.J., Muchnicky, E.E., Davidson, B.E. and Jago, G.R. (1977) Purification and Properties of the Pyrrolidonecarboxylate Peptidase of *Stretococcus faecium. Australian Journal of Biological Science* **30**: 543-552.

Szewczuk, A. and Kwiatkowska, J. (1970) Pyrrolidone Peptidase in Animal, Plant and Human Tissues. Occurrence and some Properties of the Enzyme. *European Journal of Biochemistry* **15**: 92-96.

Szewczuk, A. and Mulczyk, M. (1969) Pyrrolidonyl Peptidase in Bacteria. The Enzyme from *Bacillus subtilis. European Journal of Biochemistry* **6**: 63-67.

-T-

Tanaka, H., Chinami, M., Mizushima, T., Ogasahara, Ota, M., Tsukihara, T. and Yutani, K. (2001) X-Ray Crystalline Structures of Pyrrolidone Carboxyl Peptidase from a Hyperthermophile, *Pyrococcus furiosus*, and Its Cys-Free Mutant. *Journal of Biochemistry* **130**: 107-118.

Taylor, J. E. Dixon, (1978) Characterization of a pyroglutamate aminopeptidase from rat serum that degrades thyrotropin-releasing hormone, *Journal of Biochemistry*. U.S.A. **253** : 6934-6940.

Tsunasawa, S., Nakura, S., Tanigawa, T., Kato, I. (1998) "Pyrrolidone carboxyl peptidase from the hyperthermophilic ArchaeonPyrococcus furiosus: cloning and overexpression in Escherichia coli of the gene, and its application to protein sequence analysis *"Journal of Biochemistry* **124**: 778-783.

Tsuru D., Fujiwara, K. and Kado, K. (1978) "Purification and characterization of L-pyrrolidonecarboxylate peptidase from *Bacillus amyloliquefaciens*" *Journal of Biochemistry*. **84**: 467-476.

Turk, B., Krizaj, I., Kralj, B., Dolenc, I., Popovic, T., Bieth, J.G., Turk, V. (1993) Bovine stefin C, a new member of the stefin family. " *Journal of Biological chemistry*. **268**: 7323-7329.

-Y-

Yamada, M. and Mori, M. (1990) "Thyrotropin -releasing hormone-degrading enzyme in human serum is classified as type II of pyroglutamyl aminopeptidase: influence of thyroid stat us" *Proc. Soc. Exp. Biological. Medical*:**194,** 346-351.

Yoshimoto, T., Shimoda, T., Kitazono, T (1993) Pyroglutamyl peptidase gene from *Bacillus amyloliquefaciens*: cloning, sequencing, expression and crystalisation of the expressed enyme" *Journal of Biochemistry*, **113**: 67-73.

Yoshimoto, T., Fischl, M., Orlowski, R.C. & Walter, R. (1978). Post-proline

cleaving enzyme and post-proline dipeptidyl aminopeptidase. *Journal of Biological Chemistry,* **253** (10): 3708-3716.

-V-

Valdivia, A., Irazusta, J., Fernandez, D., Mugica, J., Ochoa, C. and Casis, L. (2004) Pyroglutamyl peptidase I and prolyl endopeptidase in human semen: increased activity in necrozoospermia. *Regulatory Peptides* **122**: 79-84.

7.2 Book Bibliography:

N.M. Hooper. (2002) Essays in Biochemistry. " Proteases in Biology and Medicine" London, Portland Press. **38**: 1-4

Mader, S. "Biology", (2001) 7th Edition,. McGraw Hill, New York, 162-172, 825-846.

7.3 Internet Bibliography:

http://www. burnham.org/labs/salvesen/classification)

http://prodes.toulouse.inra.fr/multalin/multalin.html

http://www.ncbi.nlm.nih.gov/UniGene/clust.cgi?ORG=Hs& CI D=6510 PPI Nucleotide Sequence:

http://www.ncbi.nlm.nih.gov:80/entrez/query.fcgi?cmd=Ret rieve&db=nucleotide&list_uids=9843747&dopt=G enBank PPII Nucleotide Sequence:

http://www.ncbi.nlm.nih.gov:80/entrez/query.fcgi?cmd=Retrieve&db=nucleotide&list_uids=6467370&dopt=G enBank

http:// www.merops.sanger.ac.uk/cgi-bin/merops.cgi?id.

7.4 Thesis Bibliography:

Buckley, S.J. (2001) The purification and characterisation of prolyl oligopeptidase from human saliva and dipeptidyl peptidase IV from bovine serum. PhD thesis, Dublin City University.

Ruth, D.M. (2004) Exploration of dipeptidyl peptidase IV and recombinant *fasciola hepatica cathepsin* L1 as potential biocatalysts. PhD thesis, Dublin City University.

Vaas, P.-R. (2005) Molecular characterisation of a recombinant human neuropeptide-inactivating proteinase. PhD thesis, Dublin City University